Dr. Leonid Zotov

POLAR MOTION AND LOD VARIABILITY IN THE LIGHT OF CLIMATE CHANGE

Warsaw 30/10/2020

Do we see Climate change in the fundamentals of Geodesy?

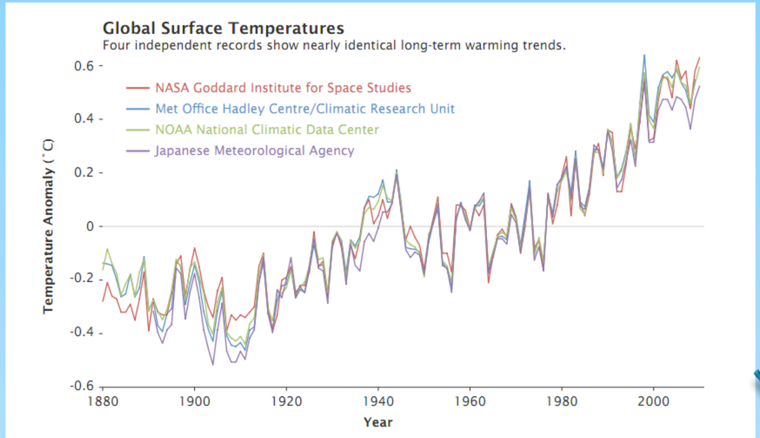

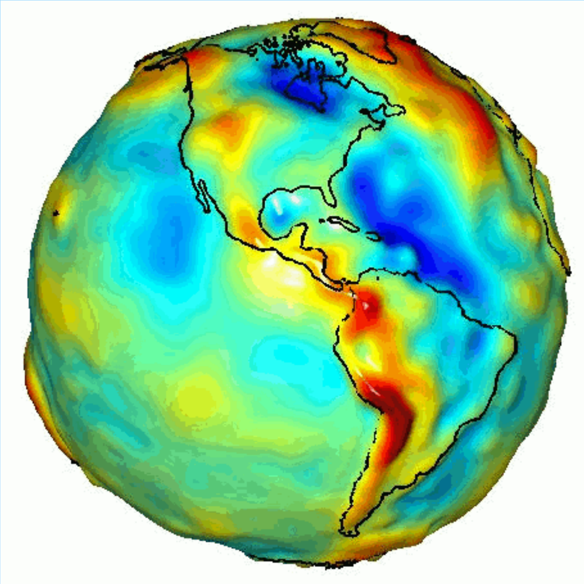

In the gravity field - YES

In the planet's rotation – WHY NOT?

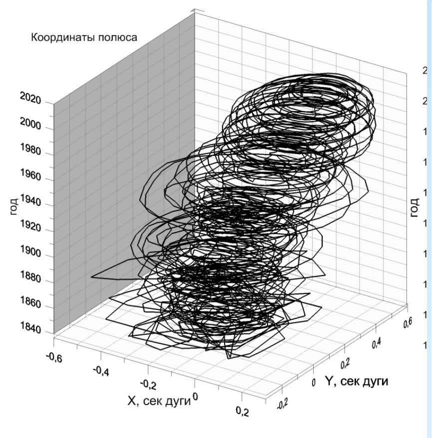

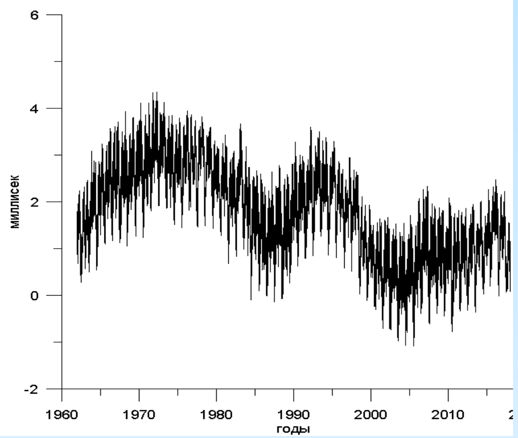

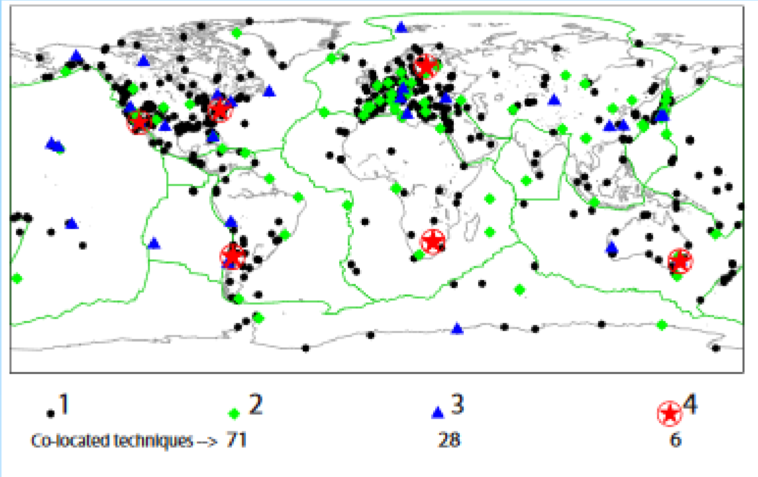

In reference systems – most likely YES

Inter-Commission Committee on Geodesy for Climate Research (ICCC)

President: **Annette Eicker** (Germany)
Vice-President: **Carmen Boening** (USA)

Internet site: https://iccc.iag-aig.org/
Twitter: @IAG_climate

Joint Working Groups

Joint Working Group JWG C.1: Climate Signatures in Earth Orientation Parameters

Affiliation: Commission 3, GGOS, IERS

Chair: Jolanta Nastula (Poland)
Vice-Chair: Henryk Dobslaw (Germany)

Introduction

Earth orientation parameters comprising variations of both the position of the rotational pole and the spin rate are precisely observed by modern space geodetic techniques for several decades already. Moreover, optical astrometric observations extending back in time over more than 100 years provide even carry information about the mass transport and mass distribution processes acting on Earth at historical times that might be explored to quantify slow and subtle variations in the Earth's climate. This working group will study the various contributors of the global and interactively coupled climate system to the observed changes of the Earth's orientation on time-scales from days to centennials. It will explore possibilities to validate numerical climate models and its individual components by means of assessing the angular momentum budget and the associated torques. The working group will further investigate predictive limits of various Earth system state and flux variables in order to aid short- and long-term prediction of polar motion and changes in the length-of-day, and might ultimately foster the incorporation of Earth Orientation Parameters into contemporaneous global re-analyses of the Earth System by means of data assimilation.

Members

- Christian Bizouard (France)
- Sigrid Boehm (Austria)
- Aleksander Brzezinski (Poland)
- Benjamin Fong Chao (Taiwan)
- Yavor Chapanov (Bulgaria)
- Jianli Chen (USA)
- Alexandre Couhert (France)
- Robert Dill (Germany)
- Alberto Escapa (Spain)
- José Manuel Ferrandiz (Spain)
- Laura Fernandez (Argentina)
- Franziska Goettl (Germany)
- Richard Gross (USA)
- Robert Heinkelmann (Germany)
- Sébastien Lambert (France)
- Vladimir Pashkevich (Russia)
- Elena Podladchikova (Belgium)
- Cyril Ron (Czech Republic)
- David Salstein (USA)
- Michael Schindelegger (Germany)
- Nikolay Sidorenkov (Russia)
- Leonid Zotov (Russia)

https://www.dropbox.com/s/u8pfpvbvqozq1cn/ToR_ICCC_2020.pdf

Proposal for a Joint IERS, IAG, GGOS Working Group: Climate Signatures in Earth Orientation Parameters

Towards an

International Panel for Earth Rotation and Climate Changes (IPERCC)

in the frame of the Inter-Commission Committee on Geodesy for Climate Research

Provisional list of the members:

- Chair: NASTULA Jolanta - Space Reseach Center (Warsaw)
- Vice-Chair: DOBSLAW Henryk - GFZ (Postdam)

- BIZOUARD Christian - Paris Observatory
- BOEHM Sigrid - TI Wien
- BRZEZINSKI Aleksander - Space Reseach Center (Warsaw)
- CHEN Jianli - USA
- DILL Robert - GFZ (Postdam)
- EICKER Annette - Germany
- FERNANDEZ Laura - National University of La Plata
- GROSS Richard - JPL
- HEIKELMANN Robert - GFZ (Postdam)
- LAMBERT Sébastien - Paris Observatory
- PASHKEVICH Vladimir - Pulkovo Observatory
- SALSTEIN David - MIT (Boston)
- SIDORENKOV Nikolay - Hydrometcenter of the Russian Federation (Moscow)
- ZOTOV Leonid - Astronomical Sternberg Institute of the Moscow State University

Bibliographic references:

- Regional atmospheric influence on the Chandler wobble. ZOTOV L., BIZOUARD C. (2015)
- Heartbeat of the Sun from Principal Component Analysis and prediction of solar activity on a millenium timescale. V. V. ZHARKOVA, S. J. SHEPHERD, E. POPOVA, and S. I. ZHARKOV (2015)
- About possible interrelation between Earth rotation and climate variability on a decadal time-scale? ZOTOV L., BIZOUARD C., SHUM C.K. (2016).
- The response of clouds and aerosols to cosmic ray decreases. J. SVENSMARK, M. B. ENGHOFF, N. J. SHAVIV, and H. SVENSMARK (2016)
- Does an Intrinsic Source Generate a Shared Low-Frequency Signature in Earth's Climate and Rotation Rate? Steven L. MARCUS (2016)
- Climate-driven polar motion: 2003-2015. Surendra ADHIKARI and Erik R. IVINS (2016)
- Decade fluctuations in Earth's rotation as evidences of lithospheric drift over the asthenosphere. SIDORENKOV N., DIONIS E., BIZOUARD C., ZOTOV L. (JSR 2019)

https://syrte.obspm.fr/~bizouard/ipercc/index.html.

Observed EOP

x, y pole coordinates

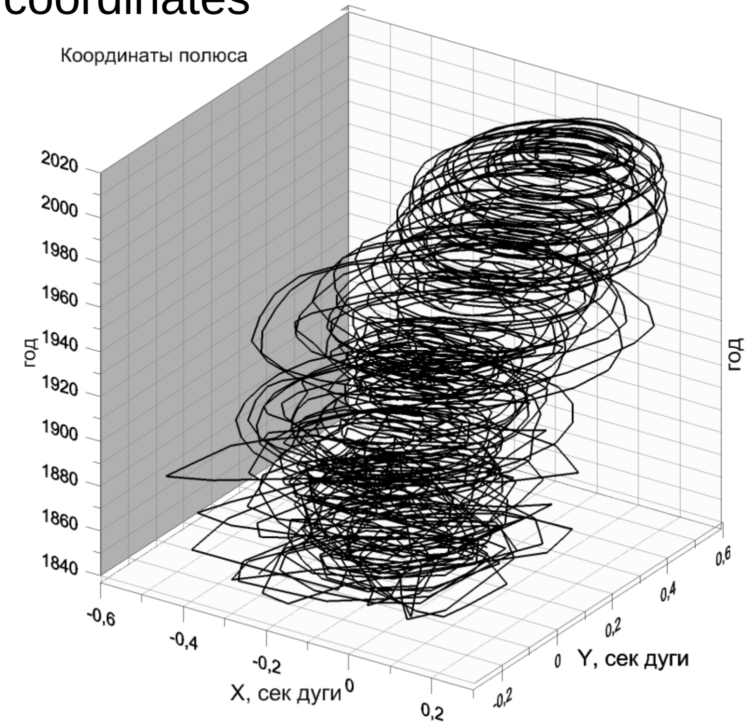

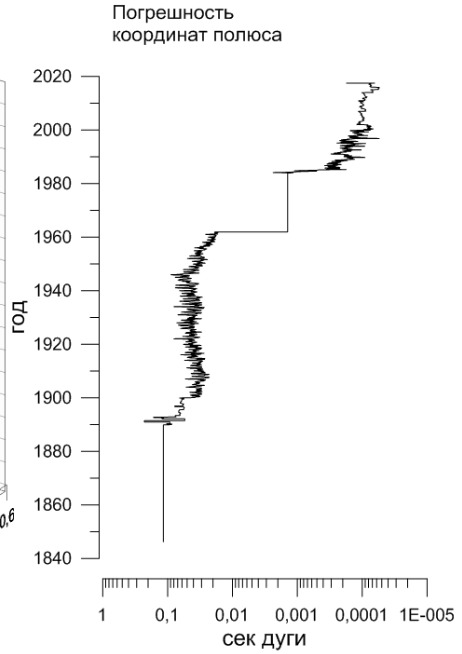

Earth orientation parameters:

- x, y pole coordinates
- UT1-UTC
- dX, dY nutation corrections

nutation corrections

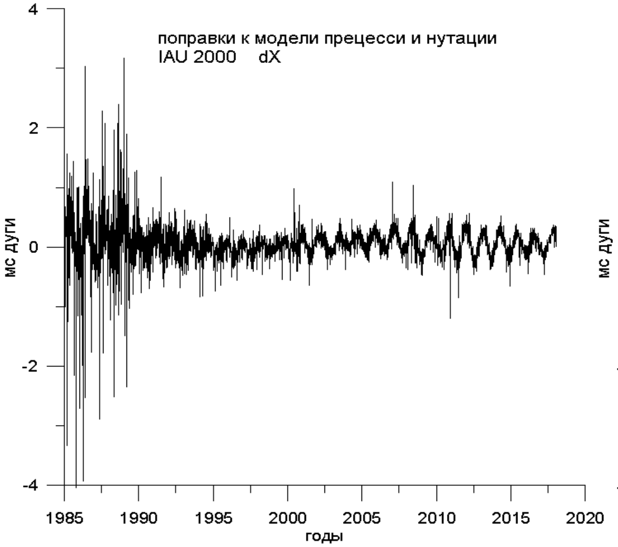

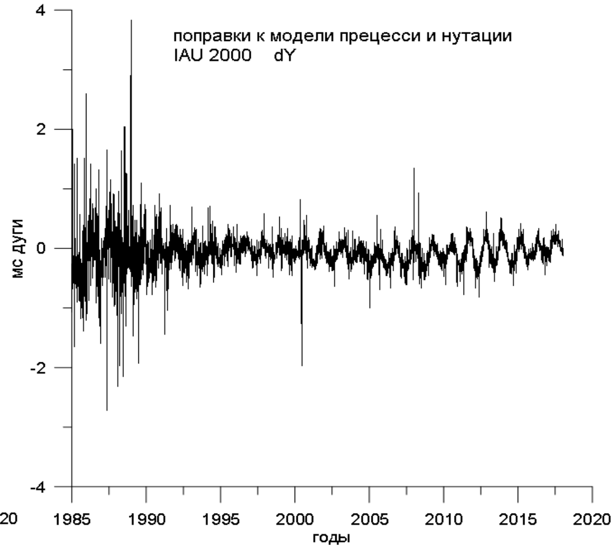

Length o day
LOD

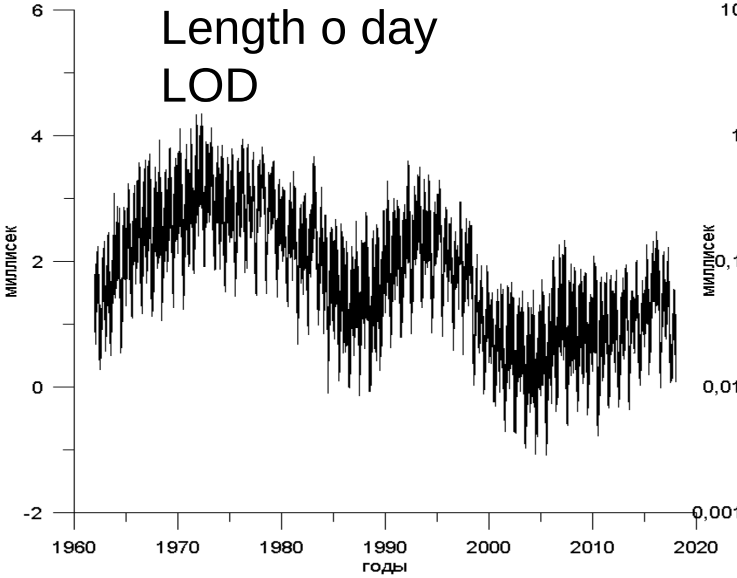

precision

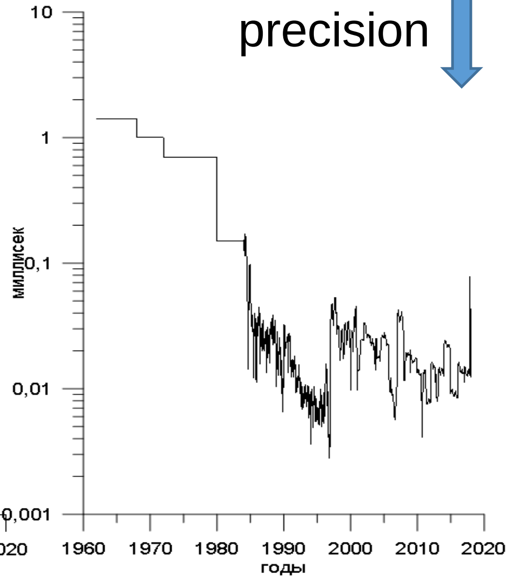

Aspects of the Earth rotation theory

$$\frac{\partial \mathbf{H}}{\partial t} + (\omega \times \mathbf{H}) = \mathbf{\Lambda},$$

$$\mathbf{H} = \mathbf{I}\omega + \mathbf{h}.$$

Angular momentum balance

In non-rotating   in rotating frame

$$\left(\frac{d\mathbf{H}}{dt}\right)_S = \mathbf{L}, \qquad \frac{d\mathbf{H}}{dt} + \mathbf{\Omega} \times \mathbf{H} = \mathbf{\Gamma},$$

Euler equations of solid body rotation

$$\frac{d\omega_1}{dt} + \frac{I_3 - I_2}{I_1}\omega_2\omega_3 = 0,$$
$$\frac{d\omega_2}{dt} + \frac{I_1 - I_3}{I_2}\omega_3\omega_1 = 0,$$
$$\frac{d\omega_3}{dt} + \frac{I_2 - I_1}{I_3}\omega_1\omega_2 = 0.$$

$$\frac{d\omega_1}{dt} = -\sigma_e\omega_2, \qquad \frac{d\omega_2}{dt} = \sigma_e\omega_1,$$

Euler frequency

$$\sigma_e = \Omega\frac{C - \frac{A+B}{2}}{\frac{A+B}{2}}.$$

Complex linearized Euler-Liouville Equation for equatorial components

$$\frac{i}{\sigma_e}\dot{m} + m = \Psi,$$

$$\dot{m}_3 = \dot{\Psi}_3,$$

For axial component

Excitation functions

$$\Psi_1 = \frac{1}{\Omega^2(C-A)}\left(\Omega^2 c_{13} + \Omega\dot{c}_{23} + \dot{h}_2 + \Omega h_1\right),$$
$$\Psi_2 = \frac{1}{\Omega^2(C-A)}\left(\Omega^2 c_{23} - \Omega\dot{c}_{13} - \dot{h}_1 + \Omega h_2\right).$$

$$\Psi_3 = \frac{1}{\Omega^2 C}\left(-\Omega^2 c_{33} - \Omega\dot{h}_3\right).$$

$$\Psi = \Psi_1 + i\Psi_2$$

$$m = m_1 + im_2, \; c = c_{13} + ic_{23}, \qquad h = \dot{c}_{13} + i\dot{c}_{23}$$

Tensor of Inertia

$$\mathbf{I} + \delta\mathbf{I} = \begin{bmatrix} A + c_{11} & c_{12} & c_{13} \\ c_{21} & B + c_{22} & c_{23} \\ c_{31} & c_{32} & C + c_{33} \end{bmatrix}.$$

Angular velocity vector

$$\omega_0 + \delta\omega = \Omega\begin{bmatrix} m_1 \\ m_2 \\ 1 + m_3 \end{bmatrix}.$$

Complex angular momentum function

$$\chi = \frac{c}{(C-A)} + \frac{h}{\Omega(C-A)},$$

Tensor of inertia changes, mass component *c* motion component *h*

$$m = p - \frac{i}{\Omega}\dot{p}.$$

$$\frac{i}{\sigma_e}\dot{p} + p = \chi^{mass} + \chi^{motion} = \chi.$$

Precession, nutation and motion of the pole

Precession and nutation with periods of
26 000 and 18.6 years caused by the tidal influence of
the Sun and Moon

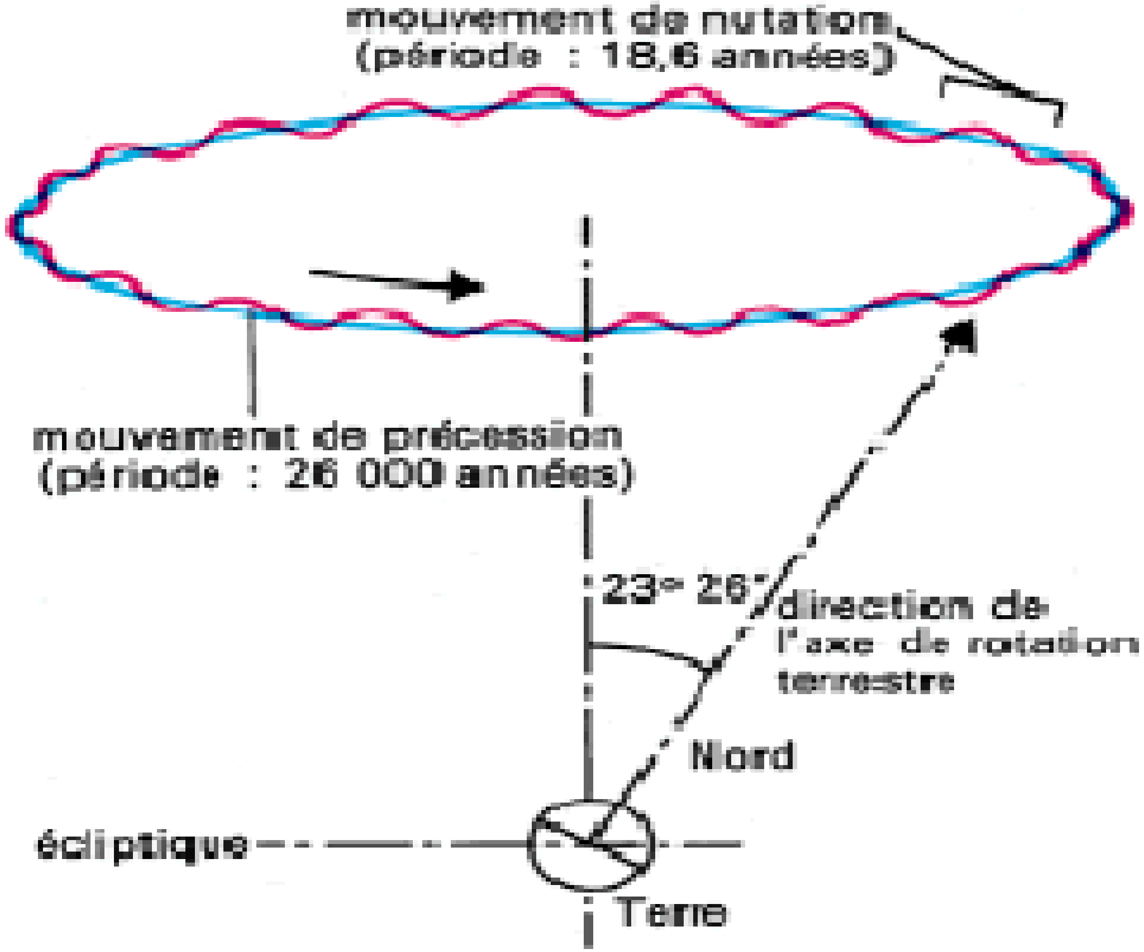

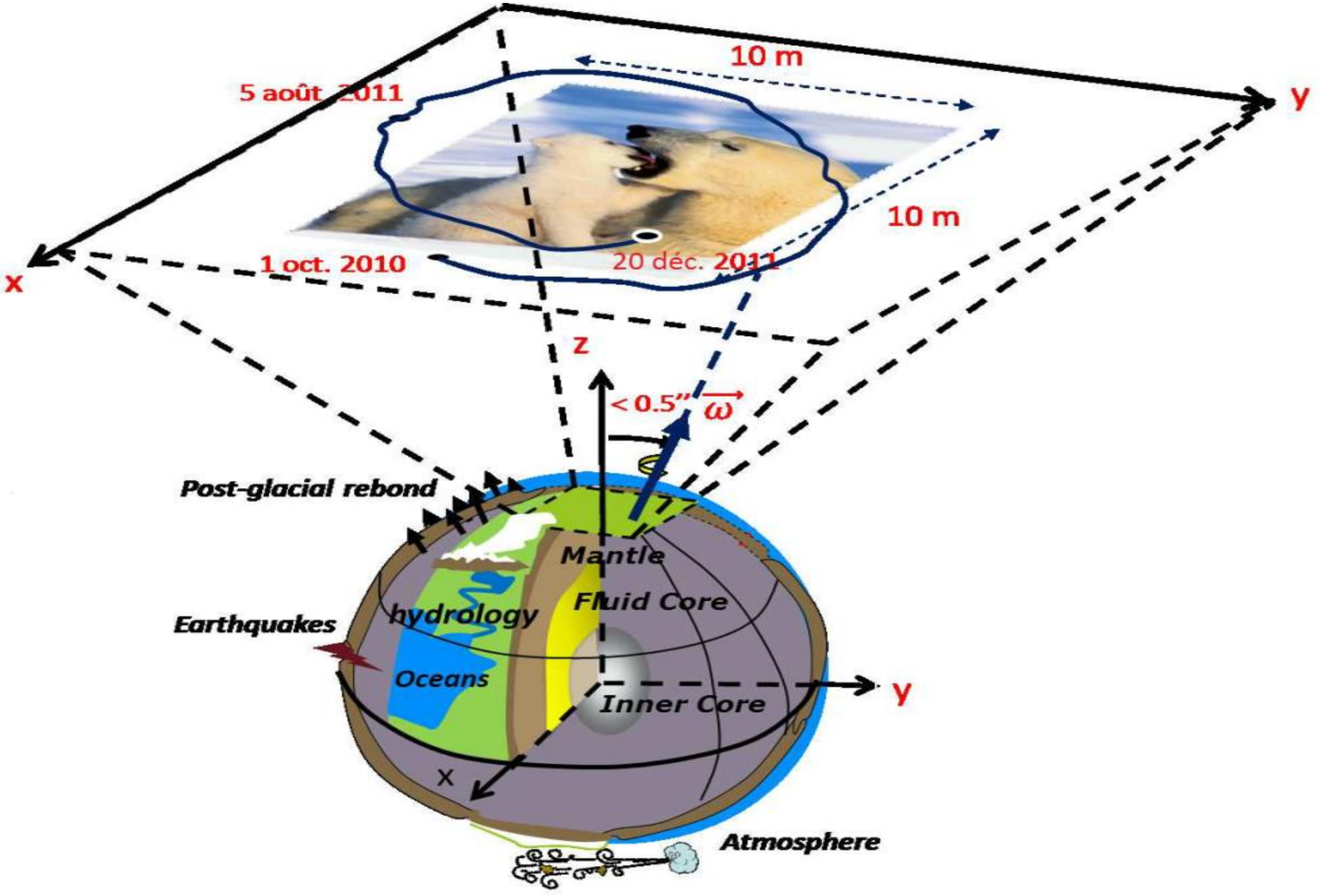

Polar motion with amplitude up to 10 m
Is caused by geophysical processes –
Angular momentum exchange between
ocean, atmosphere, core, and solid Earth

Paleoclimate over 1 million years

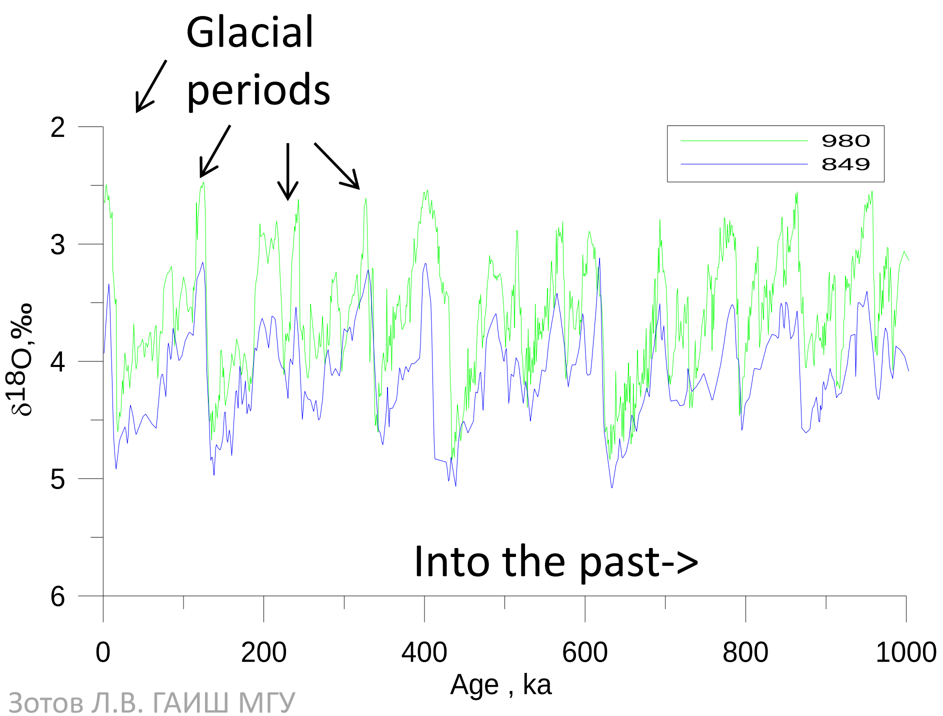

Зотов Л.В. ГАИШ МГУ

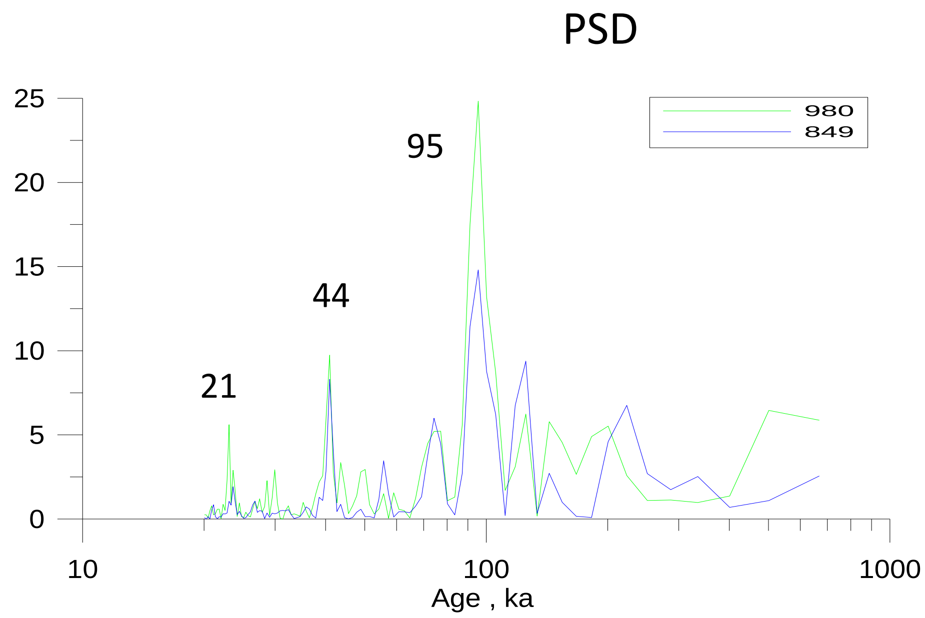

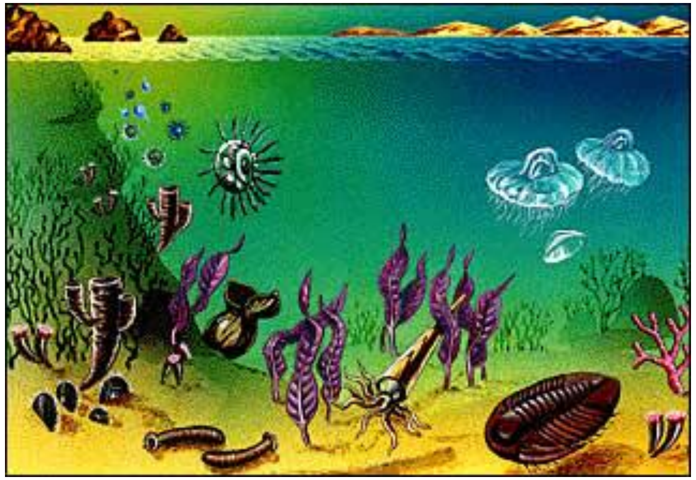

OCEAN DRILLING PROGRAM
SCIENCE OPERATOR

Chandler wobble

Centrifugal potential

$$U_{cf} = -\frac{1}{2}\Omega^2 r^2 \sin^2\theta = -\frac{1}{2}\Omega^2 r^2 + \frac{1}{2}\Omega^2 r^2 \cos^2\theta.$$

Polar tide potential

$$U_{cf} = -\frac{1}{2}\Omega^2(x^2+y^2) + \Omega^2 z(m_1 x + m_2 y).$$

Additional potential expressed through second Love number k_2~0.3

$$U_i = k_2\Omega^2 z(m_1 x + m_2 y).$$

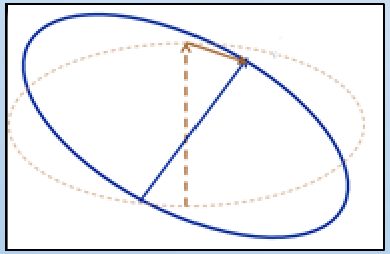

Secular Love number k_s

$$k_s = 3G(C-A)/\Omega^2 R^5 \approxeq 0.94,$$

Substitution gives

$$\Omega\left[A + \frac{k_2}{k_s}(C-A)\right]\dot{m} - i\Omega^2(C-A)\left(1-\frac{k_2}{k_s}\right)m = 0$$

Complex Love number

$$\tilde{k}_2 = k_2^{re} + ik_2^{im} = k_2(1+i\varepsilon),$$

Complex Chandler frequency

$$\sigma_c = \sigma_e \frac{(1-\frac{\tilde{k}_2}{k_s})}{(1+e\frac{\tilde{k}_2}{k_s})} = 2\pi f_c\left(1+\frac{i}{2Q}\right).$$

Earth's axis position

$$\frac{i}{\sigma_c}\dot{m} + m = \frac{\Psi^{pure}}{1-\frac{\tilde{k}_2}{k_s}},$$

Modified Chandler frequency

$$\sigma_c = \Omega\frac{(C-A)(1-k_2/k_s)}{A+(k_2/k_s)(C-A)},$$

$$m = p - i\dot{p}/\Omega$$

Ocean influence on dissipation, polar tide response, modifies eigen frequency, provides excitation

Euler-Liouville equation for polar motion

Geodetic excitation

Geophysical excitation

p(t) – complex polar motion trajectory

$$\frac{i}{\sigma_c}\frac{dp(t)}{dt} + p(t) = \chi^{tot}(t),$$

Excitation is given in form of effective angular momentum functions

$$\chi_e^{mass} = \frac{1+k_2'}{1-\tilde{k}_2/k_s}\chi^{mass}, \qquad \chi_e^{motion} = \frac{1}{1-\tilde{k}_2/k_s}\chi^{motion}.$$

Complex chandler frequency fc=365.25/433 cycles per year period T=433 days

$$\sigma_c = \sigma_e \frac{(1-\frac{\tilde{k}_2}{k_s})}{(1+e\frac{\tilde{k}_2}{k_s})} = 2\pi f_c\left(1+\frac{i}{2Q}\right).$$

Q – quality factor from 60 to 150, we used Q=100

Journal of Geophysical Research: Solid Earth

RESEARCH ARTICLE

10.1002/2014JB011825

Chandler wobble parameters from SLR and GRACE

J. Nastula[1] and R. Gross[2]

[1]Space Research Centre, Polish Academy of Sciences, Warsaw, Poland, [2]Jet Propulsion Laboratory, California Institute of Technology, Pasadena, California, USA

Key Points:
- The period and Q of the Chandler wobble are estimated from SLR and GRACE data
- Atmosphere, ocean, and hydrology models were also used
- Preferred values are the period = 430.9 ± 0.7 days and Q = 127 (56, 255)

Correspondence to:
J. Nastula,
nastula@cbk.waw.pl

Citation:
Nastula, J., and R. Gross (2015), Chandler wobble parameters from SLR and GRACE, *J. Geophys. Res. Solid Earth*, *120*, 4474–4483, doi:10.1002/2014JB011825.

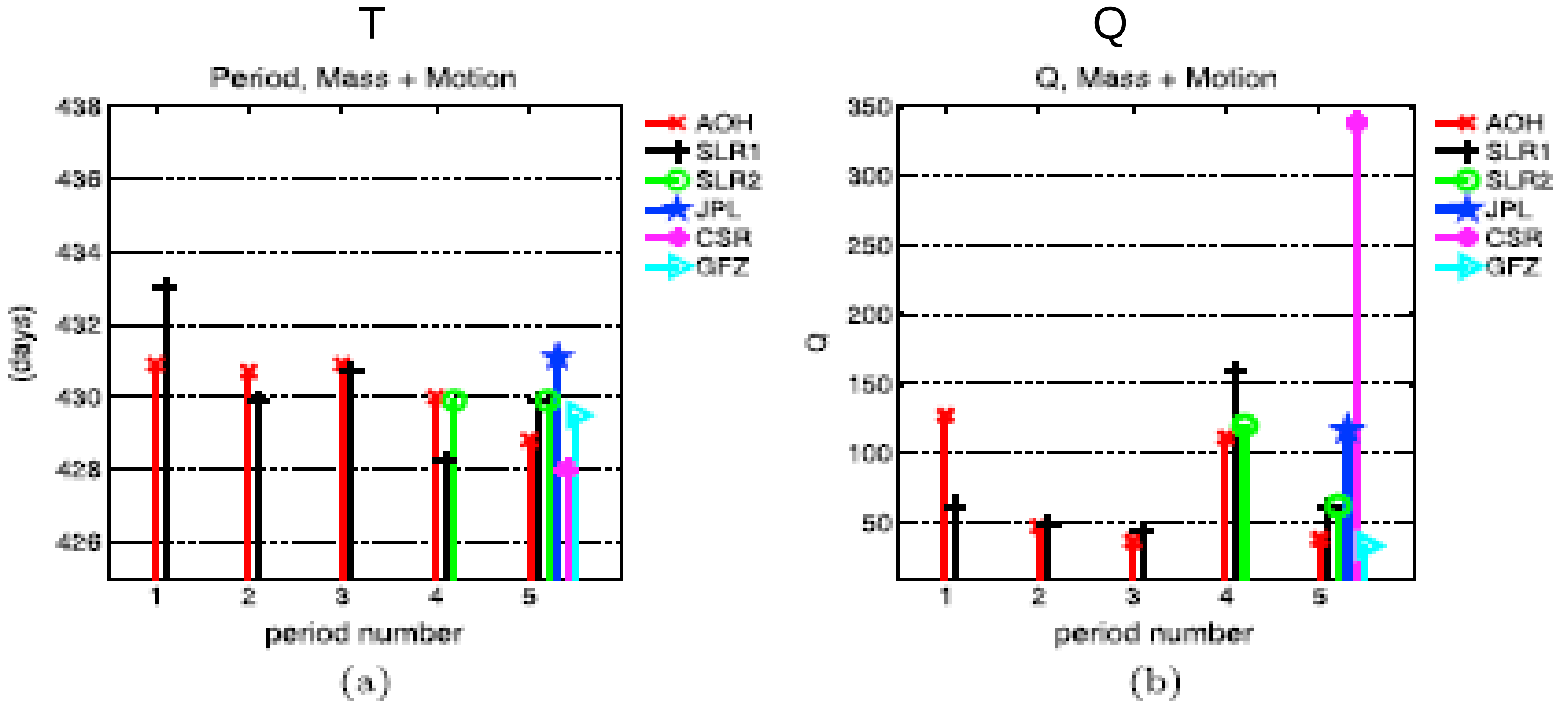

Figure 2. Comparison of estimates of the (a) period and (b) *Q* of the Chandler wobble during the five time intervals: 1, 1985–2010; 2, 1991–2010; 3, 1993–2010; 4, 2001–2010; 5, 2003–2010. Mass and motion terms were included in the excitation functions.

H. Jeffreys

Summary

The international data on the variation of latitude have been analysed in accordance with the idea that the free motion is a damped one maintained by disturbances at irregular intervals of time. The results suggest a free period of 1·202 ± 0·016 years and a time of relaxation of 15·1 ± 1·8 years. There are notable irregularities in the motion, both in the harmonic coefficients and in the means taken over 1·2-year intervals, which occur in both the international and the Greenwich data. If of geophysical origin they imply changes in the products of inertia that are difficult to explain. The damping is too great to be attributed to friction in the sea, but might be due to elastic afterworking in the body of the Earth.

Polar Motion: Historical and Scientific Problems
ASP Conference Series, Vol. 208, 2000
S. Dick, D. McCarthy, and B. Luzum, eds.

Excitation of Polar Motion

Clark R. Wilson

Department of Geological Sciences Center for Space Research and Institute for Geophysics University of Texas Austin, Austin TX 78712 USA

Current studies take advantage of greatly improved understanding and global models of climate related sources of air and water mass redistribution and motion. Mature atmospheric general circulation models are available from a number of sources. Ocean general circulation models are available, though remain relatively immature compared with atmospheric models. Least well-developed are models of the hydrologic cycle, which are required to keep track of water balance over land. There are few fully coupled climate models which track water in all its forms in the atmosphere, oceans, and on land.

Angular momentum – geophysical excitation

Mass term

Motion term

$$\mathbf{H}(t) = \mathbf{H}^{mass}(t) + \mathbf{H}^{motion}(t) = \int \rho(r,t)\mathbf{r} \times [\mathbf{\Omega} \times \mathbf{r} + \mathbf{v}(r,t)]dV.$$

$$\mathbf{H}_x^{mass}(t) = -\Omega \frac{r^4}{g} \int\int p(\phi,\lambda) \sin\phi \cos^2\phi cos\lambda d\phi d\lambda,$$

$$\mathbf{H}_y^{mass}(t) = -\Omega \frac{r^4}{g} \int\int p(\phi,\lambda) \sin\phi \cos^2\phi sin\lambda d\phi d\lambda,$$

$$\mathbf{H}_z^{mass}(t) = \Omega \frac{r^4}{g} \int\int p(\phi,\lambda) \cos^3\phi d\phi d\lambda,$$

$$\mathbf{H}_x^{motion}(t) = \frac{r^3}{g} \int\int\int [\cos\phi \sin\lambda v(r,t) - \sin\phi \cos\phi \cos\lambda u(r,t)] d\phi d\lambda,$$

$$\mathbf{H}_y^{motion}(t) = \frac{r^3}{g} \int\int\int [-\cos\phi \cos\lambda v(r,t) - \sin\phi \cos\phi \sin\lambda u(r,t)] dp d\phi d\lambda,$$

$$\mathbf{H}_z^{motion}(t) = \frac{r^3}{g} \int\int\int \cos^2\phi u(r,t) dp d\phi d\lambda,$$

Effective angular momentum

$$\chi_{x,y}^{motion} = \frac{1.5913}{\Omega(C-A)} \mathbf{H}_{x,y}^{motion}, \qquad \chi_z^{motion} = \frac{0.998}{\Omega C} \mathbf{H}_z^{motion},$$

$$\chi_{x,y}^{mass} = \frac{1.098}{\Omega(C-A)} \mathbf{H}_{x,y}^{mass}, \qquad \chi_z^{mass} = \frac{0.753}{\Omega C} \mathbf{H}_z^{mass}.$$

Oceanic Angular Momentum OAM
input to the polar motion

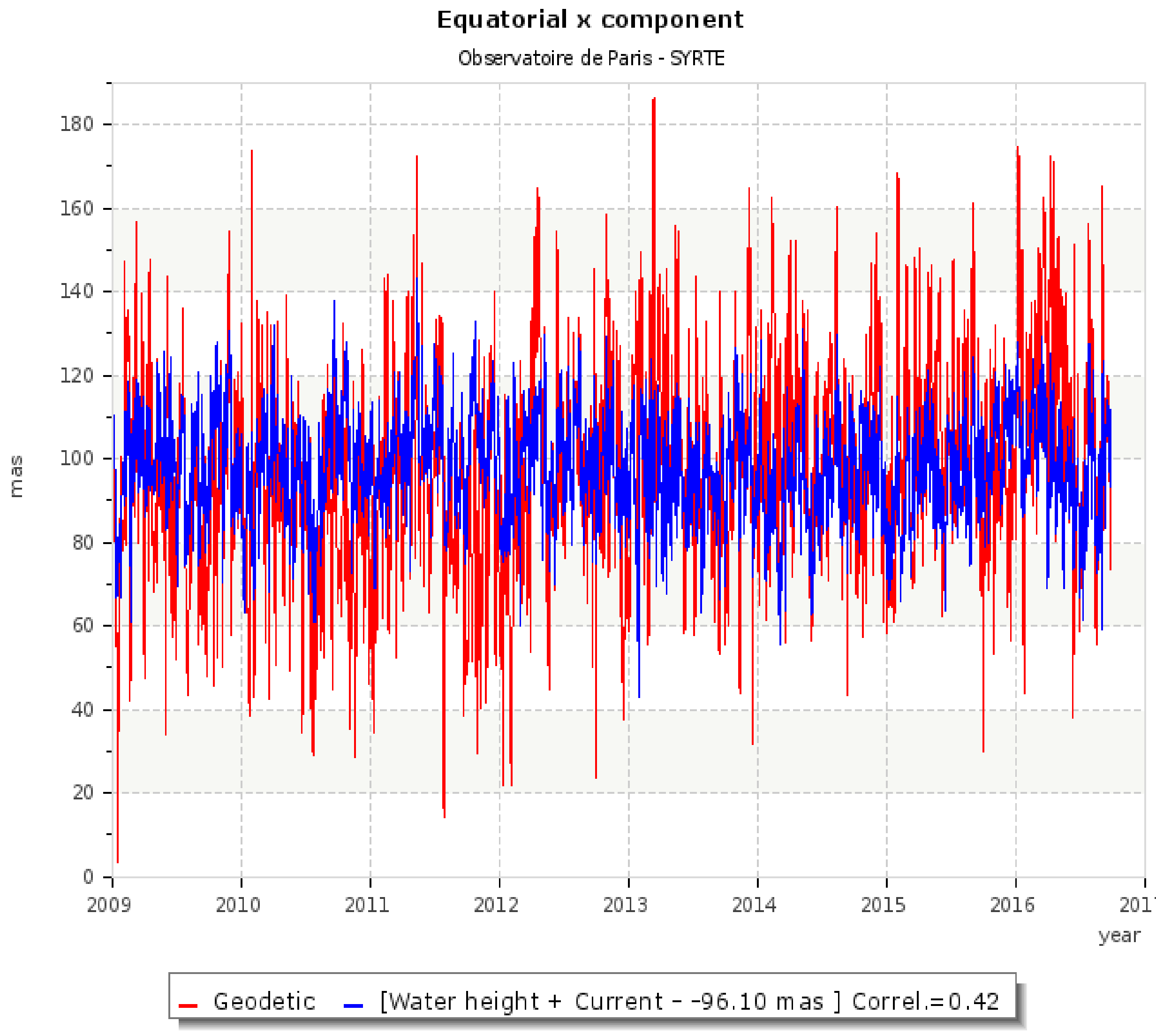

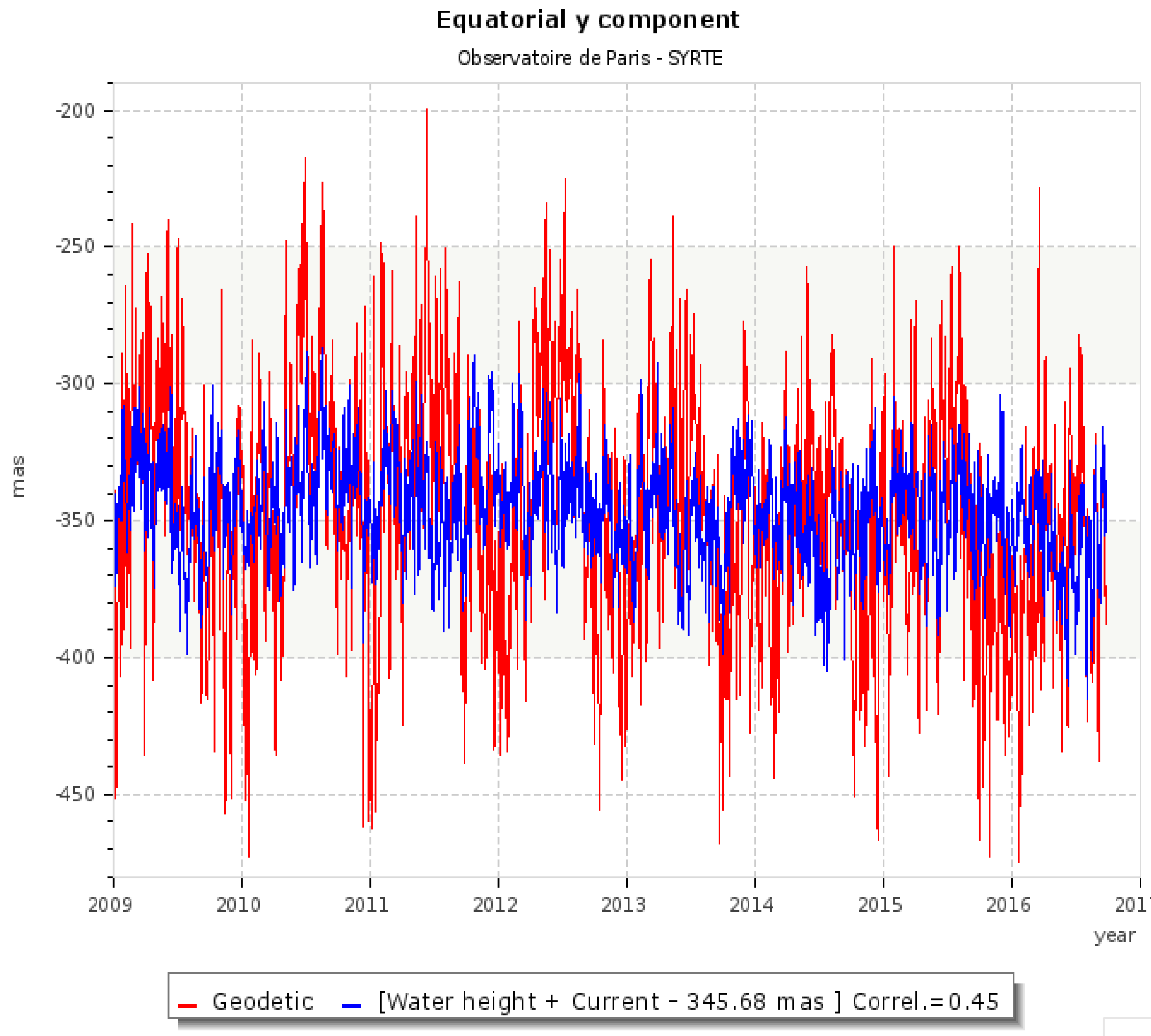

C

Oceanic Angular Momentum OAM + Atmospheric Angular Momentum AAM input to the polar motion

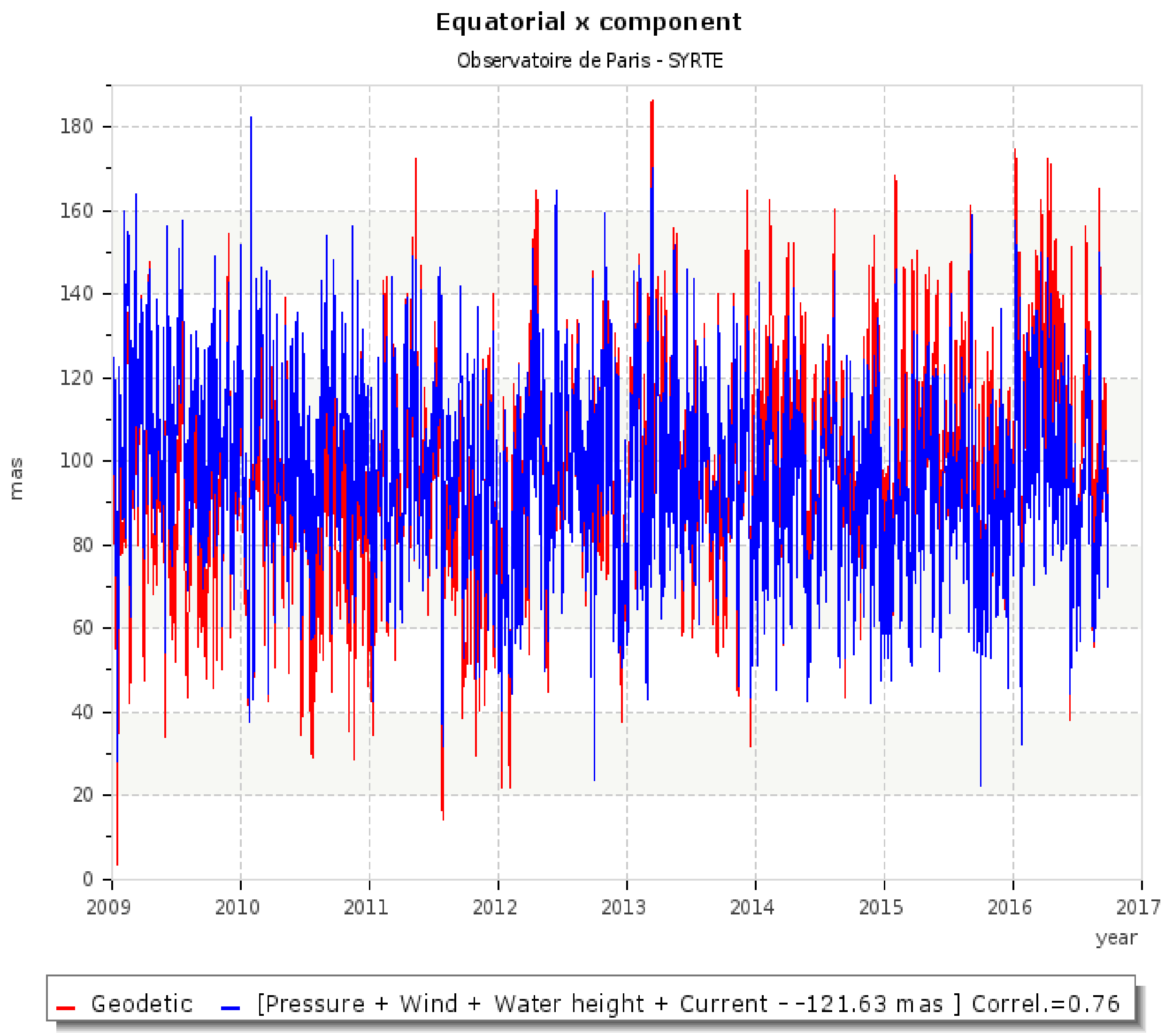

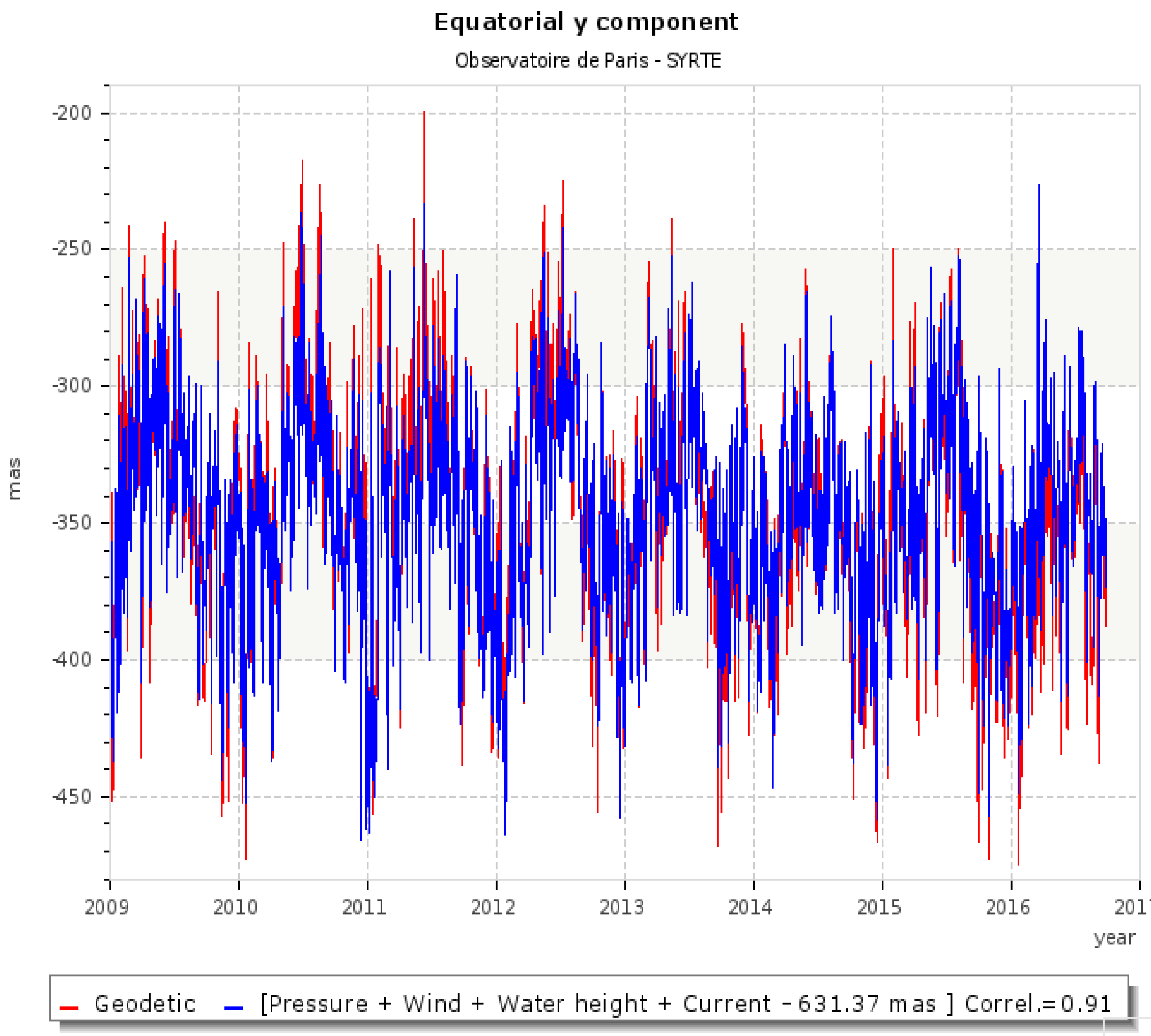

C

Acta Geophysica (2019) 67:17–39
https://doi.org/10.1007/s11600-018-0227-x

RESEARCH ARTICLE - SOLID EARTH SCIENCES

Terrestrial water storage variations and their effect on polar motion

Justyna Śliwińska[1] · Małgorzata Wińska[2] · Jolanta Nastula[1]

Received: 5 July 2018 / Accepted: 17 November 2018 / Published online: 6 December 2018

Analysis of groundwater storage changes in main Polish river basins using GRACE observations, in-situ data, and hydrological and climate models

Jolanta Nastula[1], Justyna Śliwińska[1], Zofia Rzepecka[2], Monika Birylo[2]

EGU 2020 - 13554

Long-term changes of the annual water runoff

River – hydrometric station	$\Delta W_Q/\Delta y$*	The linear trend coefficient, km³/1year	
		1935-2013	1975-2013
Sev.Dvina - Ust-Pinega	+5.3%/+15mm	+0.098	+0.091
Mezen - Malonisogorskaya	-1.7%/-6mm	+0.005	+0.029
Pechora - Ust-Tsilma	+4.6%/+20mm	+0.173	+0.184
Ob - Salekhard	-0.4%/-0.7mm	+0.089	-0.089
Yenisey - Igarka	+5.4%/+13mm	+0.696	+0.922
Olenek - Sukhana	+12.2%/+21mm	+0.066	+0.113
Lena - Kyusyur	+7.4%/+16mm	+1.080	+2.214
Yana – Jiangky/Yubileynaya	*+12.8%/+18mm*	-	-
Kolyma - Srednekolymsk	+4.6%/+9mm	+0.081	+0.451

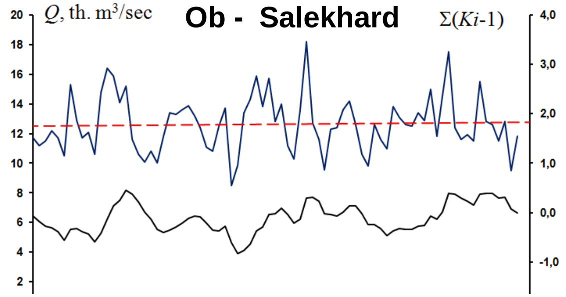

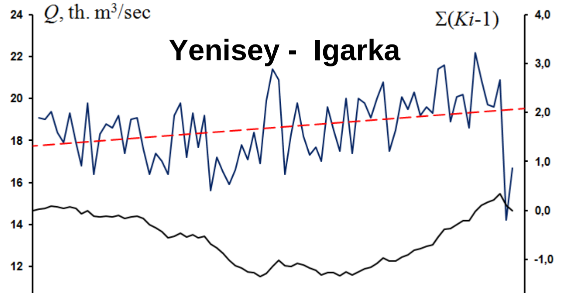

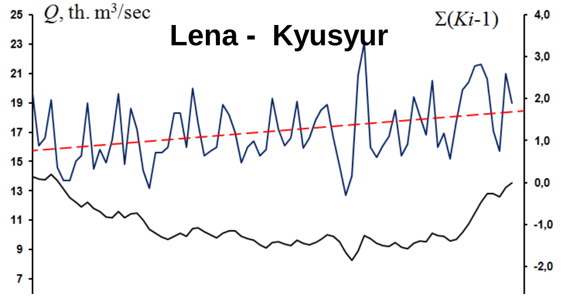

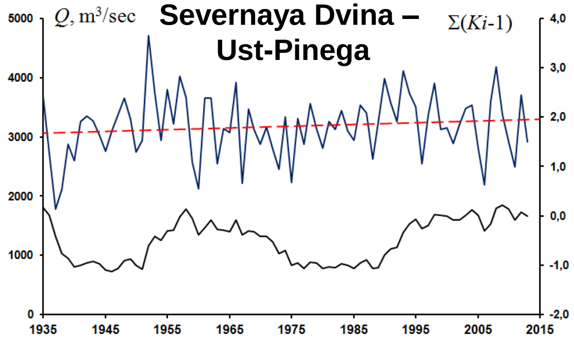

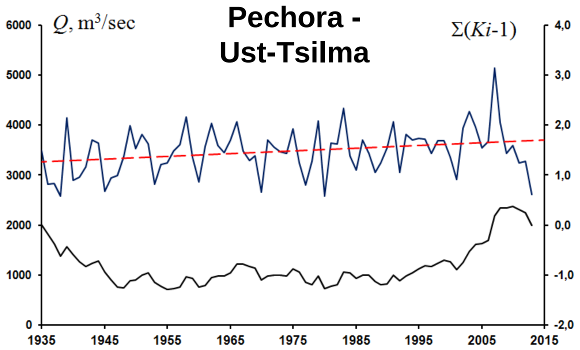

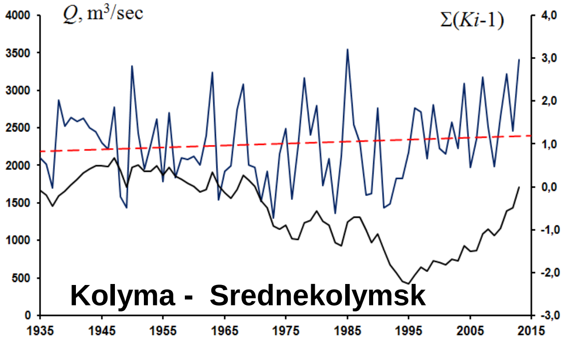

Credit:
N. Frolova

Geophysical processes influencing Earth rotation

from 1 to 1 000 000 years

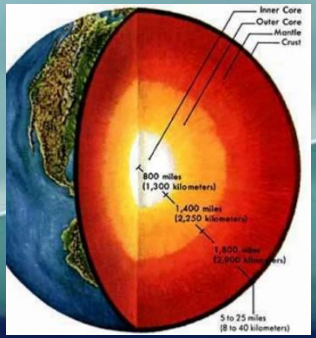

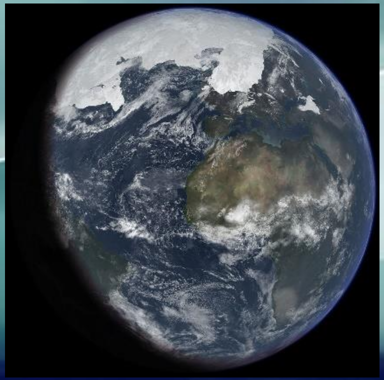

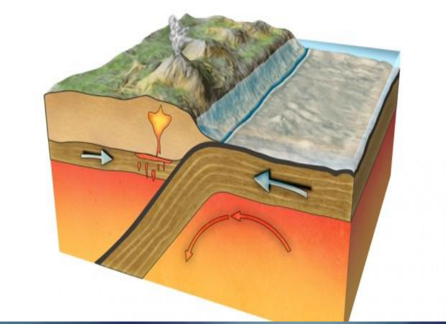

Well-modelled

Luni-solar tides

12 h 1 day 365 days 10 years 10^2 years 10^3 years 10^4 years 10^5 years 10^6

atmosphere ocean

glaciations

Hydrological effects and climate influences

Core-mantle coupling

Tectonics

credit: C. Bizouard

Motion of the Earth's pole

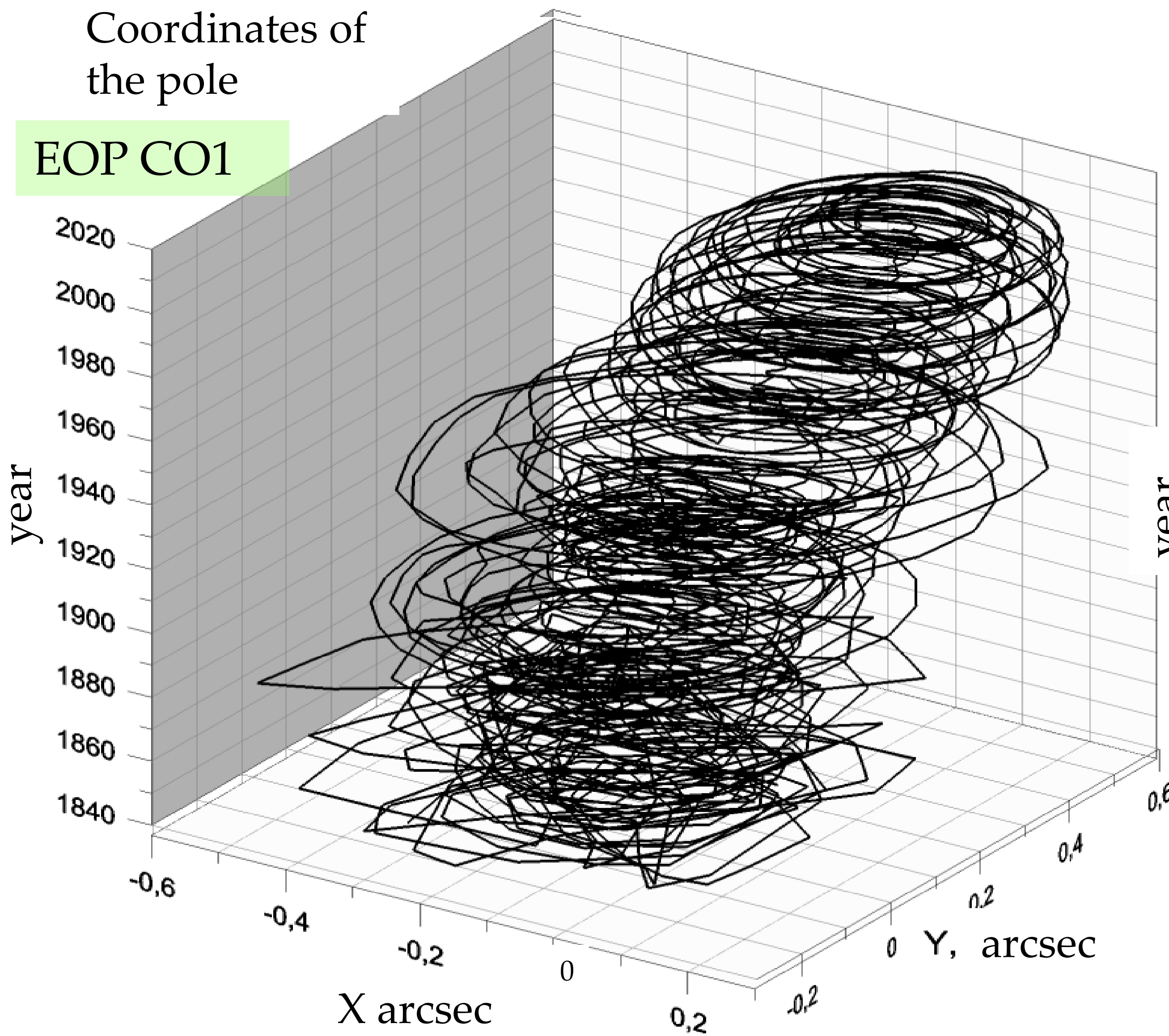

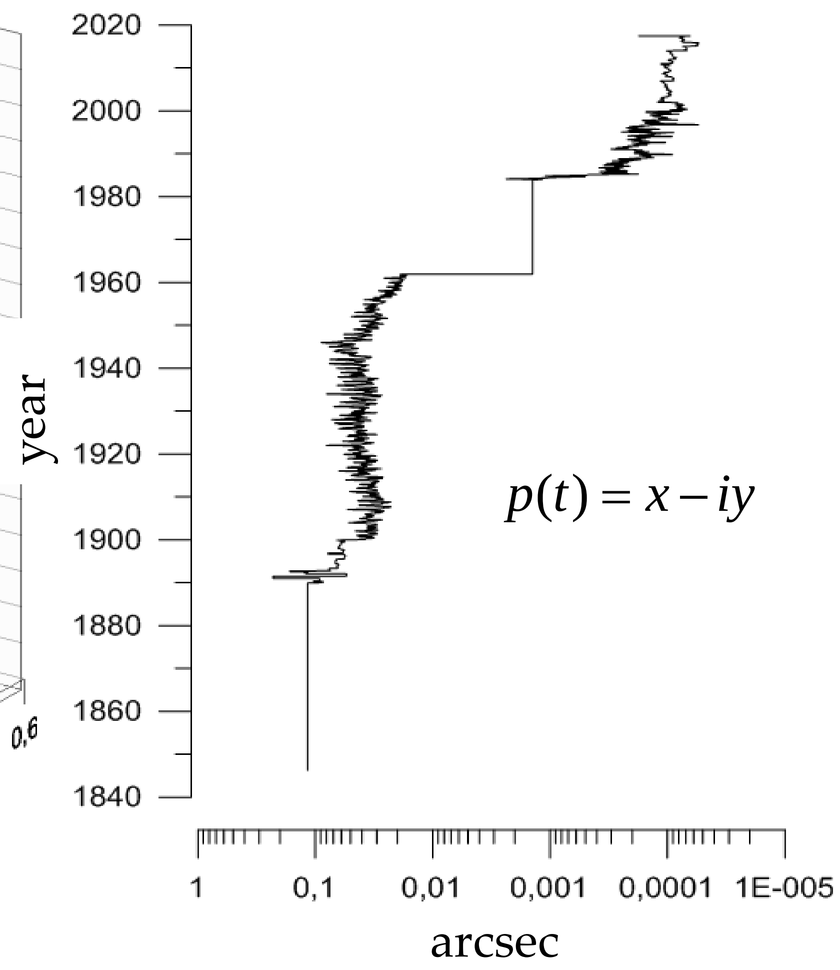

$p(t) = x - iy$

Trends in the polar motion and postglacial rebound

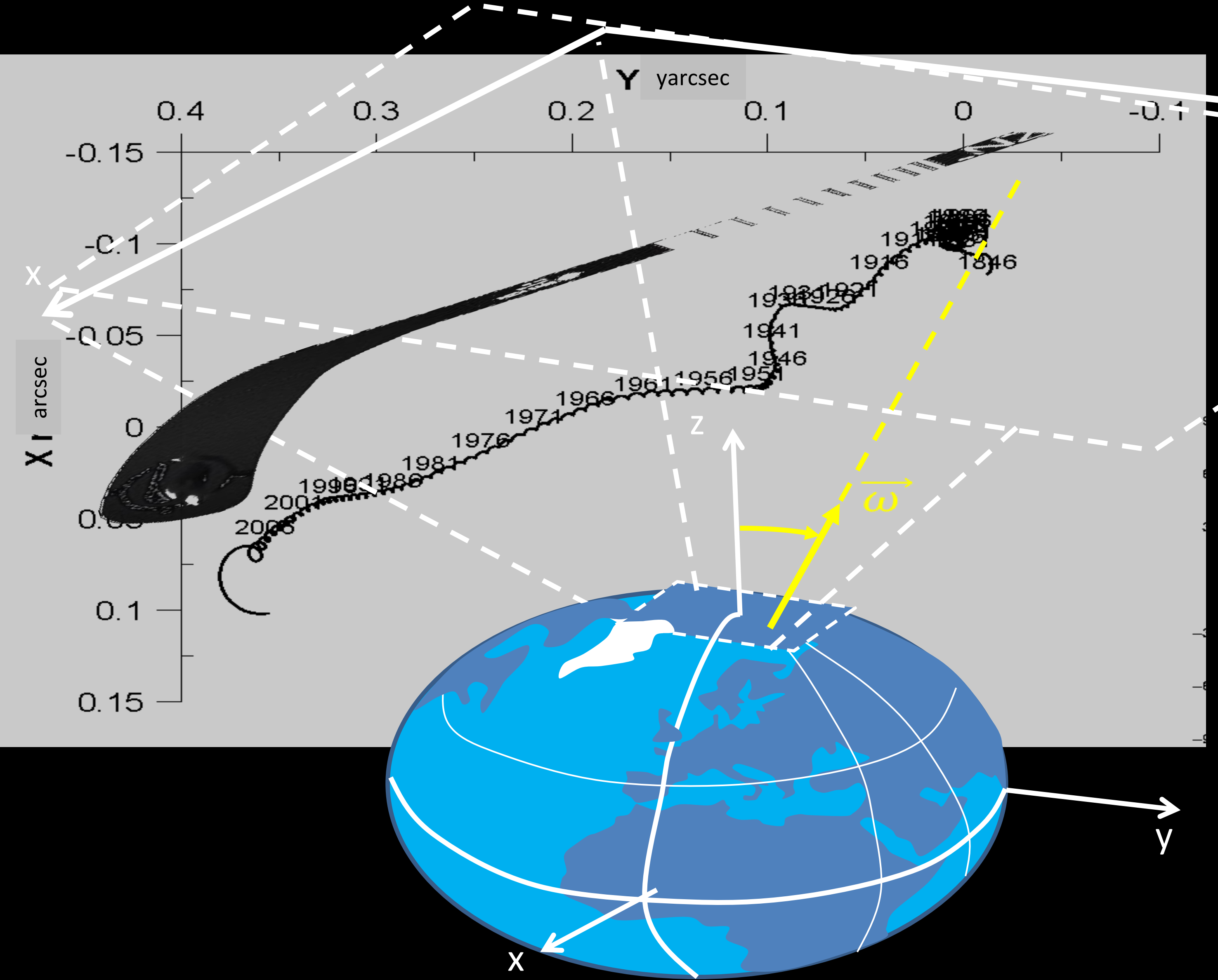

Glacial isostatic adjustment
(Paulson et al. 2007)

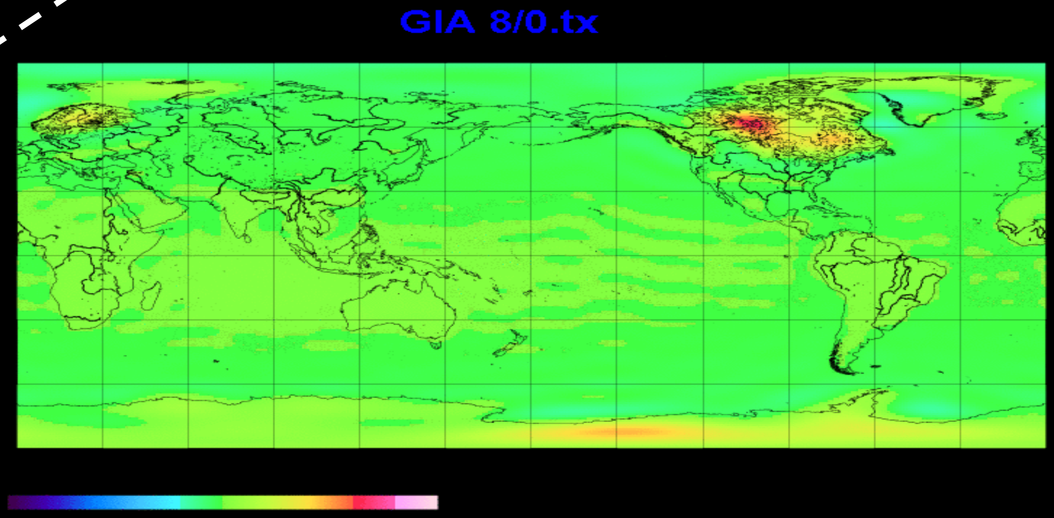

CLIMATOLOGY

Climate-driven polar motion: 2003–2015

Surendra Adhikari* and Erik R. Ivins

10.1126/sciadv.1501693

Earth's spin axis has been wandering along the Greenwich meridian since about 2000, representing a 75° eastward shift from its long-term drift direction. The past 115 years have seen unequivocal evidence for a quasi-decadal periodicity, and these motions persist throughout the recent record of pole position, in spite of the new drift direction. We analyze space geodetic and satellite gravimetric data for the period 2003–2015 to show that all of the main features of polar motion are explained by global-scale continent-ocean mass transport. The changes in terrestrial water storage (TWS) and global cryosphere together explain nearly the entire amplitude (83 ± 23%) and mean directional shift (within 5.9° ± 7.6°) of the observed motion. We also find that the TWS variability fully explains the decadal-like changes in polar motion observed during the study period, thus offering a clue to resolving the long-standing quest for determining the origins of decadal oscillations. This newly discovered link between polar motion and global-scale TWS variability has broad implications for the study of past and future climate.

Adhikari, Ivins, *Climate driven polar motion: 2003-2015*, Sci. Adv., Vol. 2, No. 4, p. e1501693, 2016, doi:10.1126/sciadv.1501693

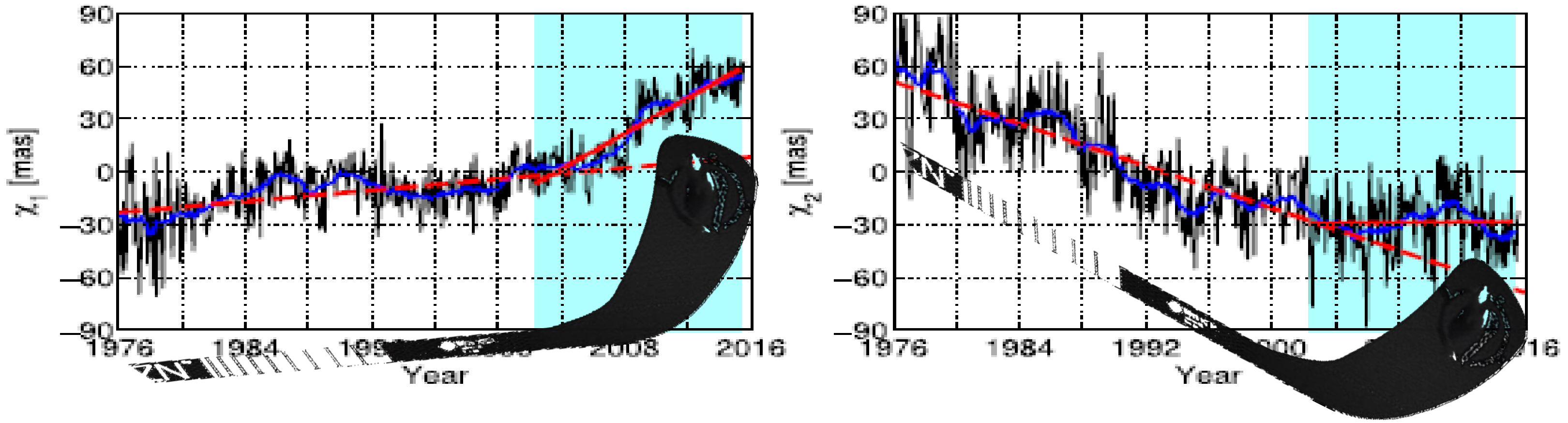

Fig. 1. Observed pole position data. Mean monthly polar motion excitations (black lines) derived from the observed daily values after removing semi-annual, annual, and Chandler wobbles. Smoothed solutions (blue lines) reveal quasi-decadal variability in the corresponding component of the 20th-century linear trend (dashed red lines). Cyan shadows in the background cover our study period, over which the drift direction deviates (solid red lines) from the long-term linear trend.

EGU2018-10300 | Orals | G3.1/CL4.20/CR8.6/GD11.6/GM11.10/NH11.17 | | **Highlight**

Toward a Unified Theory for 20th Century Secular Polar Motion

Erik Ivins, Surendra Adhikari, Lambert Caron, Bernhard Steinberger, John Reager, Kristian Kjeldsen, Ben Marzeion, and Eric Larour

Wed, 11 Apr, 11:45–12:00, Room -2.32

Agreement between C_{21} S_{21} from SLR and GRACE with PM trends

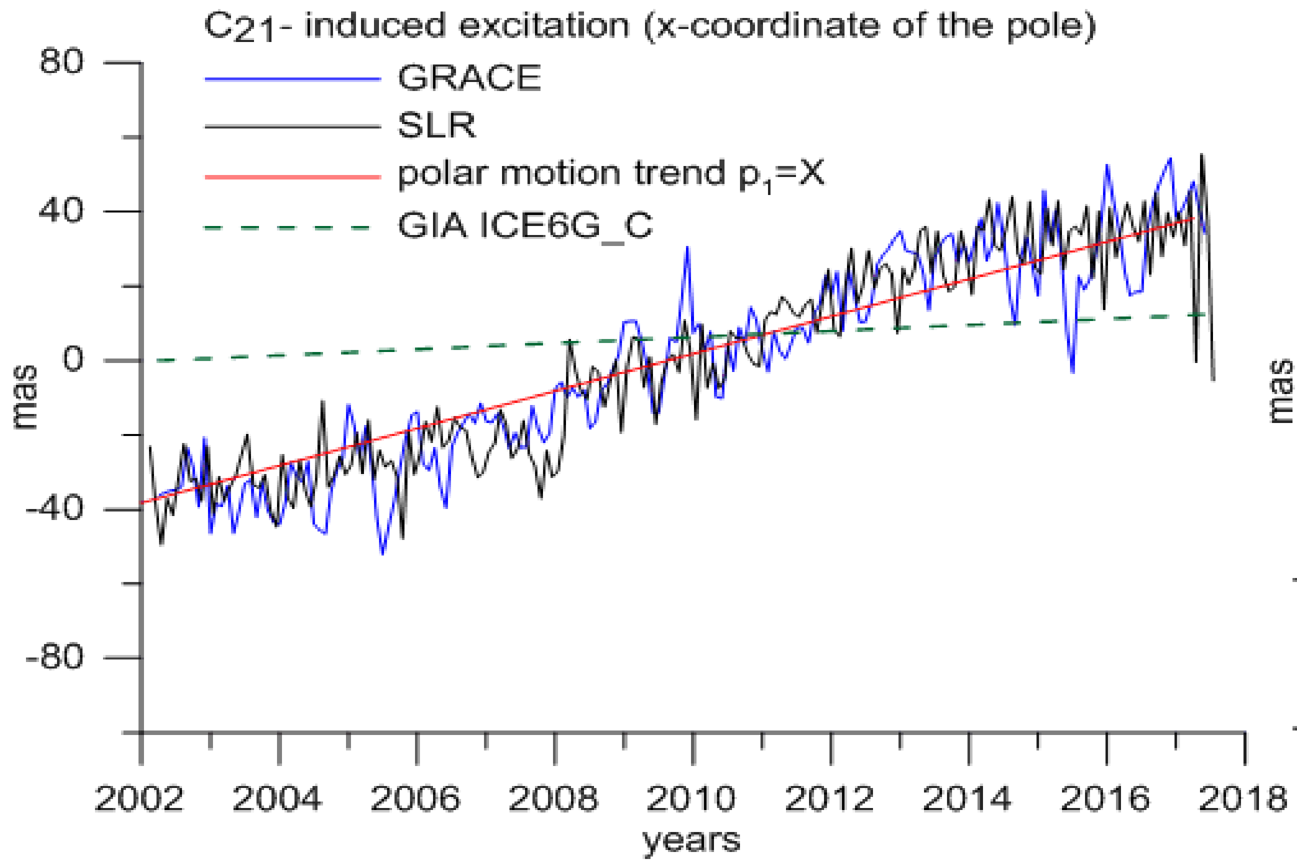

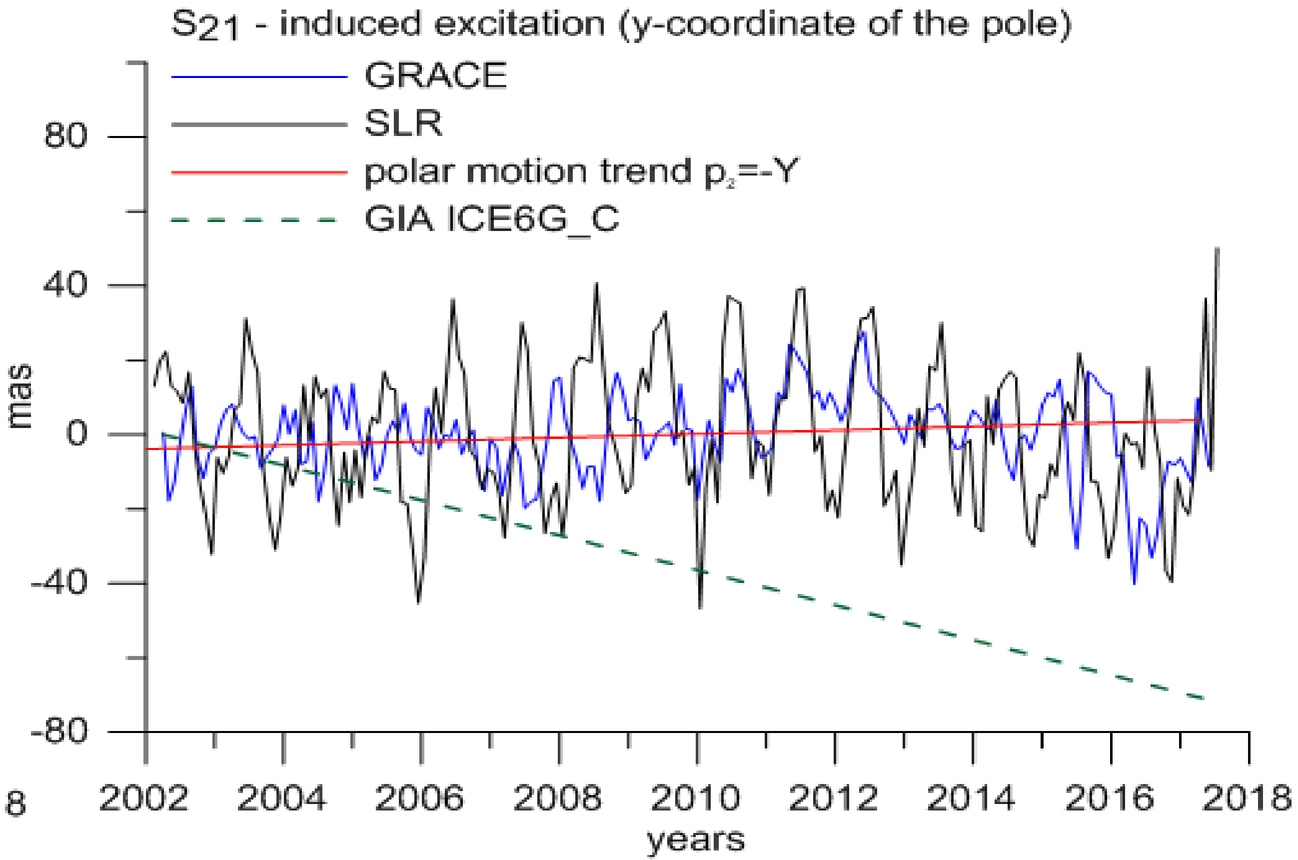

We can conclude: climatological mass redistribution is responsible for polar motion drift.

April 18, 2016 C.K. Shum wrote to Leonid: it looks like Erik and Surendra had stole your thunder and the idea that we discussed in Moscow in the train to/from St. Petersburg!

Leonid Zotov, Christian Bizouard, C.K. Shum, Vera Zinovieva, Analysis of the Second Degree Stokes Coefficients of Geopotential and Earth Rotation Trends, AIP proceedings & EGU-2018

GEODESY AND GEODYNAMICS 2016, VOL X NO X, 1–7

Available online at www.sciencedirect.com

ScienceDirect

journal homepage: www.keaipublishing.com/en/journals/geog;
http://www.jgg09.com/jweb_ddcl_en/EN/volumn/home.shtml

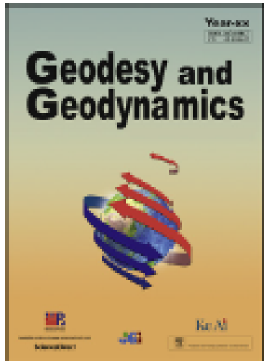

A possible interrelation between Earth rotation and climatic variability at decadal time-scale

Leonid Zotov[a,b,*], C. Bizouard[c], C.K. Shum[d,e]

[a] National Research University Higher School of Economics, Moscow Institute of Electronics and Mathematics, Moscow, Russia

[b] Lomonosov Moscow State University, Sternberg Astronomical Institute, Moscow, Russia

[c] SYRTE, Observatoire de Paris, PSL Research University, CNRS, Sorbonne Universités, UPMC Univ. Paris 06, 61 avenue de l'Observatoire, 75014 Paris, France

[d] Division of Geodetic Science, School of Earth Sciences, The Ohio State University, USA

[e] State Key Laboratory of Geodesy and Earth's Dynamics, Institute of Geodesy & Geophysics, Chinese Academy of Sciences, Wuhan, China

Global mean temperature and sea level rise

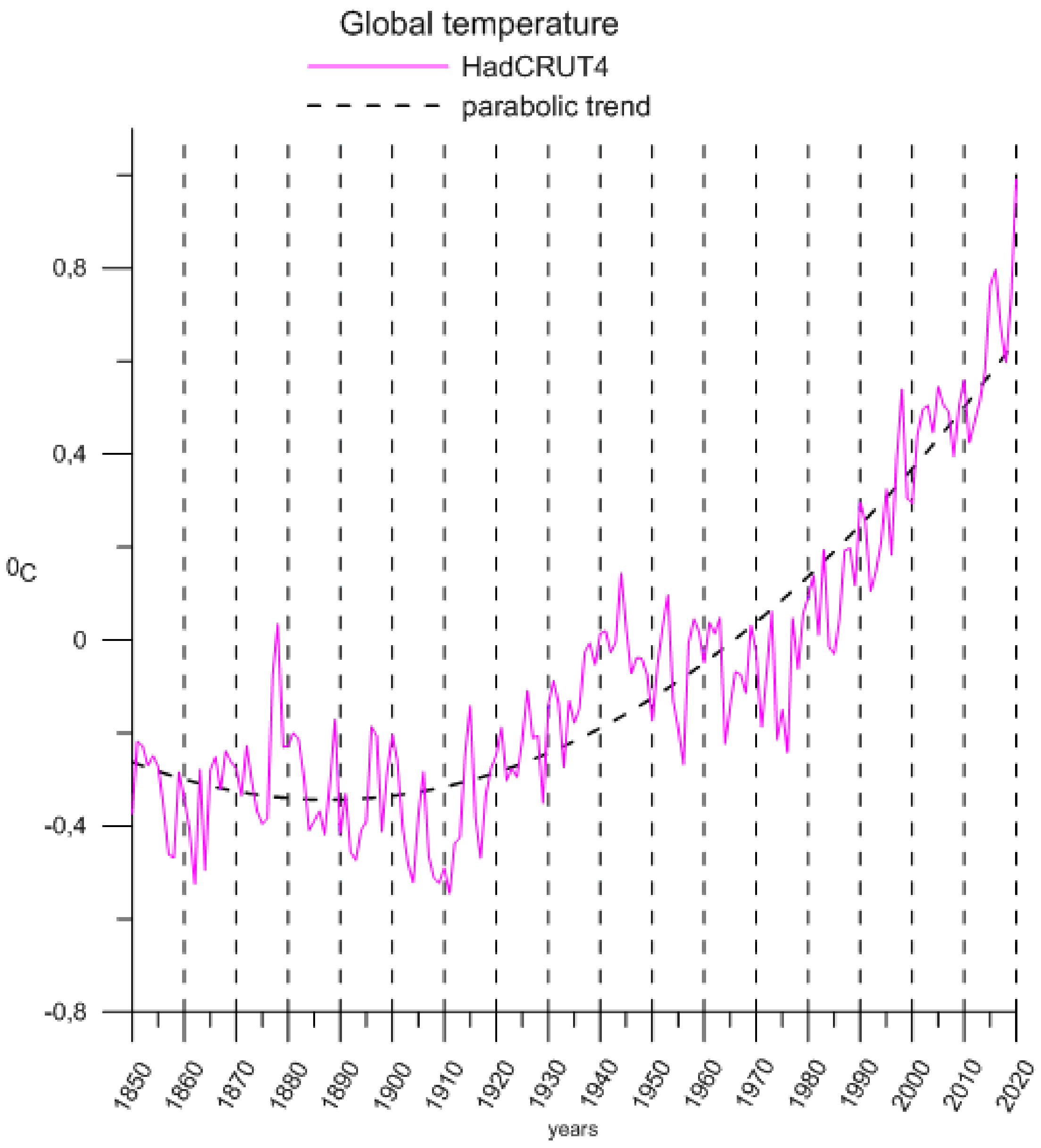

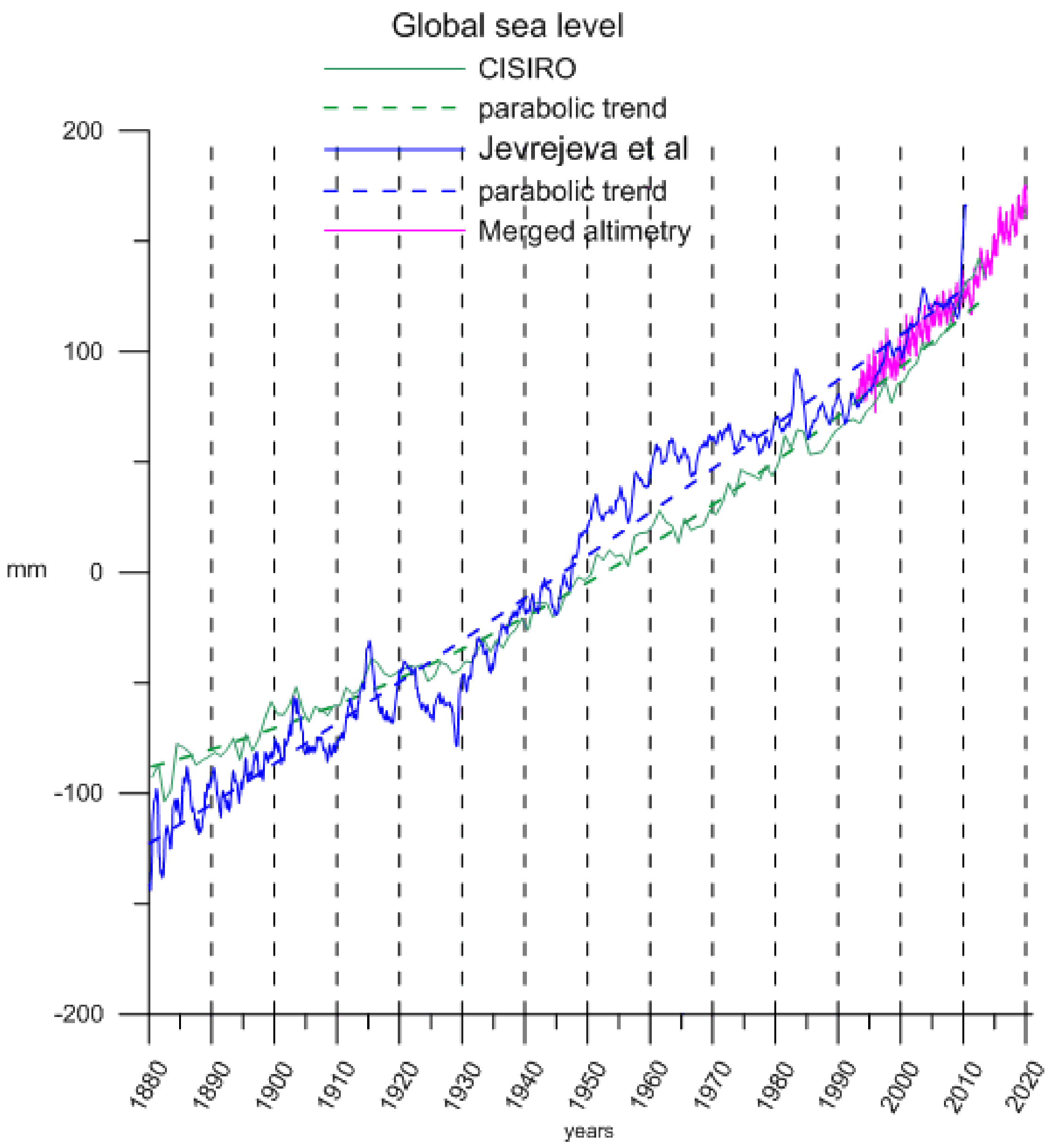

L.V.Zotov, SAI MSU

Global temperature and sea level changes

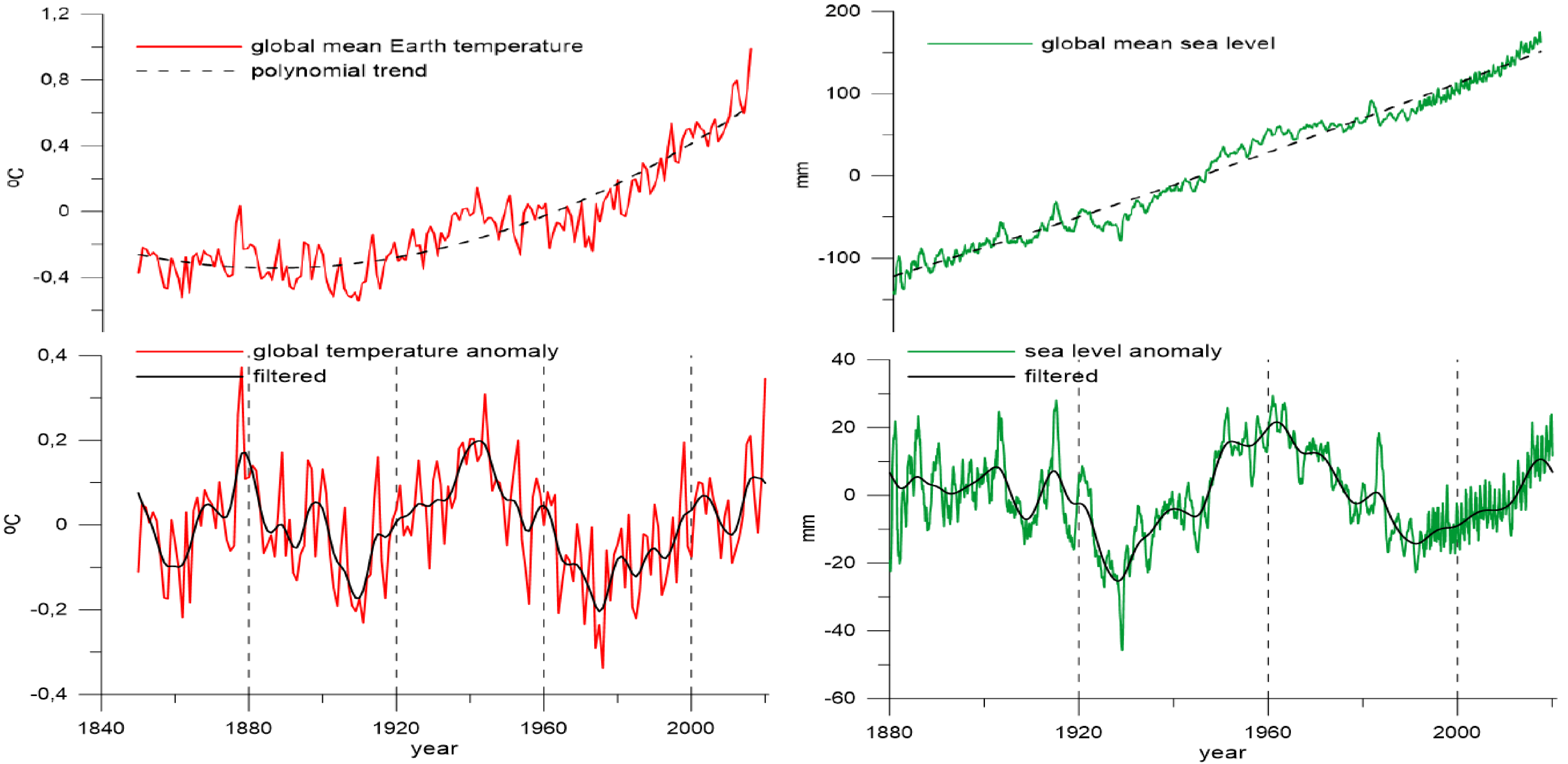

L. Zotov at all. Multidecadal and 6-year variations of LOD, IOP, 2020 in press

Cross-spectrum of Sea Level and temperature T

$FFT\{Cov(SL,T)\}$

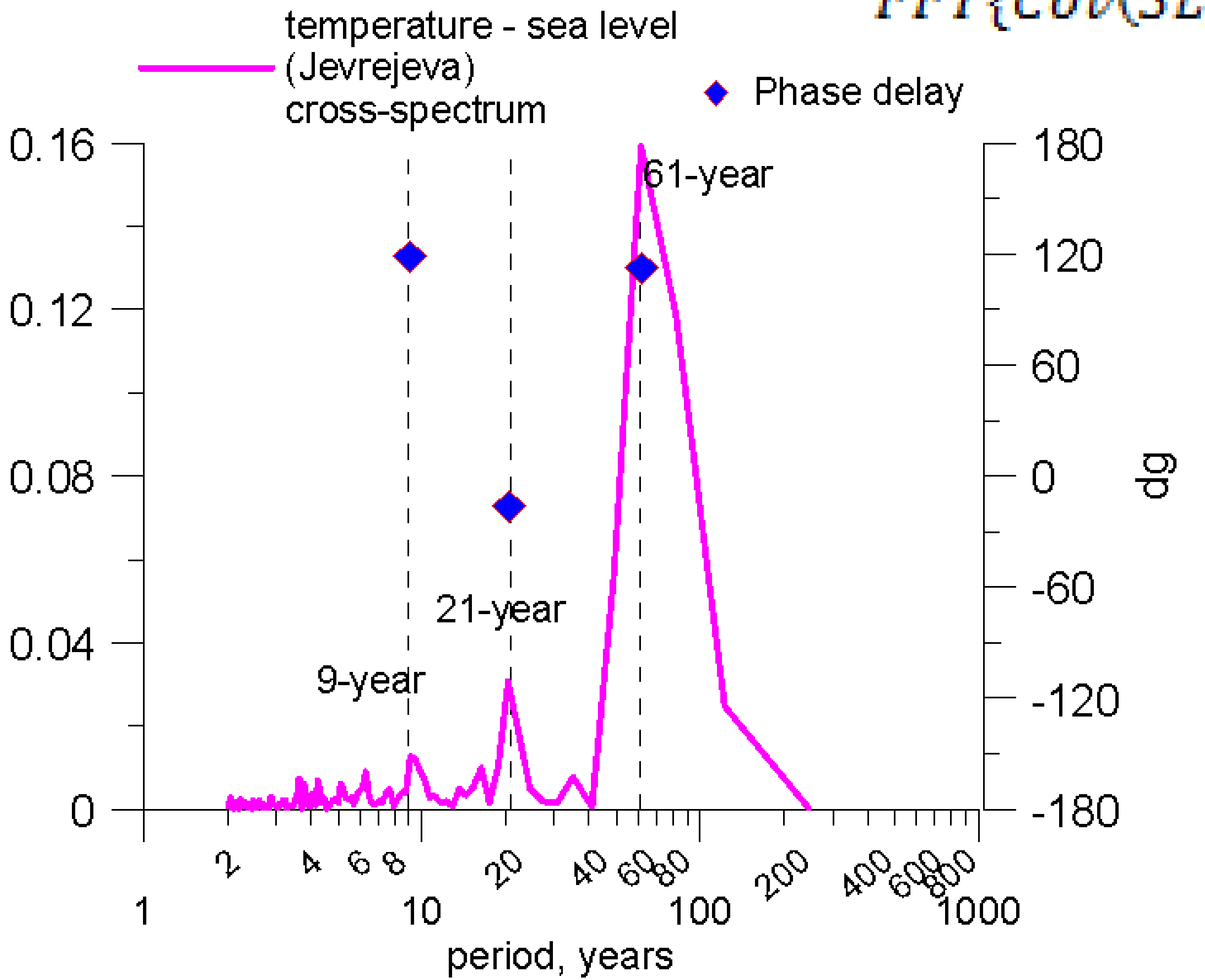

60- 20- 10-year variations of the Global temperature and Sea level, Extracted by MSSA

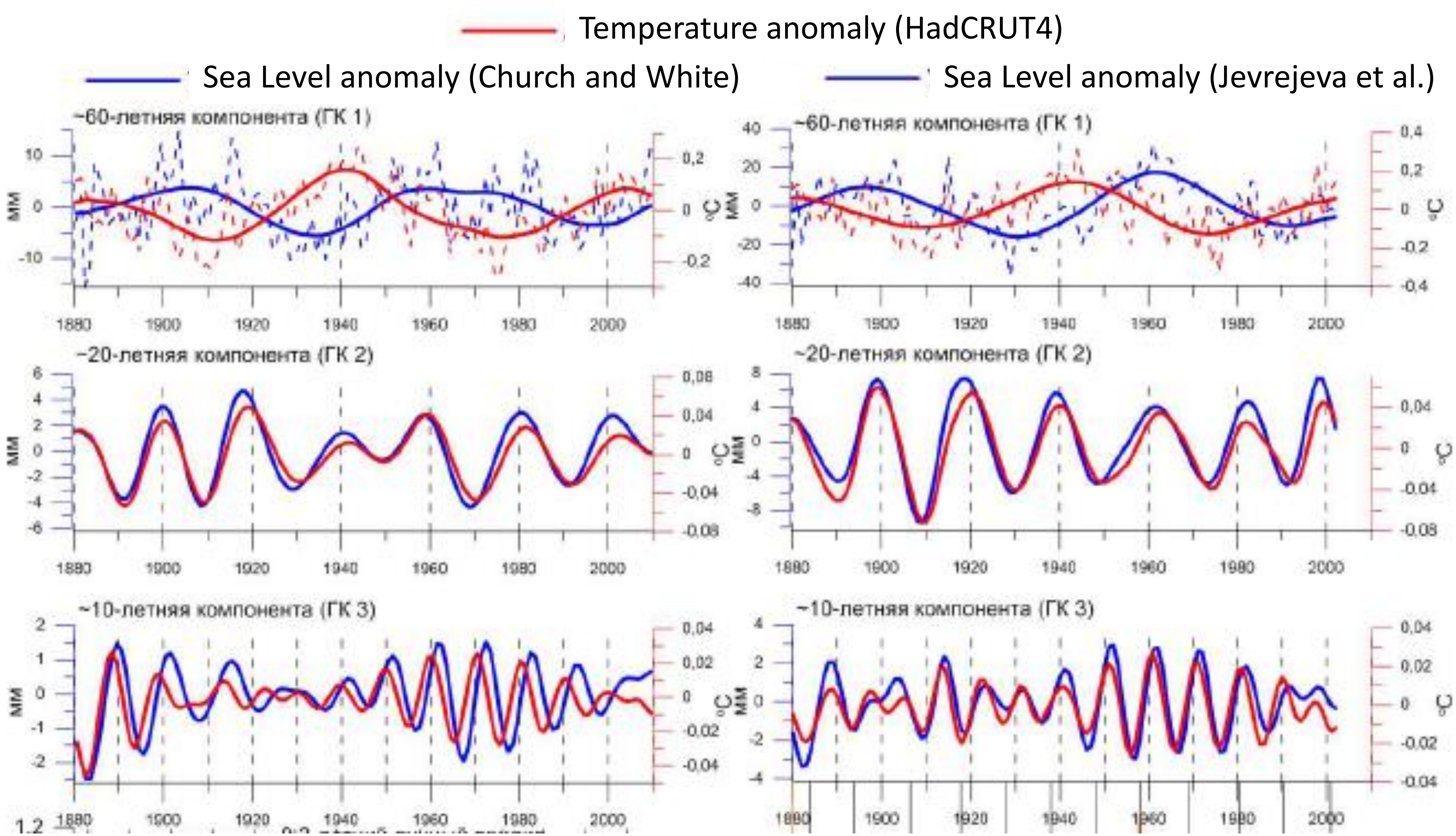

EGU2020-4643

An 8-year cycle in the rate of the global mean sea level

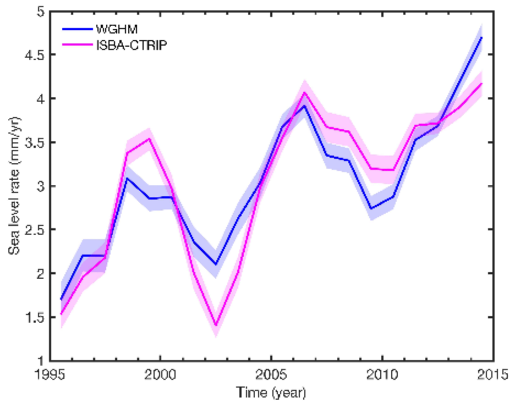

- $GMSL_{LT}$ shows a clear 8-year cycle superimposed on an increasing trend

Research question:

- What is the origin of the 8-year cycle?

Anny Cazenave

EGU2020: Sharing Geoscience Online

EGU G3.2 Session, 6th May 2020

L. Moreira, H. B. Dieng, A. Cazenave, H. Palanisamy, F. Paul, D. Cáceres and B. Decharme

International Space Science Institute (ISSI), Bern, Switzerland

Climate Change Attribution Using Empirical Decomposition of Climatic Data

Craig Loehle[1] and Nicola Scafetta[*,2]

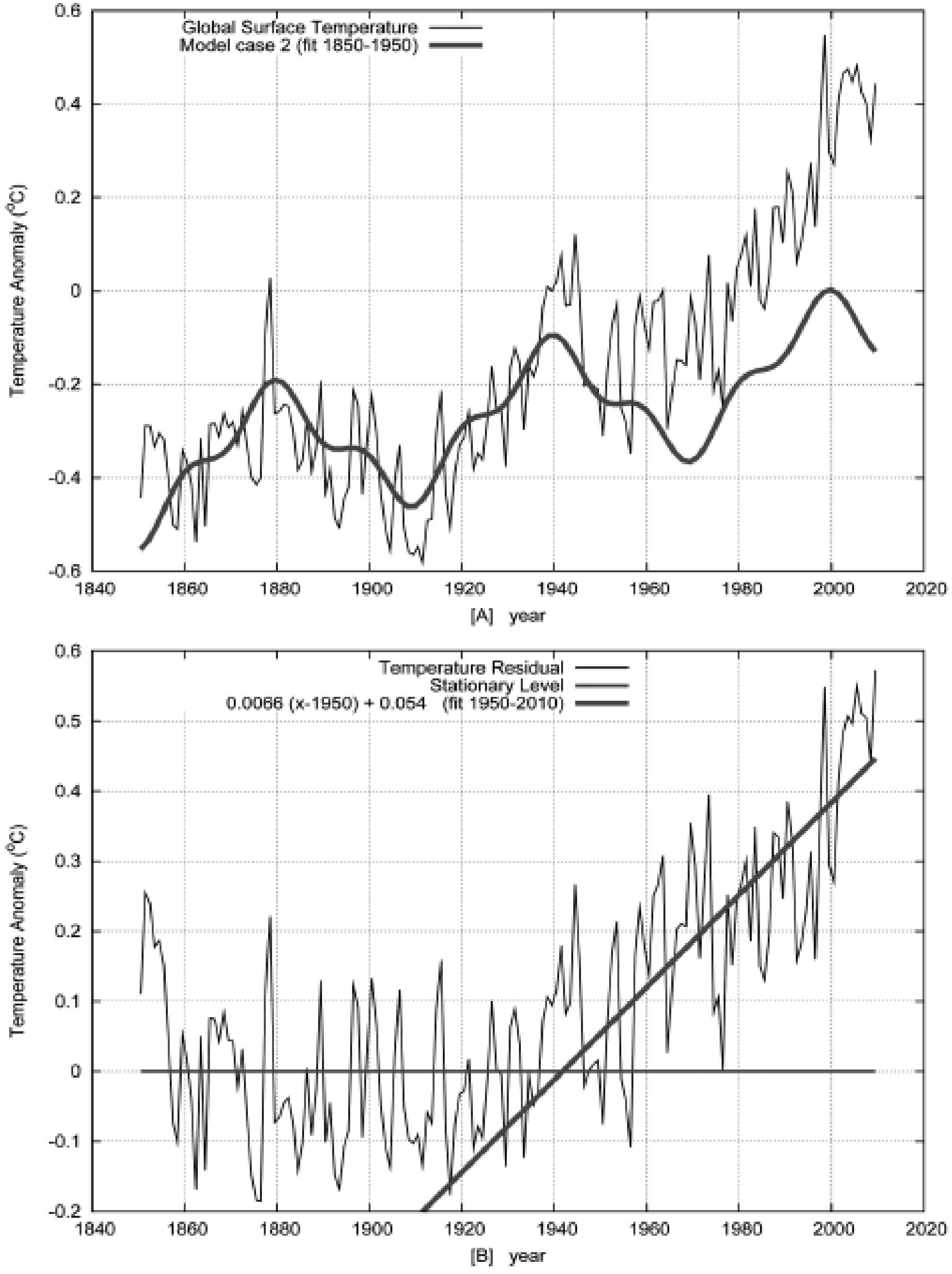

ig. (2). A) As in Fig. (1A), with model fit to pre-1950 data. B) Residuals. Before about 1950 residuals are stationary around the zero level .fter about 1942 there is a clear upward linear trend which may be associated to anthropogenic warming.

A Semi-Empirical Approach to Projecting Future Sea-Level Rise

Stefan Rahmstorf

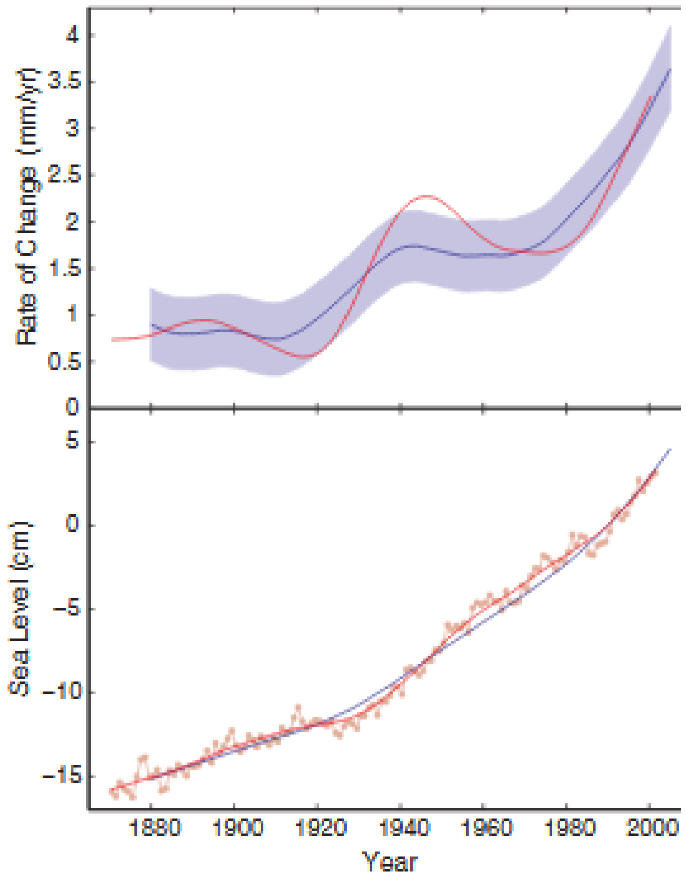

Fig. 3. (**Top**) Rate of sea-level rise obtained fro tide gauge observations (red line, smoothed a described in the Fig. 2 legend) and compute from global mean temperature from Eq. 1 (dar blue line). The light blue band indicates th statistical error (one SD) of the simple linea prediction (*15*). (**Bottom**) Sea level relative t 1990 obtained from observations (red line smoothed as described in the Fig. 2 legend) an computed from global mean temperature fro Eq. 2 (blue line). The red squares mark th unsmoothed, annual sea-level data.

Atlantic multidecadal oscillation AMO
as a cause of 60-year global temperature changes

MSSA L=22 years, parabolic trend removed

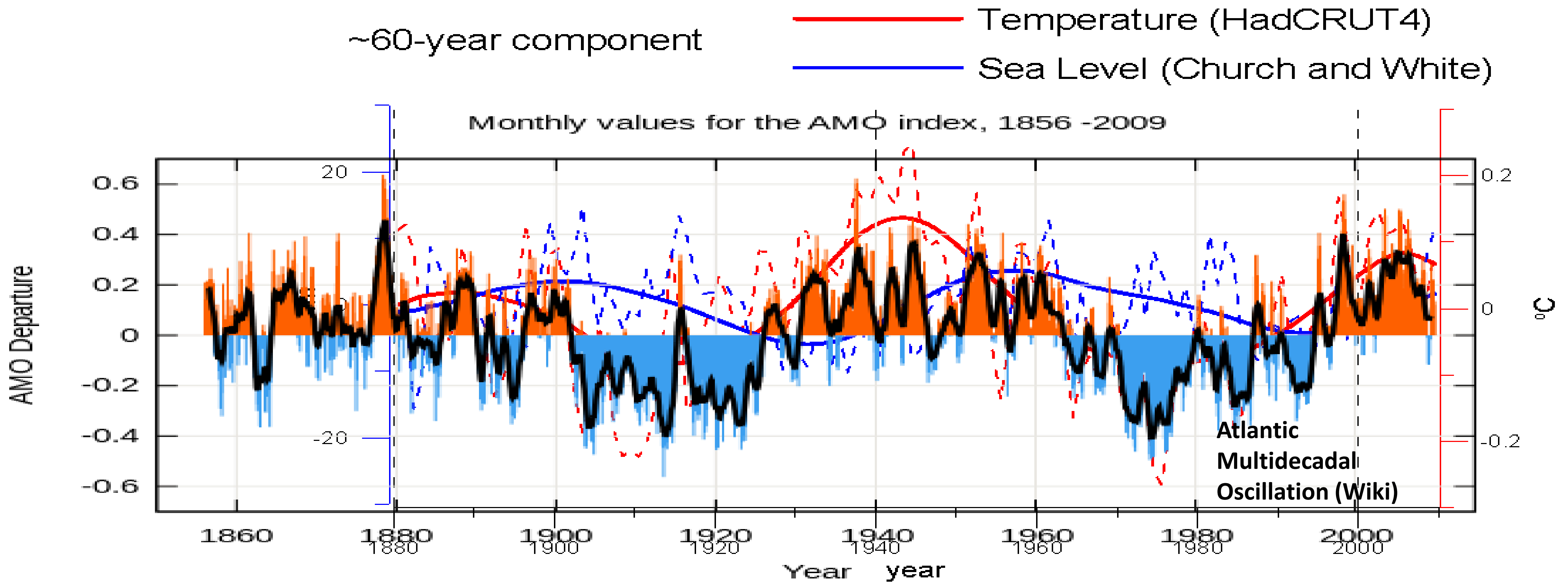

Atlantic Multidecadal Oscillation AMO

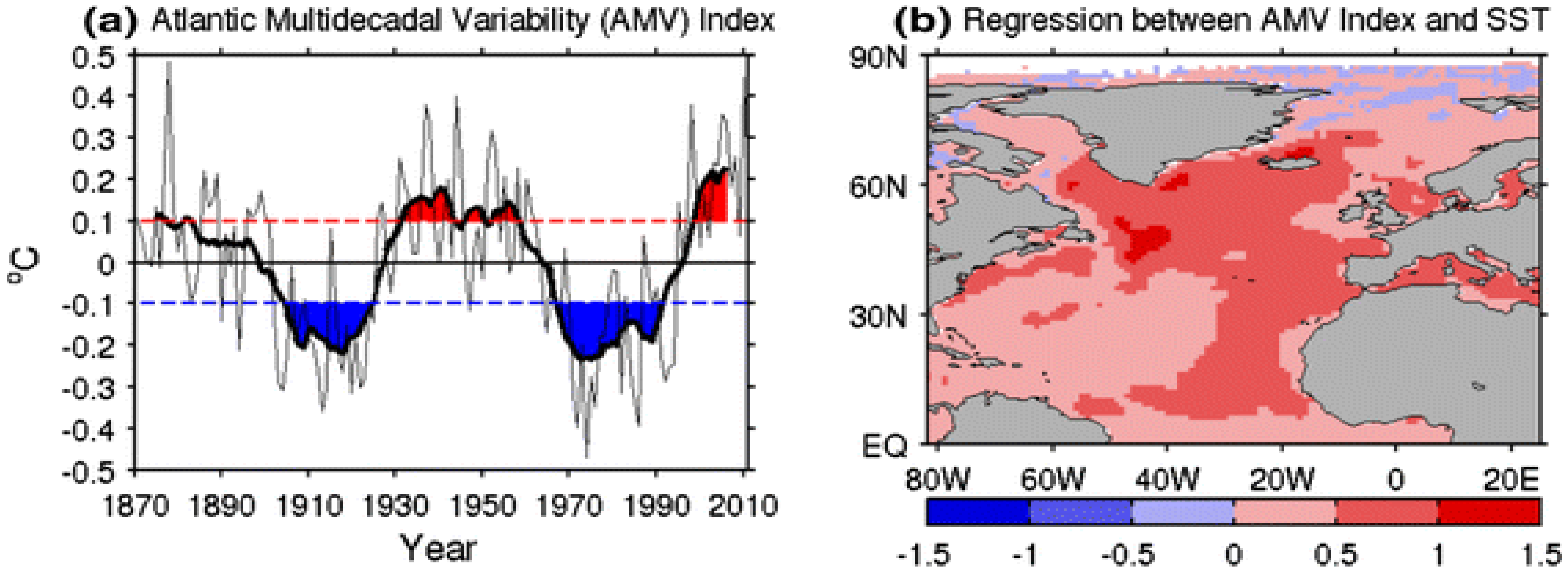

Warming whole in North Atlantic in 2018

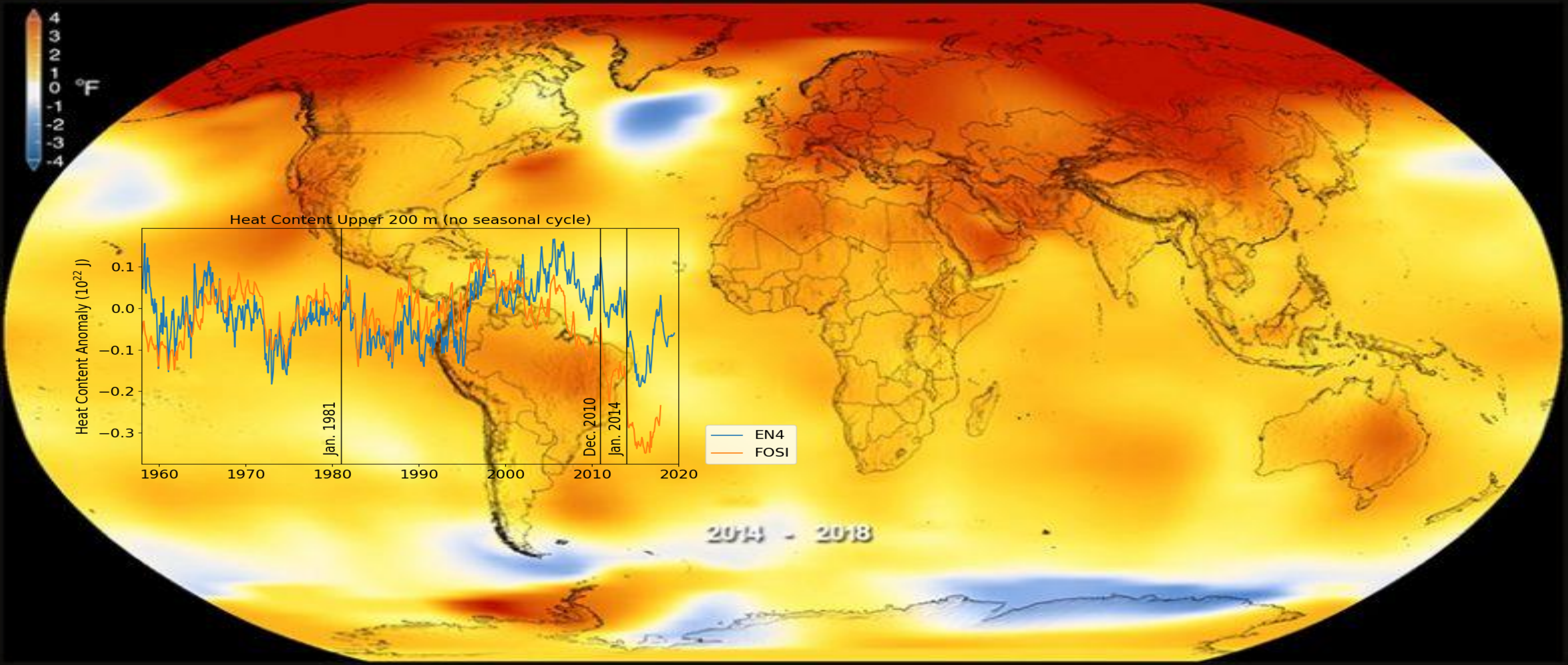

See Jennifer Mecking et all. EGU2020-6802

A satellite era warming hole in the equatorial Atlantic Ocean

Hyacinth Nnamchi[1], Mojib Latif[1], Noel Keenlyside[2] and Wonsun Park[1]

Multidecadal variability + warming effets

GEOMAR

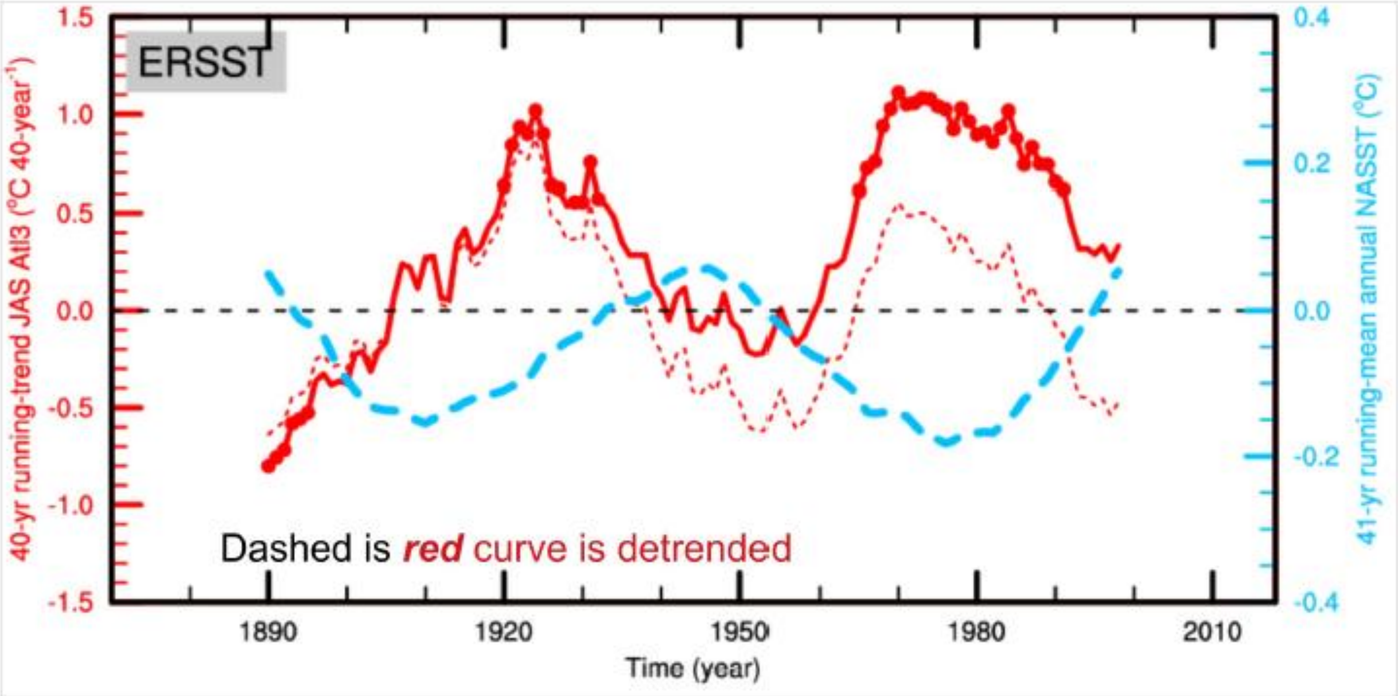

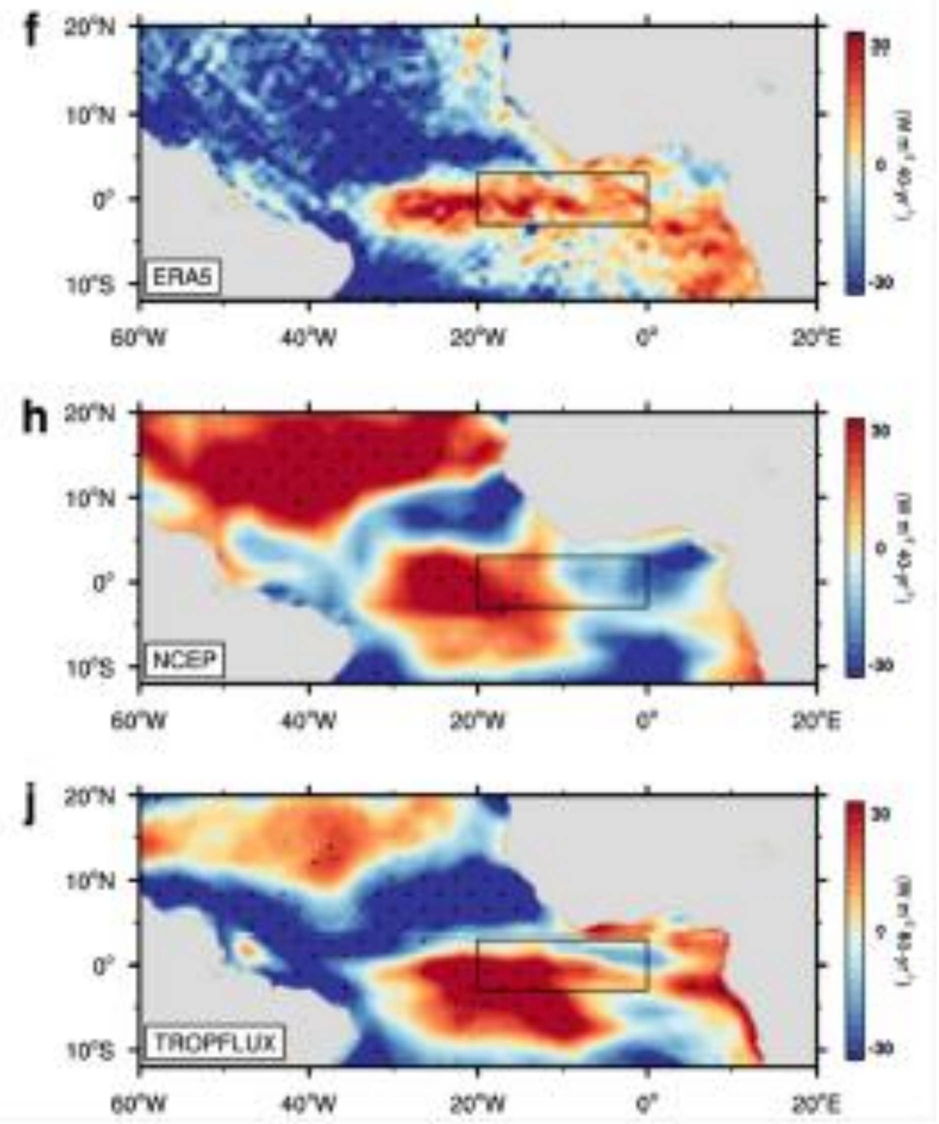

WHICH FACTORS DETERMINE VARIABILITY AND PREDICTABILITY OVER THE NORTH ATLANTIC REGION?

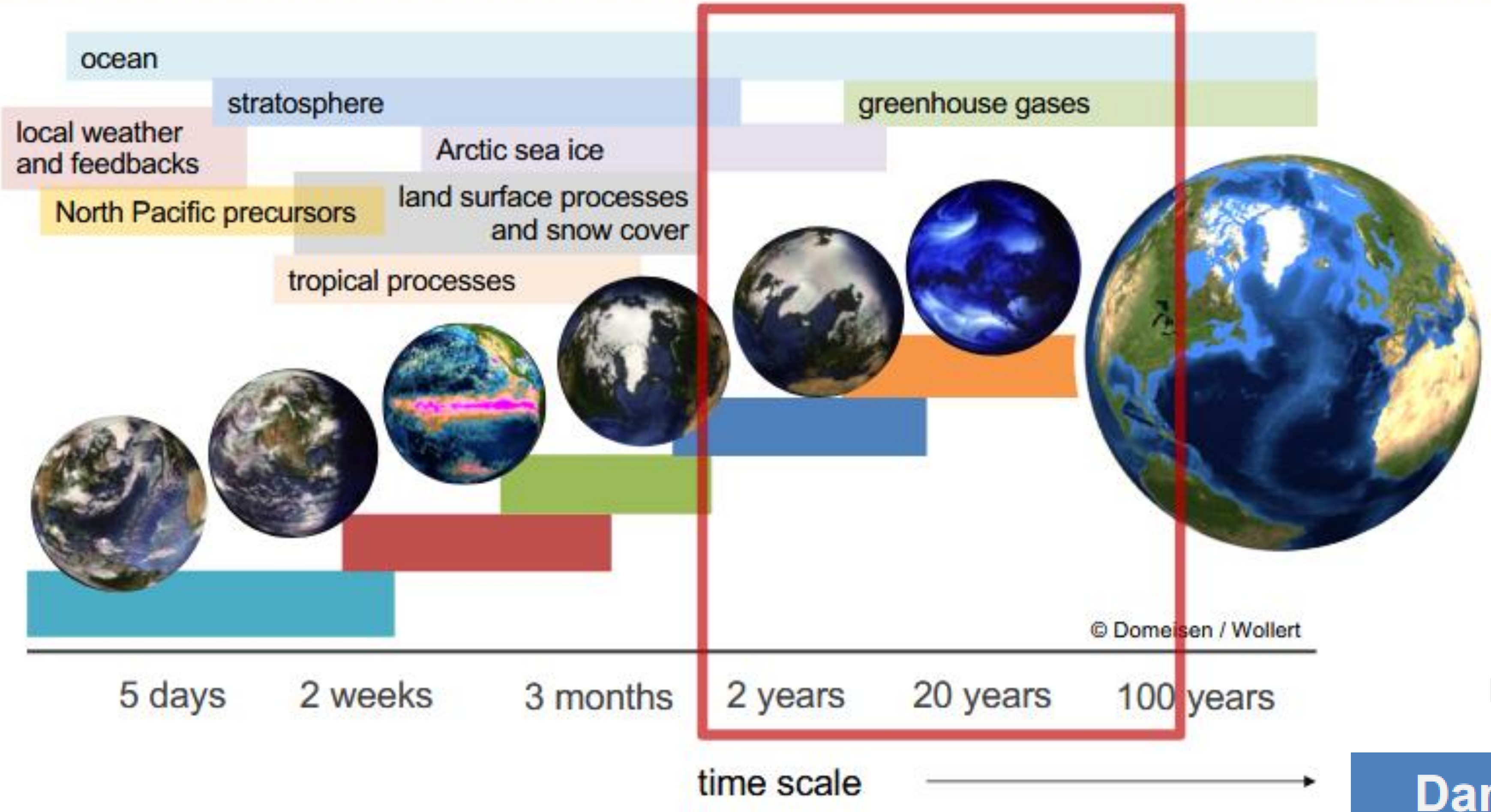

EGU2020-7815

Daniela Domeisen

EGU2020-10437

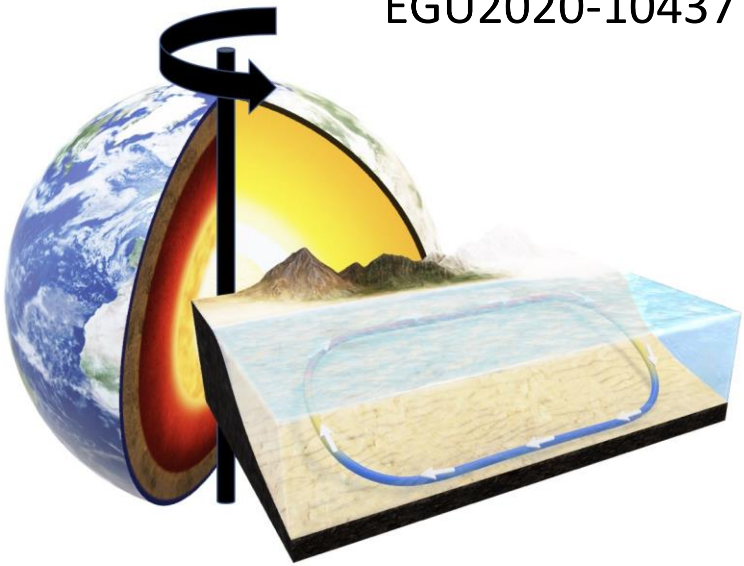

The intriguing relation between Earth's rotation, geomagnetism, and climate at multidecadal time scales

Sébastien Lambert

SYRTE, Observatoire de Paris - Université PSL, CNRS, Sorbonne Université, LNE

l'Observatoire de Paris | PSL cnrs INSU Observer & comprendre SORBONNE UNIVERSITÉ CRÉATEURS DE FUTURS DEPUIS 1257 LABORATOIRE NATIONAL DE MÉTROLOGIE ET D'ESSAIS LNE

EGU European Geosciences Union

http://syrte.obspm.fr/~lambert/lodclimate

Results: LOD vs SST

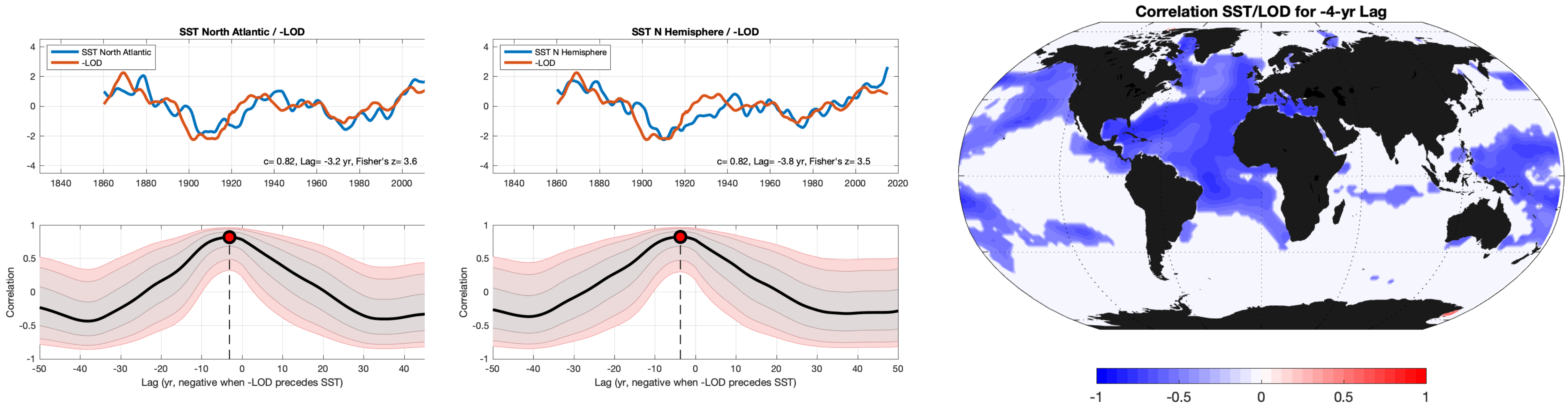

In the correlation plots, the successive shaded areas around the black line represent the 68%, 95%, and 99% confidence intervals. In the correlation maps, only correlation significant at more than 95% are reported. In both, the lag is negative when LOD precedes SST. I confirmed here the significant correlations between LOD and SST concentrated along North Atlantic (see Marcus 2016) with a small lag of a few years.

Long-term LOD, temperature changes, and magnetic dipole strength

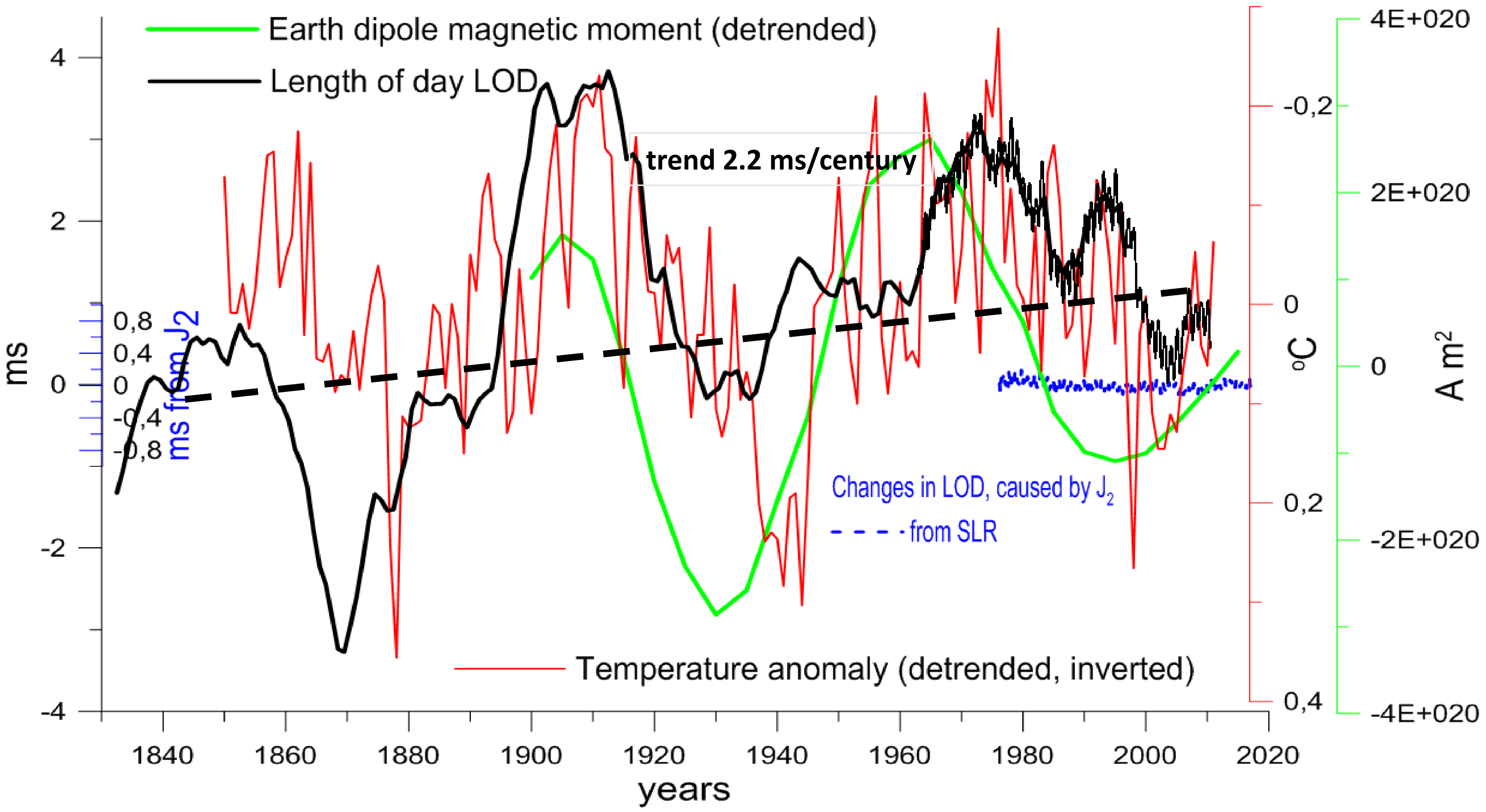

Earth dipole magnetic moment $$m_d = \frac{4\pi}{\mu_0} a^3 \sqrt{(g_1^0)^2 + (g_1^1)^2 + (h_1^1)^2},$$

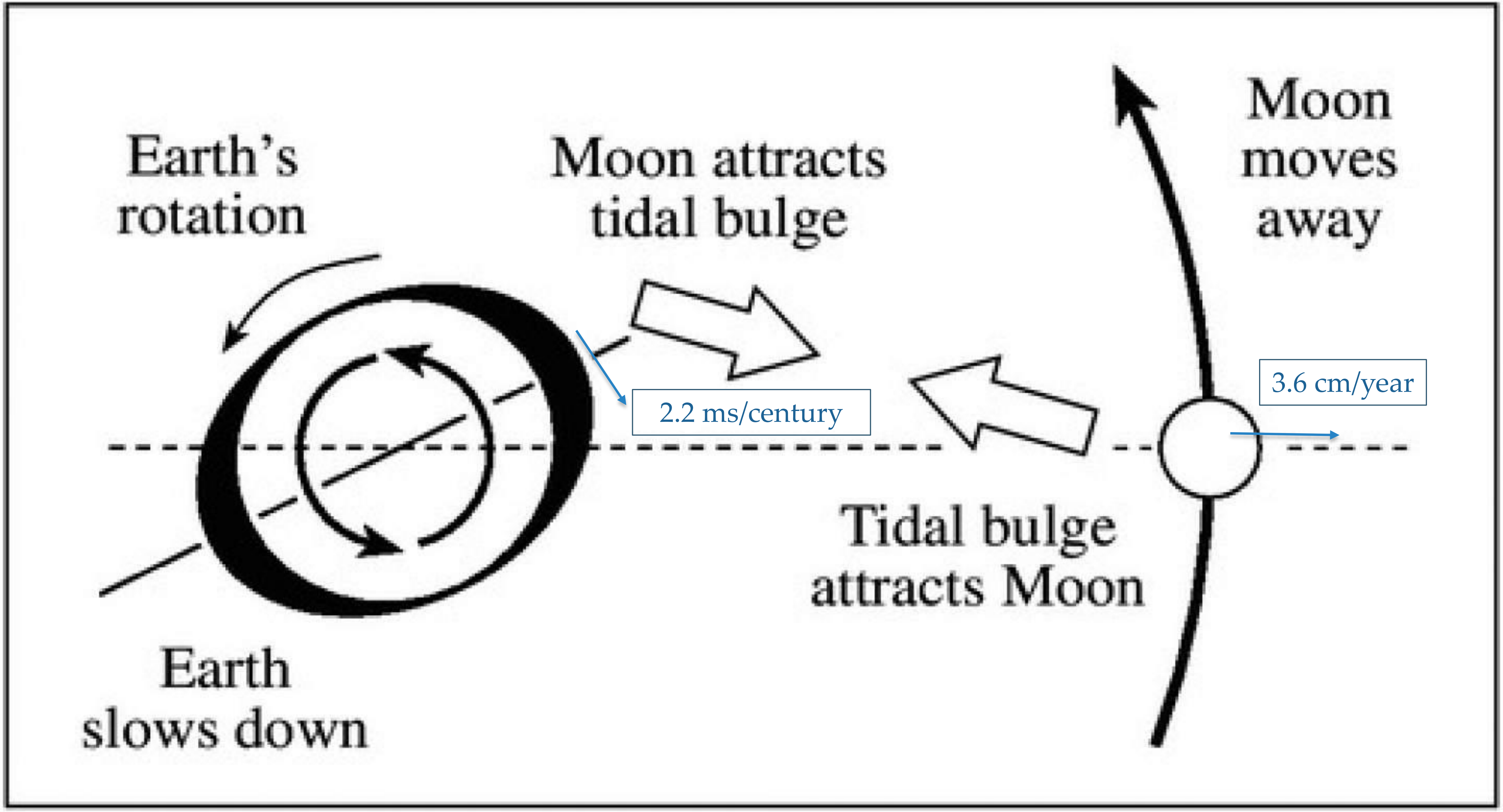

Earth's rotation
Moon attracts tidal bulge
Moon moves away
2.2 ms/century
3.6 cm/year
Tidal bulge attracts Moon
Earth slows down

Multidecadal and 6-year variations of LOD

IOP, 2020, in Press

Leonid Zotov[1,4,5], Christian Bizouard[2], Nikolay Sidorenkov[3], Artem Ustinov[4], Tatiana Ershova[4]

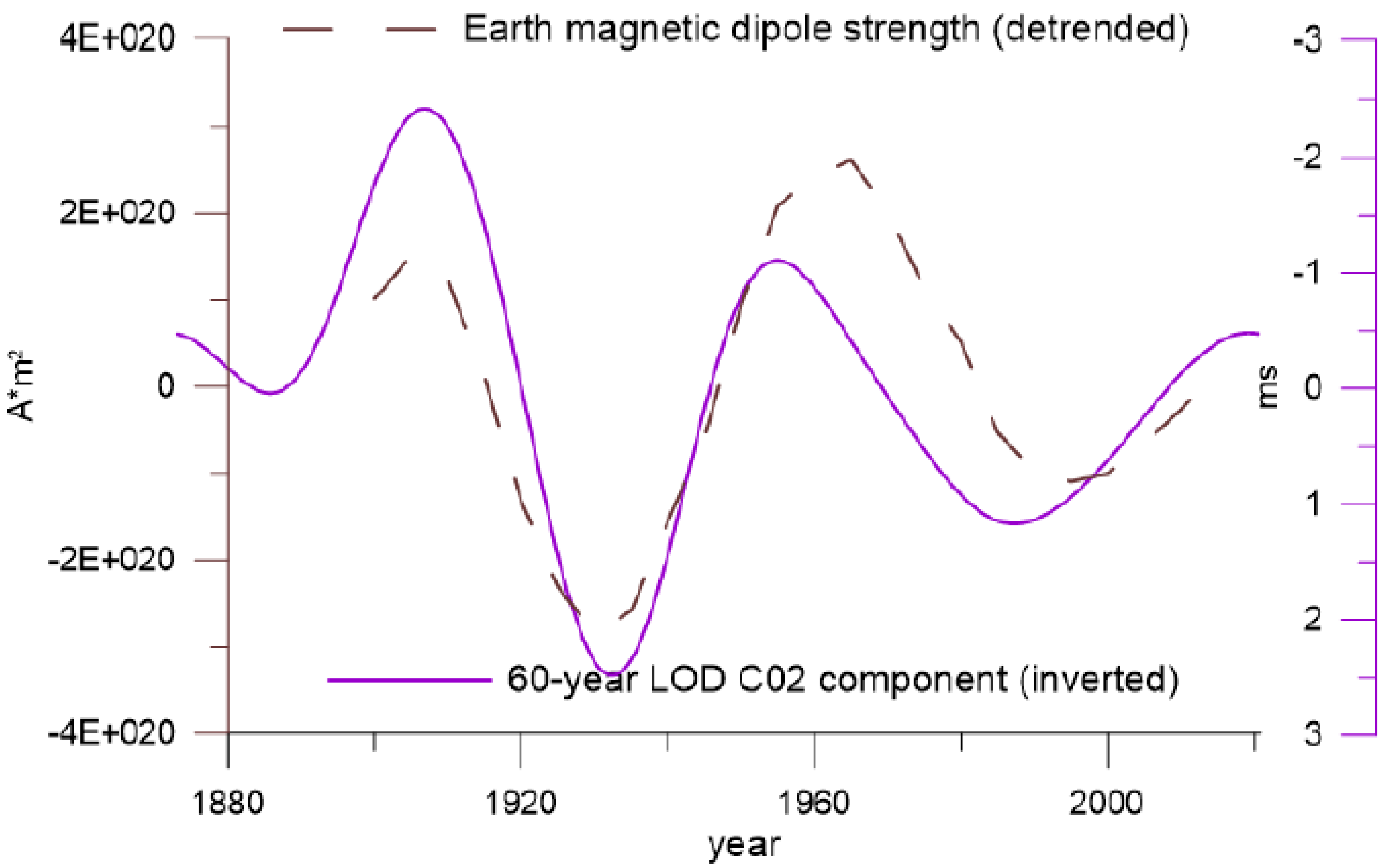

Figure 22. Comparison of the anomalies of the Earth magnetic field dipole and 60-year LOD variations.

GEOPHYSICAL RESEARCH LETTERS, VOL. 30, NO. 11, 1573, doi:10.1029/2002GL016763, 2003

Coherent interannual and decadal variations in the atmosphere-ocean system

Jean O. Dickey and Steven L. Marcus
Jet Propulsion Laboratory, California Institute of Technology, Pasadena, California, USA

Olivier de Viron
Royal Observatory of Belgium, Brussels, Belgium

Received 13 December 2002; revised 2 February 2003; accepted 31 March 2003; published 7 June 2003.

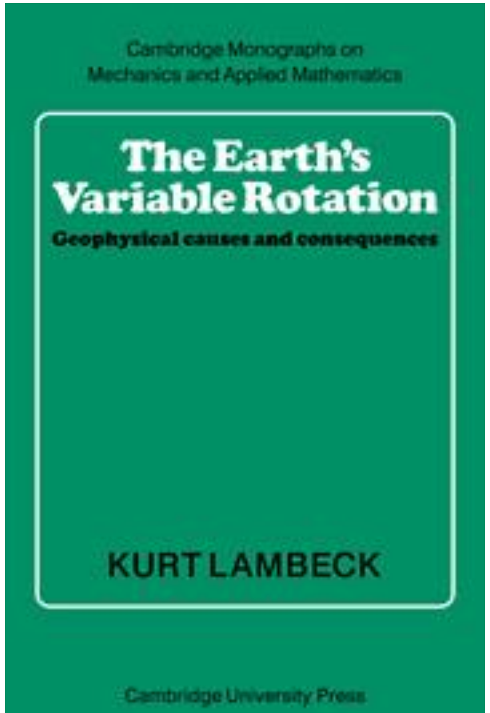

Does an Intrinsic Source Generate a Shared Low-Frequency Signature in Earth's Climate and Rotation Rate?

Steven L. Marcus*

Private Researcher, Santa Monica, California

Received 11 March 2015; in final form 24 October 2015

ABSTRACT: Previous studies have shown strong negative correlation between multidecadal signatures in length of day (LOD)—an inverse measure of Earth's rotational rate—and various climate indices. Mechanisms remain elusive. Climate processes are insufficient to explain observed rotational variability, leading many to hypothesize external (astronomical) forcing as a common source for observed low-frequency signatures. Here, an internal source, a core-to-climate, one-way chain of causality, is hypothesized. To test hypothesis feasibility, a recently published, model-estimated forced component is removed from an observed dataset of Northern Hemisphere (NH) surface temperatures to isolate the intrinsic component of climate variability, enhancing its comparison with LOD. To further explore the rotational connection to climate indices, the LOD anomaly record is compared with sea surface temperatures (SSTs)—global and regional. Because climate variability is most intensely expressed in the North Atlantic sector, LOD is compared to the dominant oceanic pattern there—the Atlantic multidecadal oscillation (AMO). Results reveal that the LOD-related

Alberto ESCAPA, J. G

Second-order effects i

Jia-Cheng LIU, N. CA

Testing the improveme

Véronique DEHANT a

Progress in understan

Elnaz NAGHIBI, S.A. K

Excitation of the Earth's Ch

Nikolay SIDORENKOV, E. D

Decadal fluctuations in Ea

asthenospere

Leonid ZOTOV, C. BIZOUA

On the variability of the Ch

Jan VONDRAK, C. RON

Determination of FCN p

geophysical excitations

José Manuel FERRANDIZ,

HEINKELMAN

Joint Working Group on The

ournées 2019

8,9 October 2019 - PARIS

rte.obspm.fr/astro/
2019/index.php?pa
ntation_pdf

DECADAL FLUCTUATIONS IN EARTH'S ROTATION AS EVIDENCES OF LITHOSPHERIC DRIFT OVER THE ASTHENOSPERE

N. SIDORENKOV[1], E. DIONIS[2], C. BIZOUARD[2], L. ZOTOV[3],

[1] Hydrometcentre of Russia, Moscow - Russia - sidorenkov@mecom.ru
[2] SYRTE, Observatoire de Paris, CNRS/UPMC - France
[3] Sternberg Astronomical Institute of Moscow State University - Russia

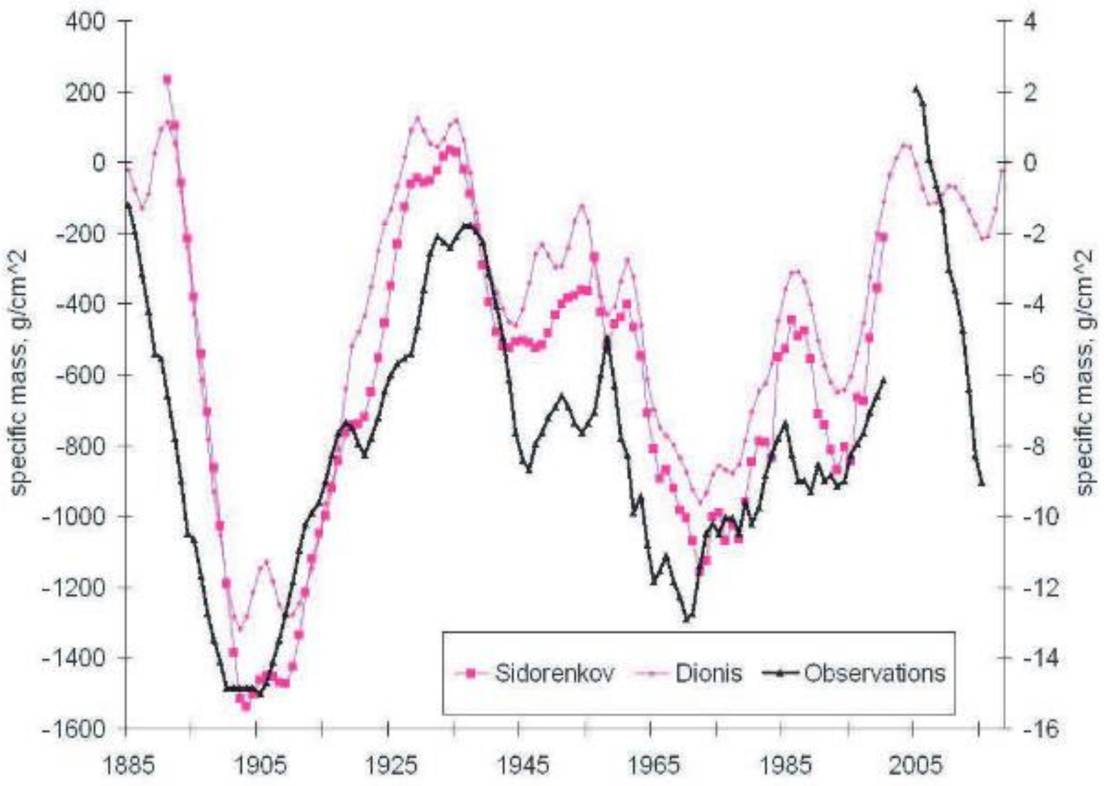

Figure 2: Temporal variations the specific mass of ice in Antarctica obtained from theoretical

One possible mechanism, proposed by anonymous reviewer of Journal of Geodesy

Global Earth temperature is inversely related to average global cloud coverage (McLean, 2014)

More solar energy comes to the atmosphere and ocean

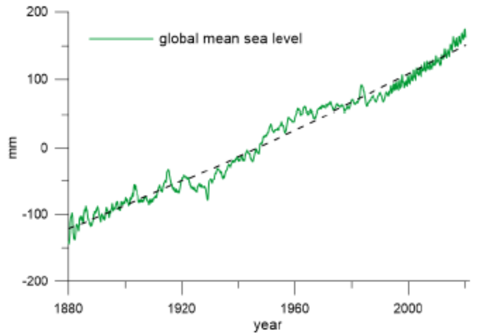

Thermal expansion of the ocean and atmosphere

Decrease of atmospheric and oceanic angular momentum

Solid Earth rotates faster

Oblatness is changing, which changes the shape of core-mantle boundary

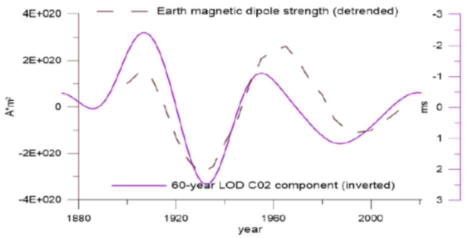

Figure 22. Comparison of the anomalies of the Earth magnetic field dipole and 60-year LOD variations.

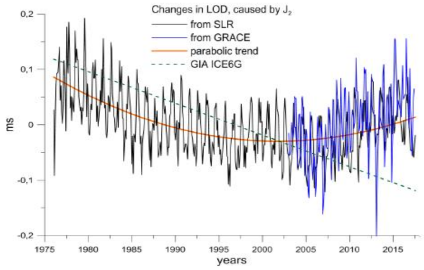

Figure 2. Effect of $J_2 = -\sqrt{5}C_{20}$, provided in LOD changes.

It influences the outer-core pressure and flow, which results in the variations of magnetic field

Тренды зонального AAM ECMWF и NCEP

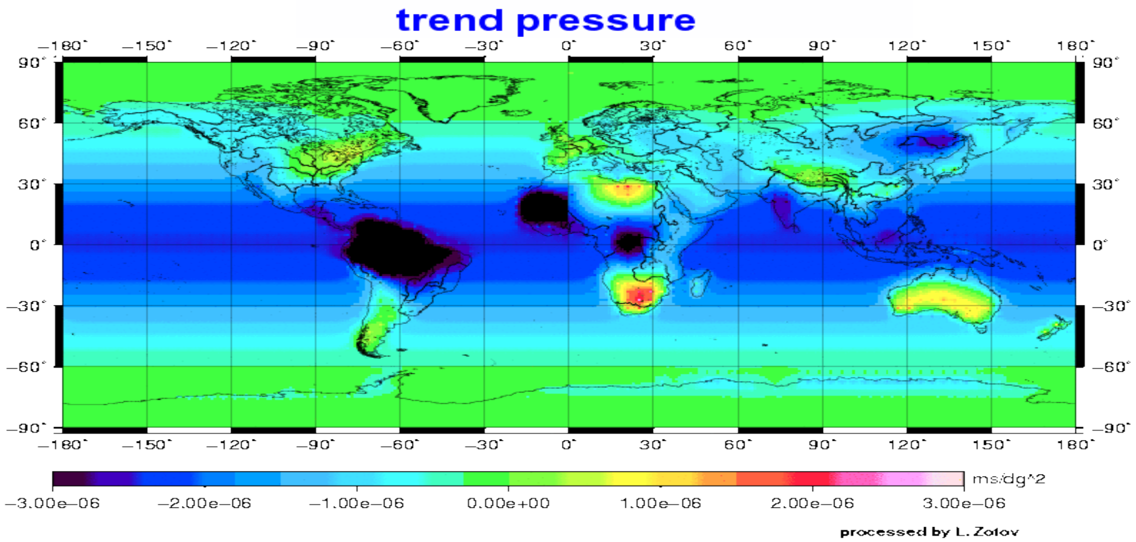

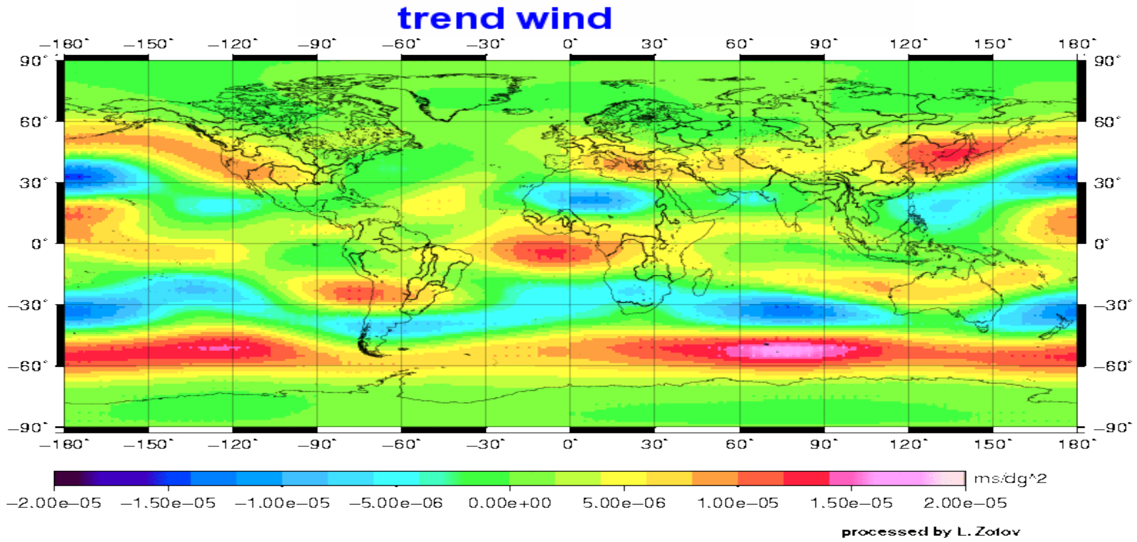

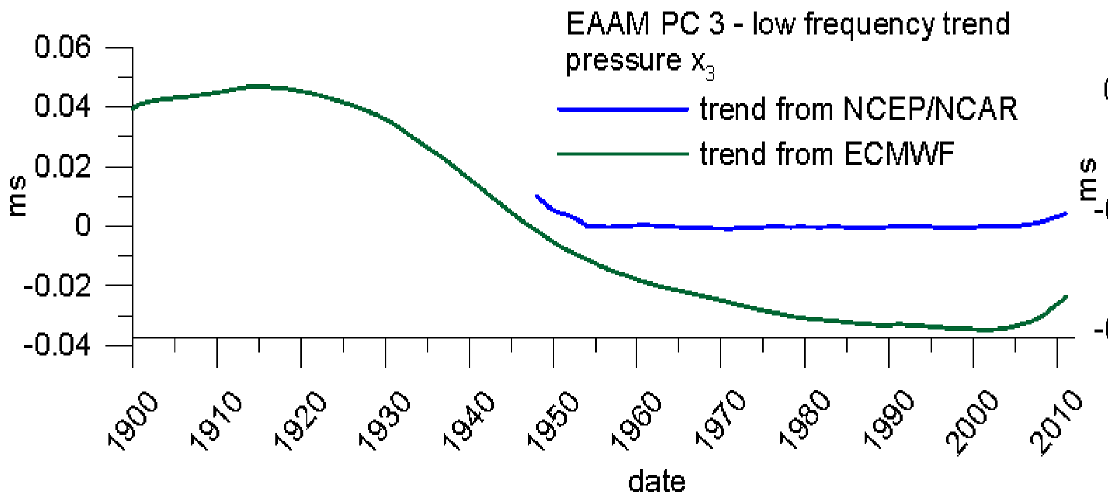

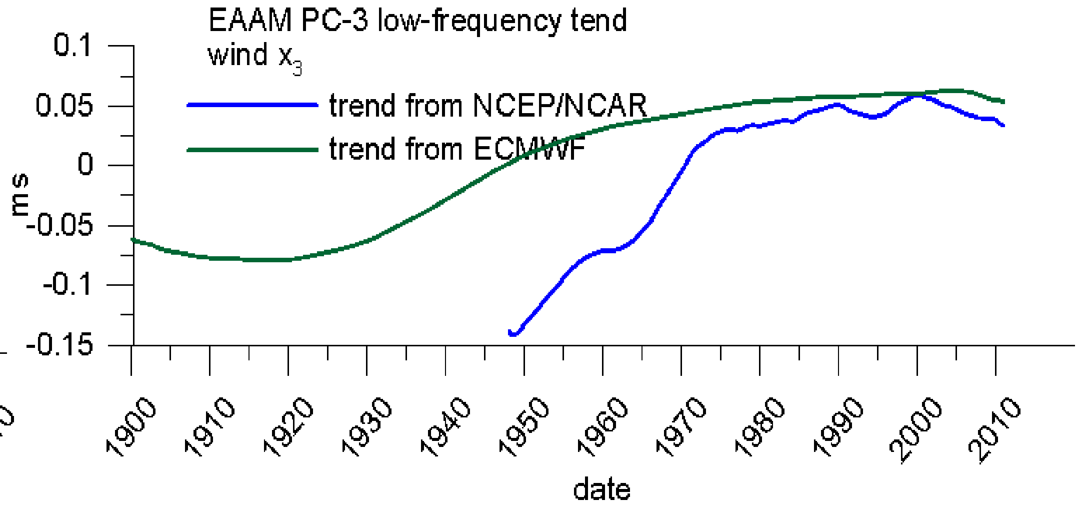

Zotov L., Sidorenkov N.S., C. Bizouard, C.K. Shum, Wenbin Shen [Multichannel singular spectrum analysis of the axial atmospheric angular momentum](), Geodesy and Geodynamics, Volume 8, Issue 6, 2017, Pages 433-442, KeAi, China, doi:10.1016/j.geog.2017.02.010.

Effect of global warming on the length-of-day

Olivier de Viron and Véronique Dehant
Royal Observatory of Belgium, Belgium

Hugues Goosse and Michel Crucifix
Institut d'Astronomie et de Géophysique G. Lemaître, Univ. Cath. de Louvain, Belgium

Participating CMIP Modeling Groups
Bureau of Meteorology Research Center, Canadian Center for Climate Modeling and Analysis, Center for Climate System Research, CERFACS, CSIRO Division of Atmospheric Research, German Climate Computing Center, Geophysical Fluid Dynamics Laboratory, Institute of Atmospheric Physics, Laboratoire de Météorologie Dynamique, Climate Research Department-Meteorological Research Institute, National Center for Atmospheric Research, Naval Research Laboratory, Hadley Center for Climate Prediction & Research

Received 23 June 2001; revised 17 September 2001; accepted 15 October 2001; published 12 April 2002.

GEOPHYSICAL RESEARCH LETTERS, VOL. 29, NO. 7, 1146, 10.1029/2001GL013672, 2002

Table 2. Source of the Variation in the LOD at Low Frequency

Source	Data	ΔLOD
Core motion	observ.	1–2 *ms*[a]
Tidal friction	observ.	20μs/year
Contin. water res.	observ.	−6μs/year
Post glacial rebound	observ.	−5 μs/year
Wind AAM	CMIP	1.81μs/year
Mass term	CMIP	−0.75 μs/year
Sea level	observ.	0.5 μs/year
Glacier	observ.	0.4 μs/year
Earthquake	observ.	−0.1 μs/year
Ocean current	CMIP	0.1 μs/year

[a] Not a trend but a decadal variation.

1. The largest contribution of the wind is mainly associated with an increase in the zonal wind between 10–60 degrees of latitude in both hemispheres. The effect is larger in the Southern Hemisphere than in the Northern Hemisphere, as can be seen in Figure 1. This increase in the zonal wind, by AM conservation, induces an increase in LOD.

2. The effect of the pressure is strongly coherent for nearly all the models. The decrease of the pressure contribution is associated with a decrease of the atmosphere global flattening, i.e. mass displaced from the equator to the pole, inducing a decrease in LOD.

3. The change of the contribution of the oceanic currents is mainly associated with variation in the Southern ocean, a region of strong zonal currents that display a large response to the increase in greenhouse gases, e.g. [*Boer et al.*, 2000].

Multidecadal and 6-year variations of LOD

IOP, 2020, in Press

Leonid Zotov[1,4,5], Christian Bizouard[2], Nikolay Sidorenkov[3], Artem Ustinov[4], Tatiana Ershova[4]

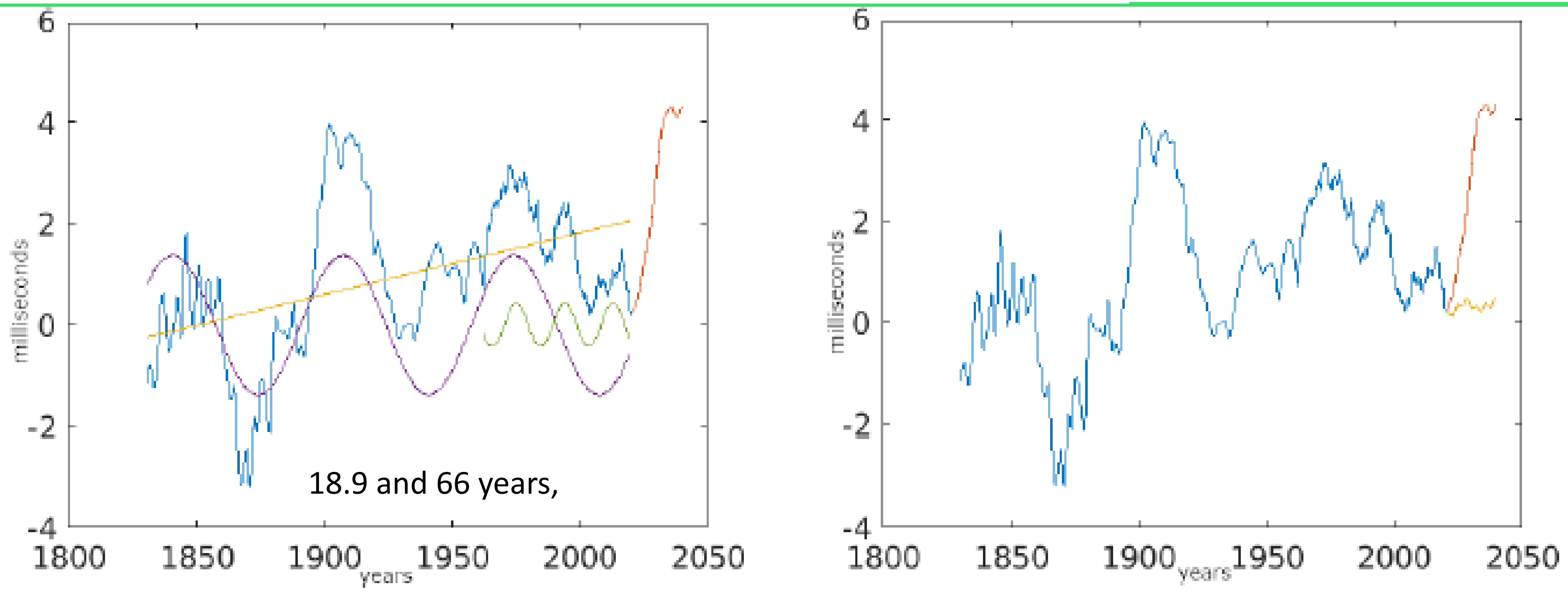

Figure 6. Adjustment for LOD. LOD C02 series in blue, linear trend yellow, 20-year harmonic green, 60-year harmonic purple.

Figure 7. C02 LOD series and its prediction based on above model (orange) and neural network (yellow).

Tidal variations and LOD

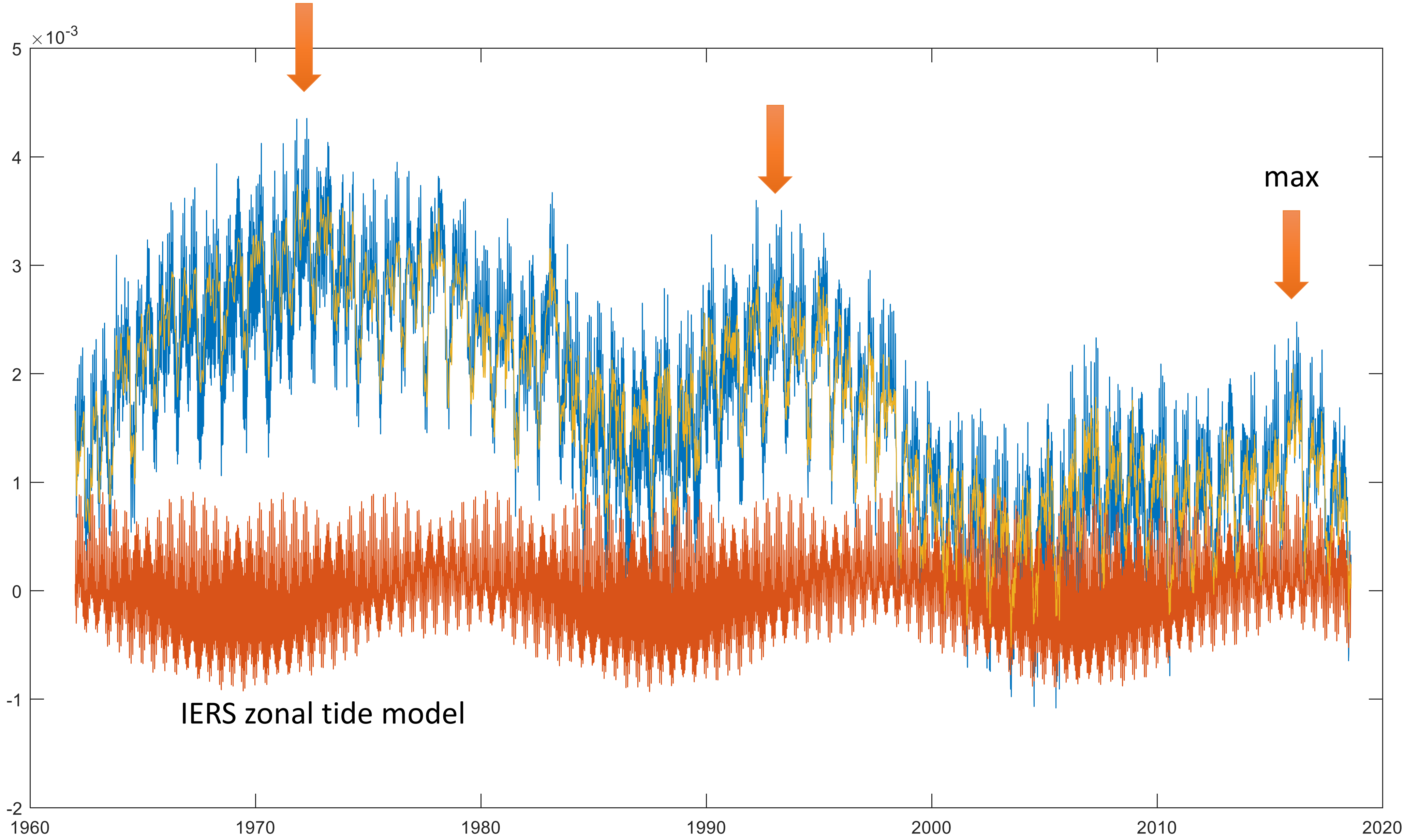

Tidal Earth rotation velocity changes

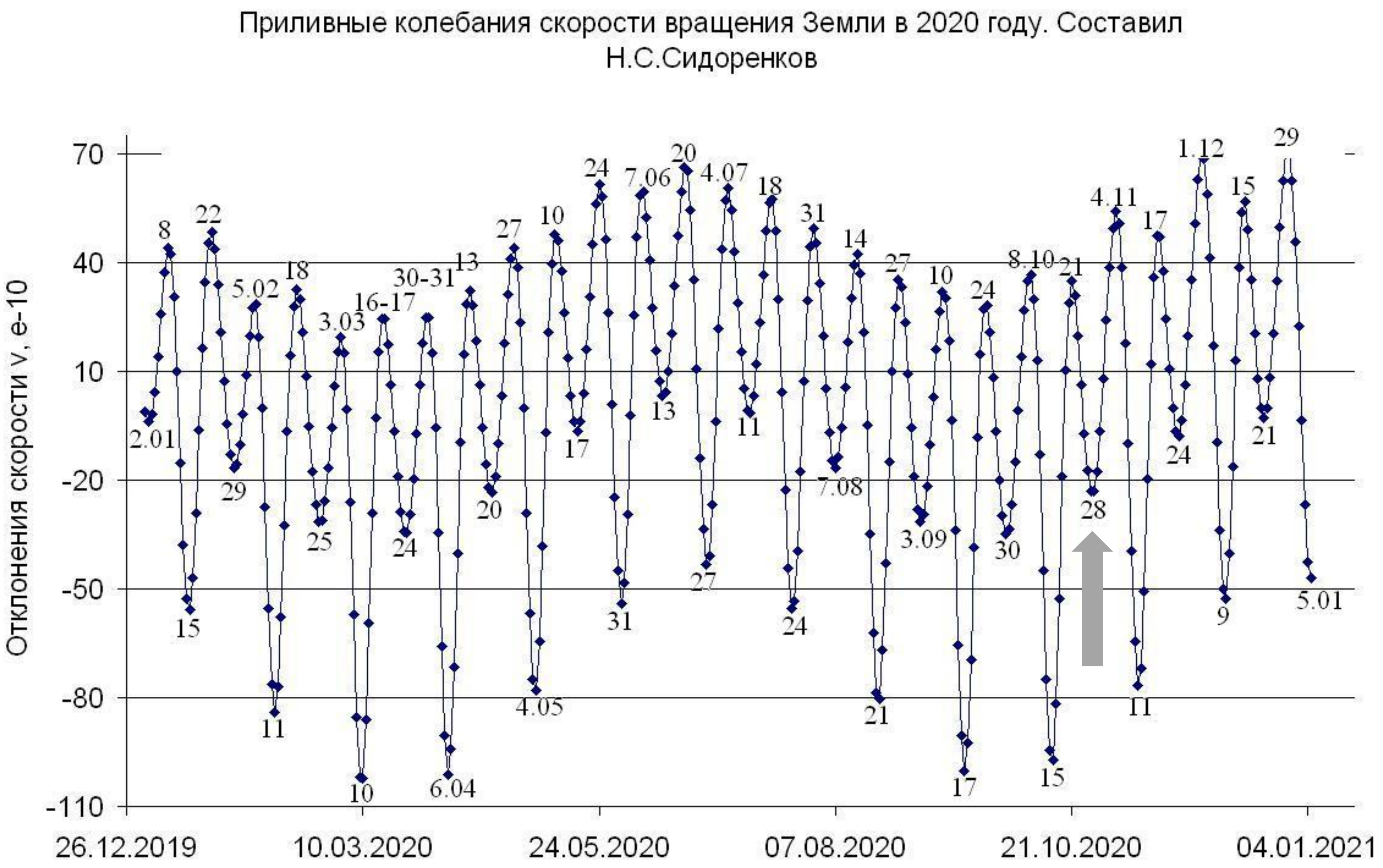

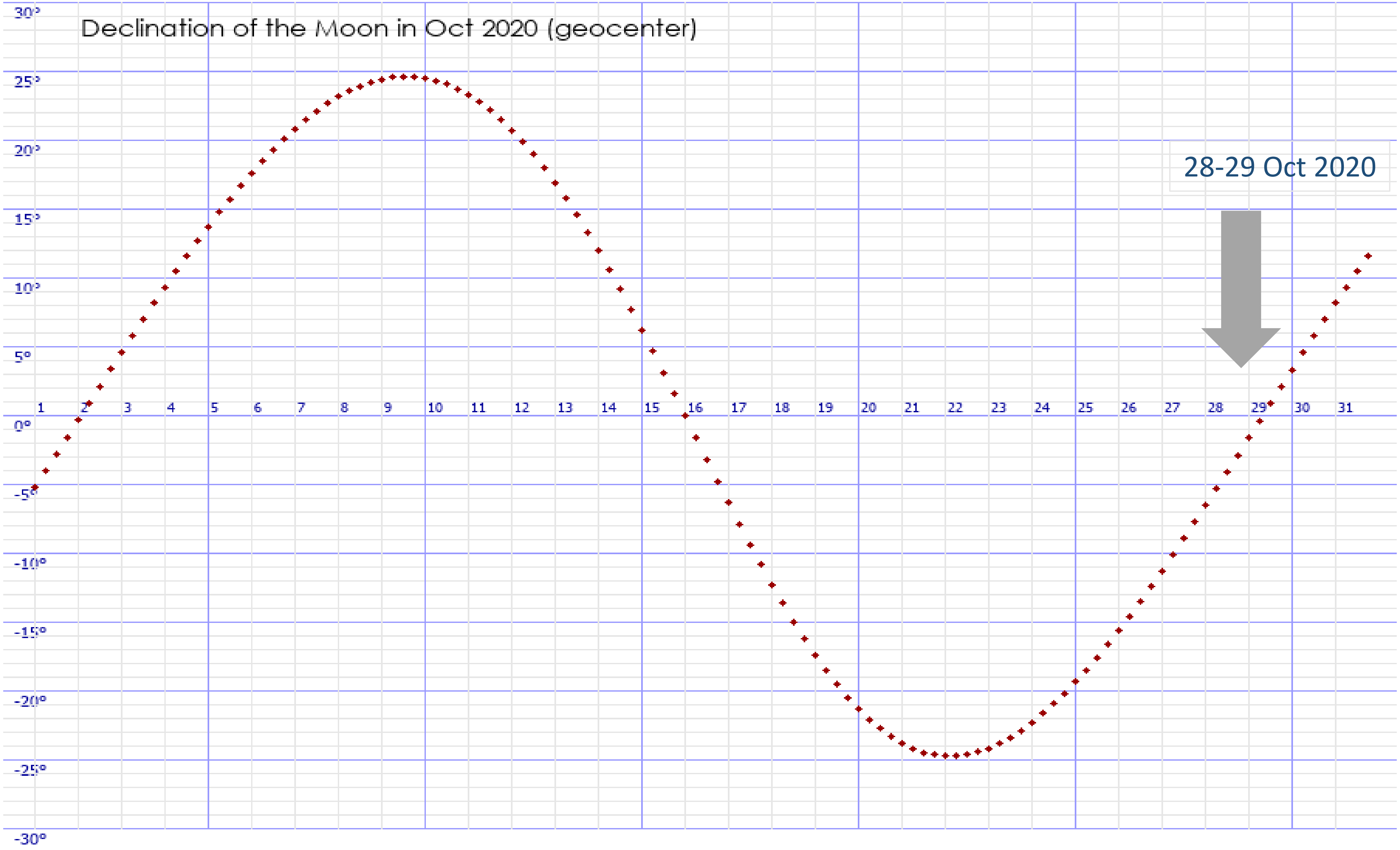
Declination of the Moon in Oct 2020 (geocenter)
28-29 Oct 2020
30°
25°
20°
15°
10°
5°
0°
-5°
-10°
-15°
-20°
-25°
-30°
1 2 3 4 5 6 7 8 9 10 11 12 13 14 15 16 17 18 19 20 21 22 23 24 25 26 27 28 29 30 31

El Nino fingerprint in LOD, acceleration of the Earth since 2015

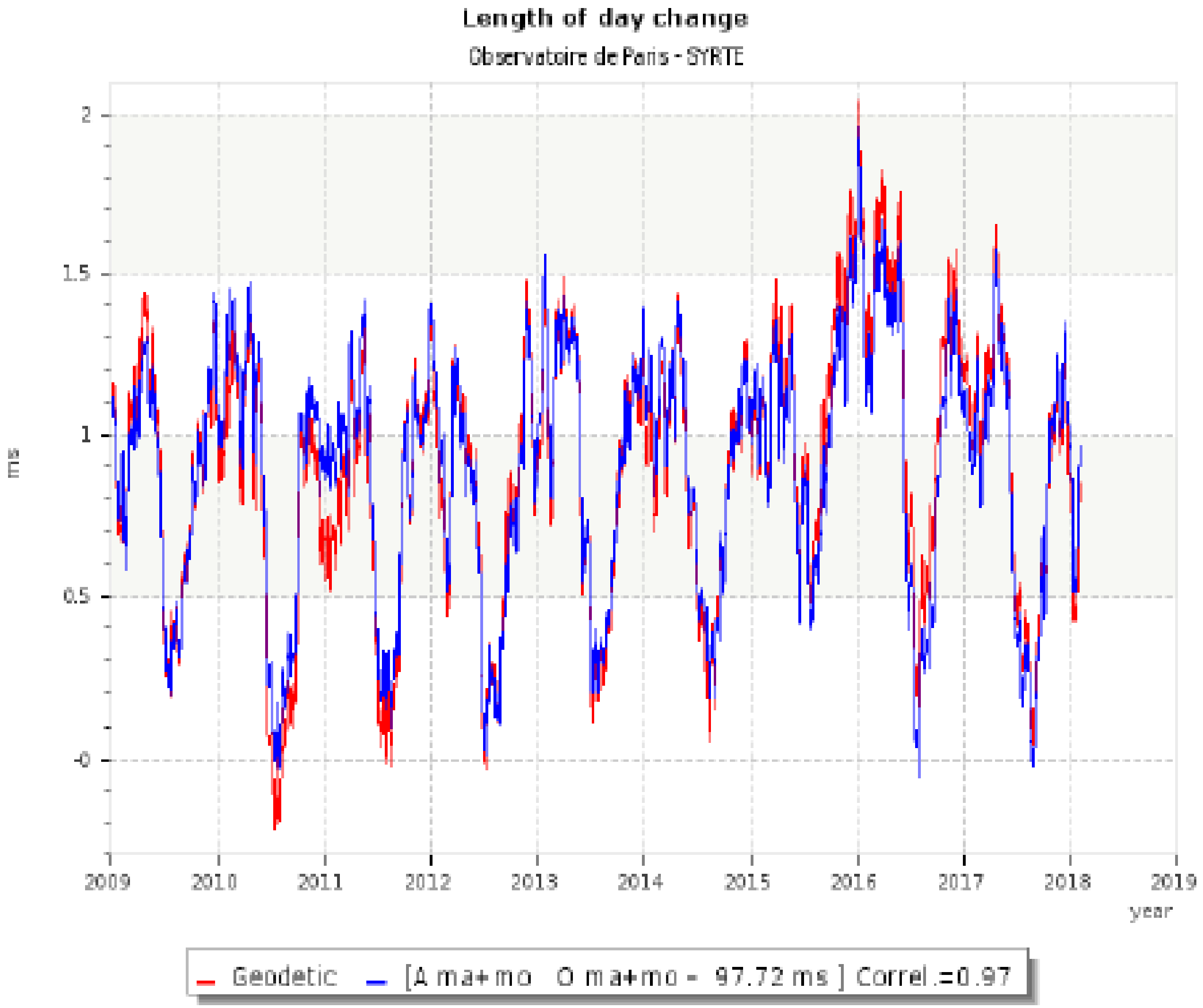

Figure 16. Comparison of LOD (geodetic, red) with the sum of OAM and AAM contributions (geophysical, blue) in the interannual band from EOP PC site.

LOD and Atmospheric processes

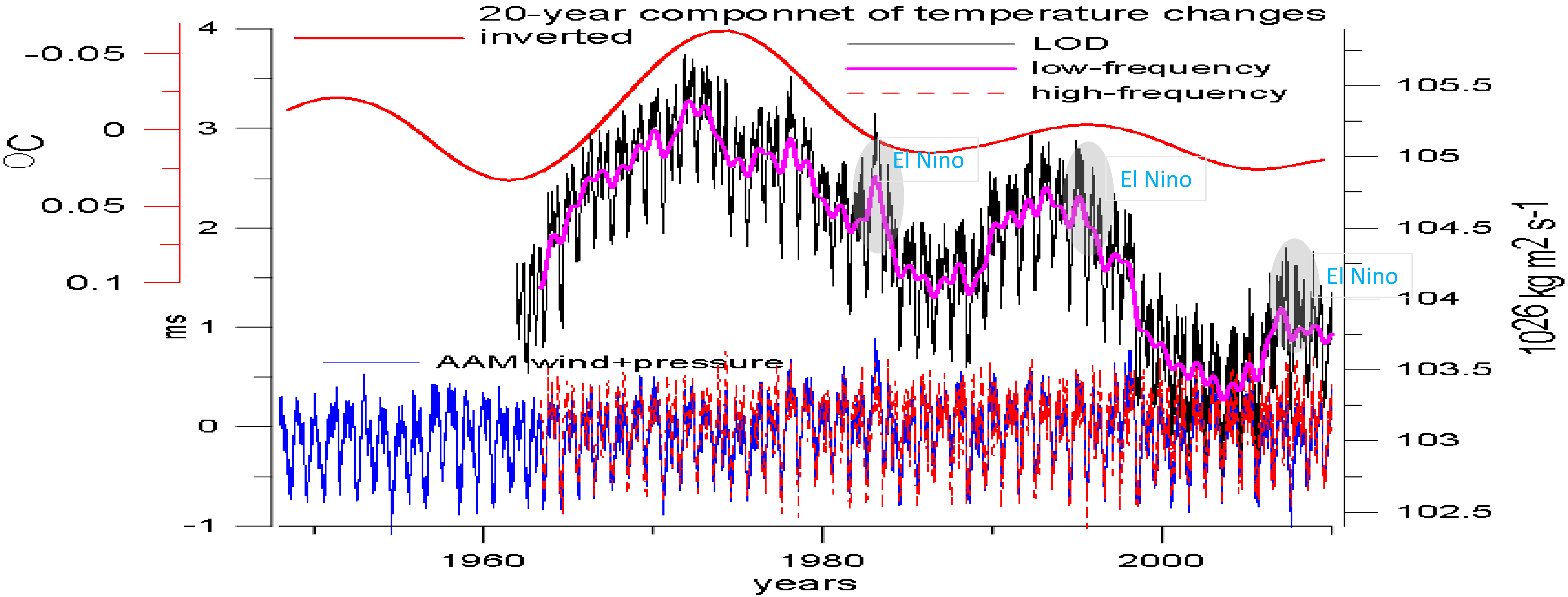

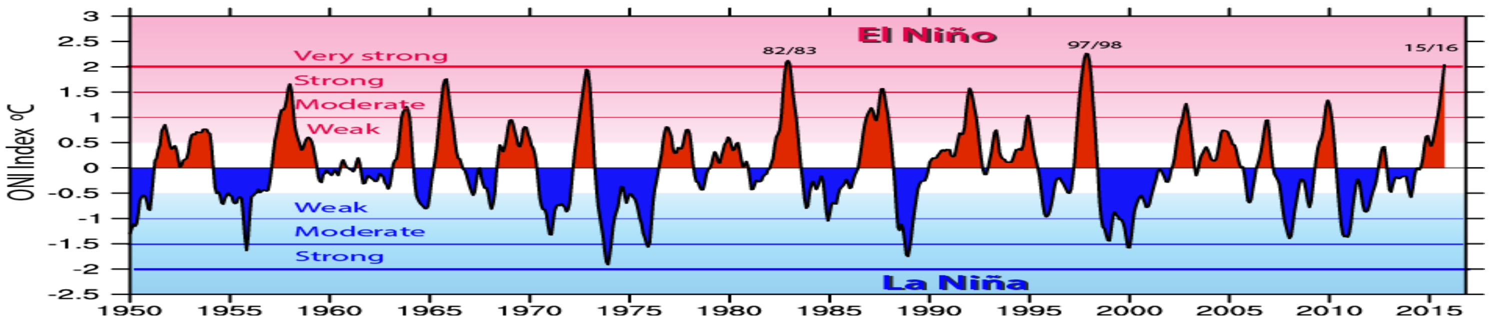

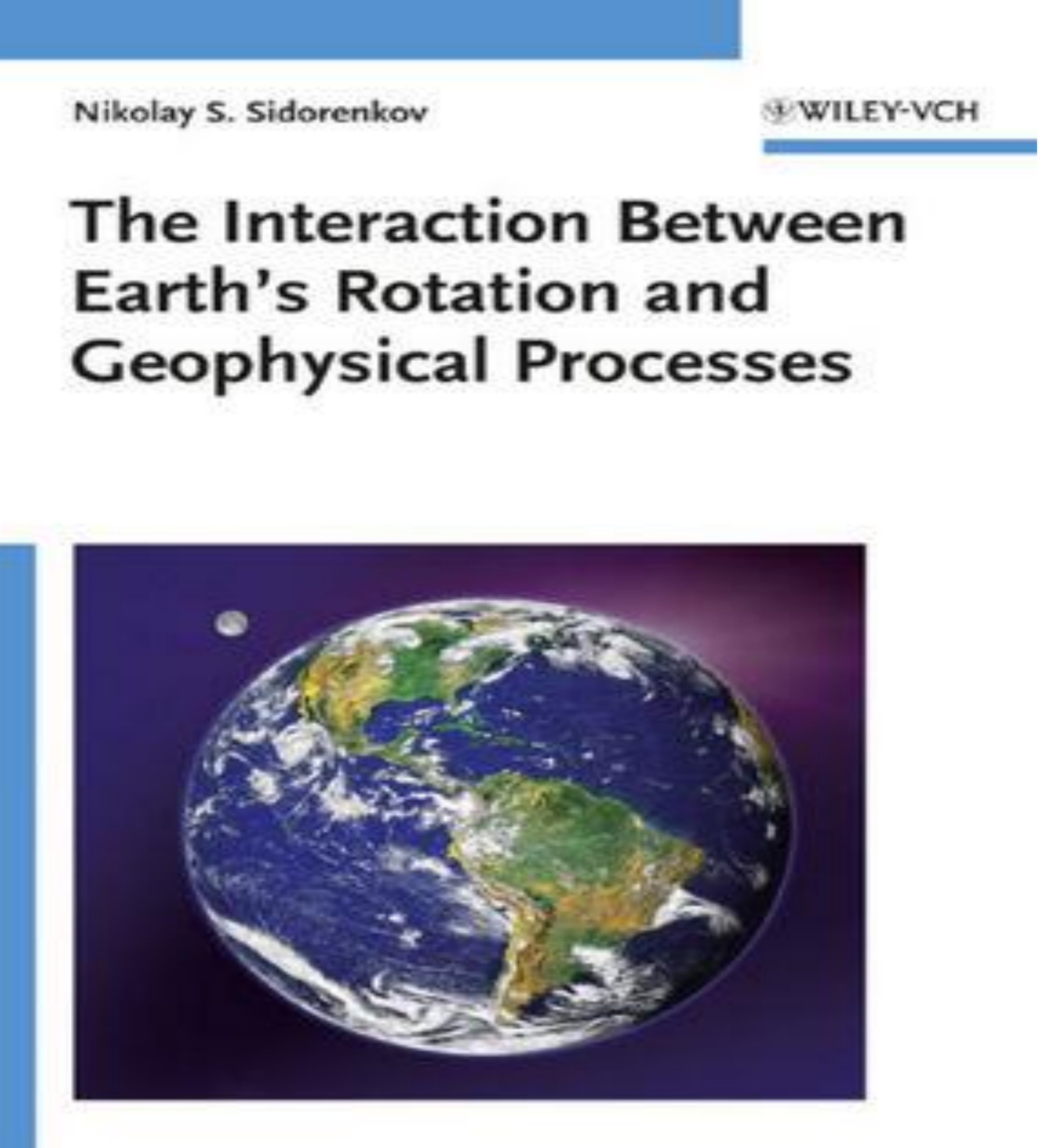
Nikolay S. Sidorenkov
WILEY-VCH
The Interaction Between Earth's Rotation and Geophysical Processes

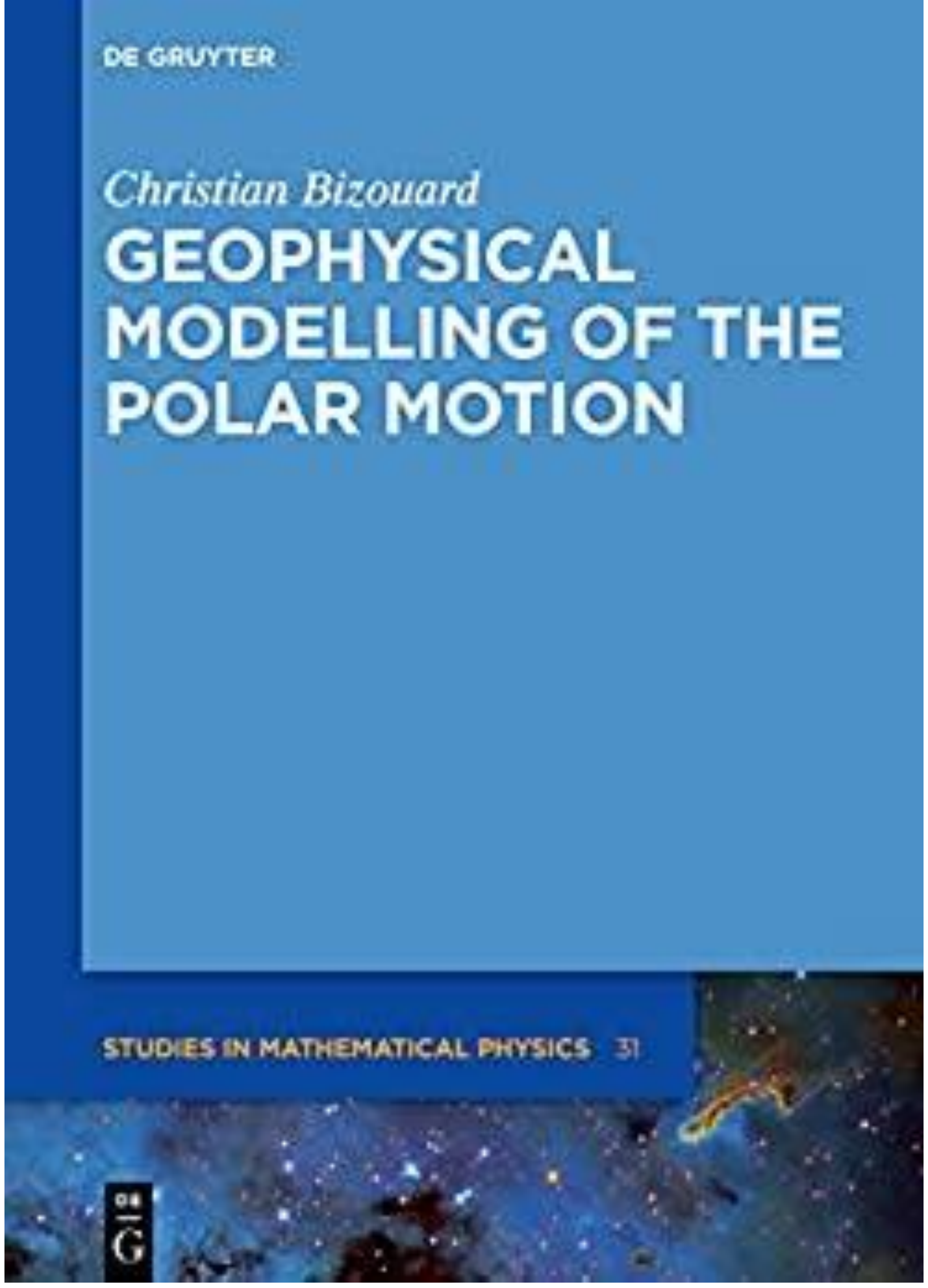
DE GRUYTER
Christian Bizouard
GEOPHYSICAL MODELLING OF THE POLAR MOTION
STUDIES IN MATHEMATICAL PHYSICS 31

To conclude:

It could be, that LOD variability and natural climate variations are coupled stronger then it was expected.

Mechanisms could be more complicated, than in case of polar motion drift.

It could be that:

Moon tides modulate geophysical processes and LOD (currents in North Atlantic, El Nino, tidal deceleration of the Earth).

.

Internal processes in the Earth reflected in the magnetic field, can influence planet's rotation and heat release.

Singular spectrum analysis of polar motion

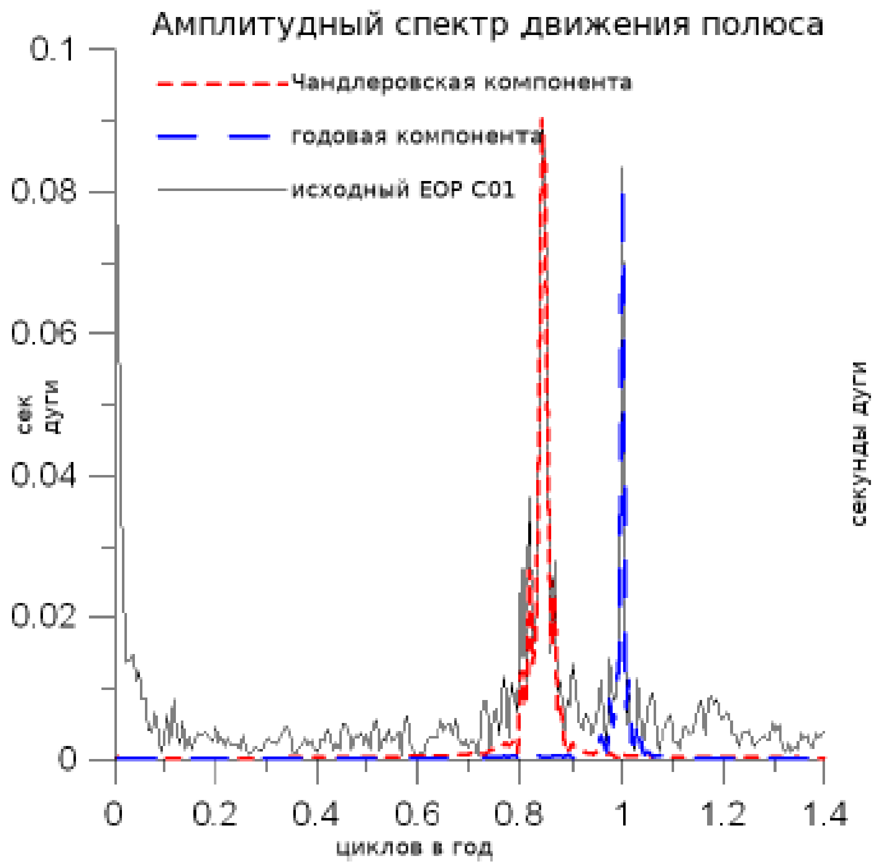

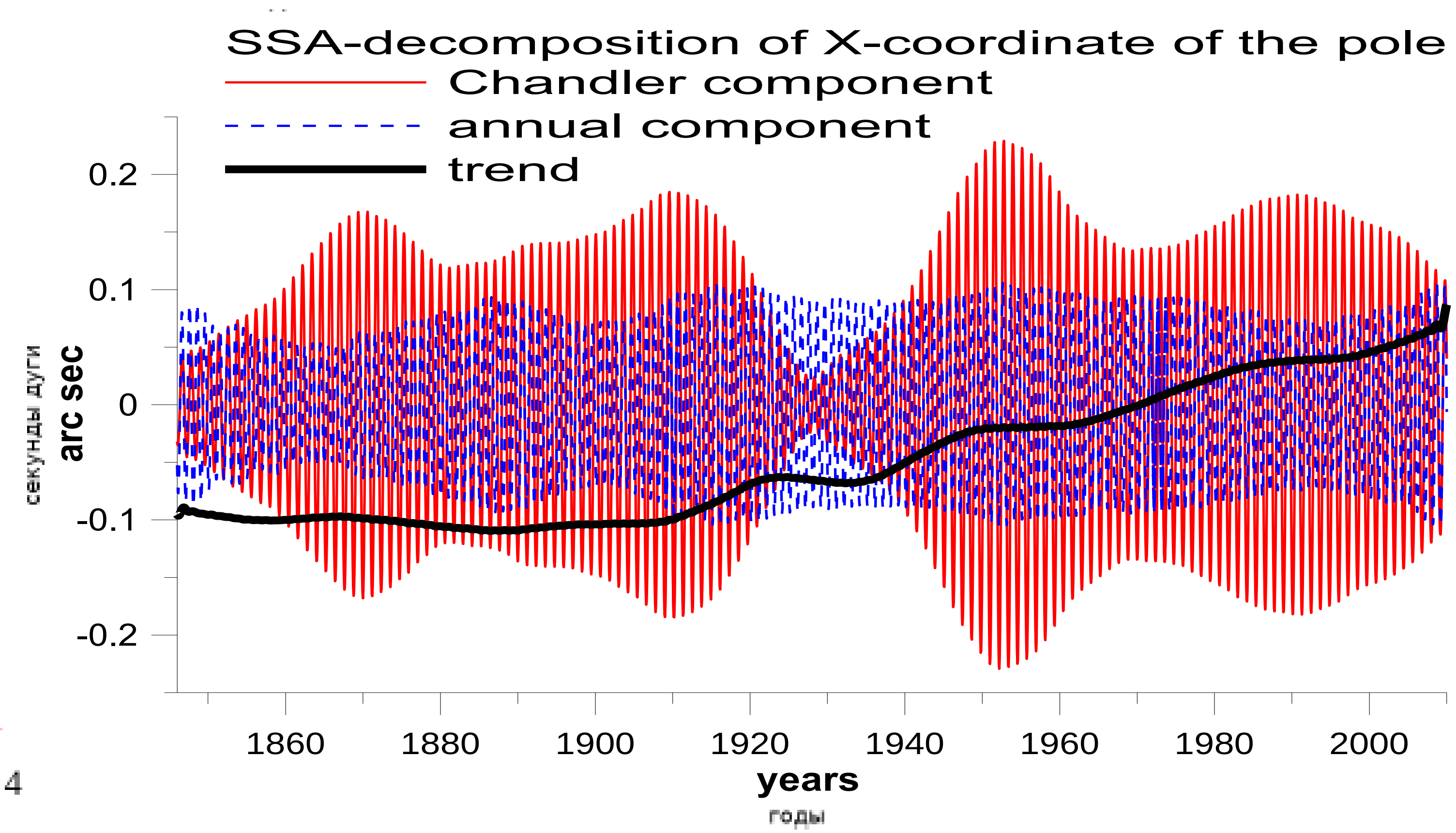

Рис. 3.2: Спектры движения полюса (слева) и его компоненты (x-координата), полученные комплексным ССА (справа).

Variable Chandler and Annual Wobbles in Earth's Polar Motion During 1900–2015

Surv Geophys (2016) 37:1075–1093
DOI 10.1007/s10712-016-9384-0

Guocheng Wang[1] · Lintao Liu[1] · Xiaoqing Su[2] · Xinghui Liang[1] · Haoming Yan[1] · Yi Tu[3] · Zhonghua Li[1] · Wenping Li[4]

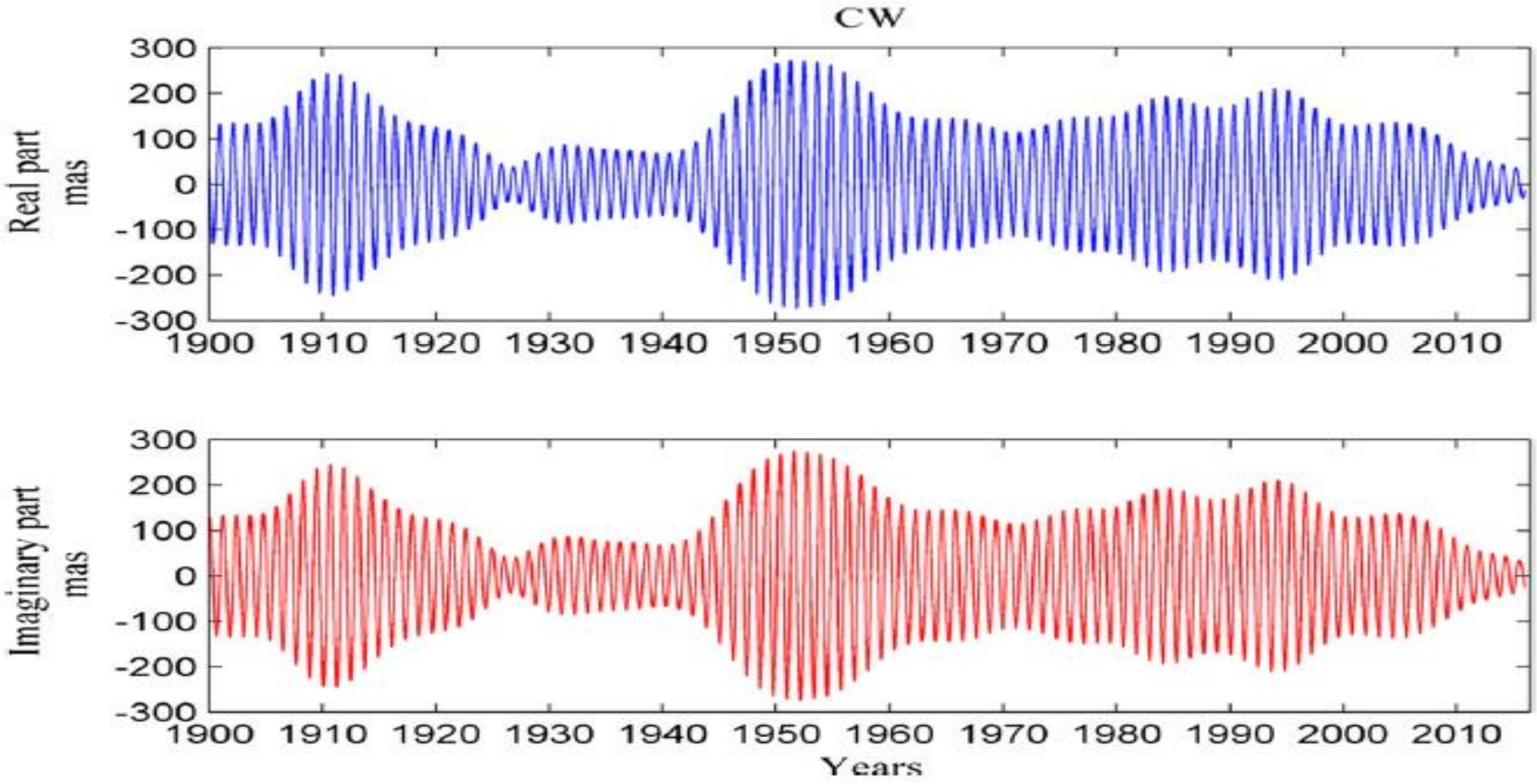

Fig. 8 Reconstruction of the CW using the FBPBPF method

Amplitude and phase variations of Earth's Chandler wobble under continual excitation

Benjamin F. Chao[a,b,*], Wei-Yung Chung[b]

[a] Institute of Earth Sciences, Academia Sinica, Taipei, Taiwan
[b] Department of Earth Sciences, National Central University, Chungli, Taiwan

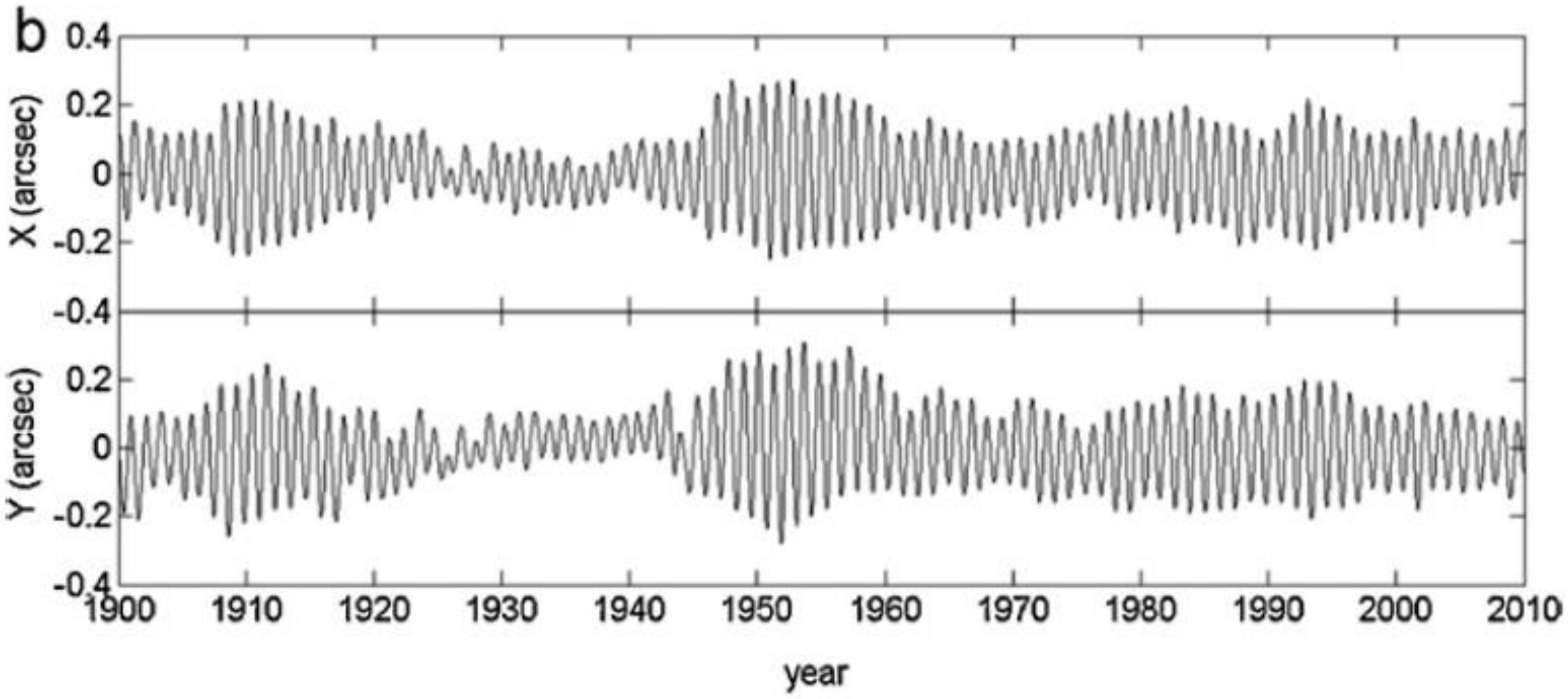

Fig. 1. (a) The x and y components of the Hipparcos polar motion series (for the period 1899.7–1992.0) concatenated with EOP-C01 (for the period 1992.0–2010.0) for the total span of 110 years at 5-day intervals. (b) The Chandler wobble series $m(t)$ obtained from (a) after removing the least-squares estimates of the annual wobble and a linear trend.

Chandler wobble: two more large phase jumps revealed

Zinovy Malkin and Natalia Miller

FT-filtered PM series

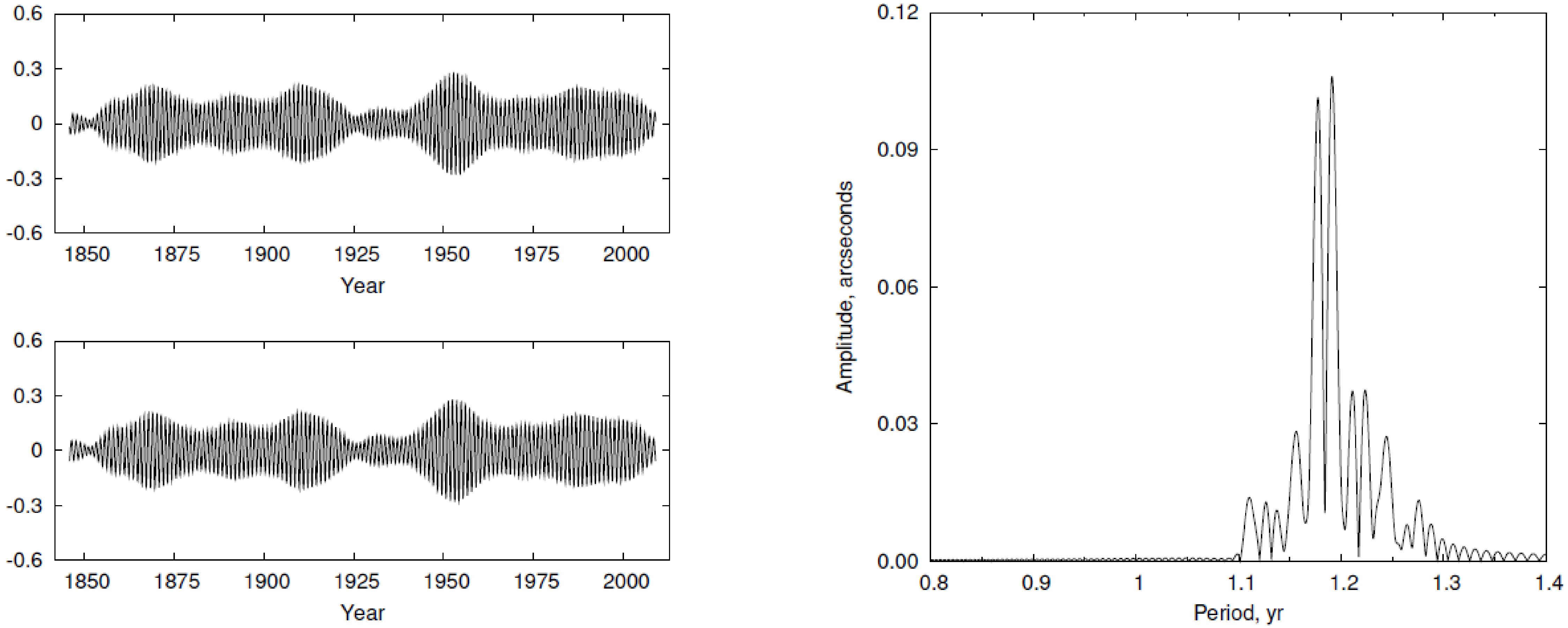

Filtered Chandler wobble and its envelope

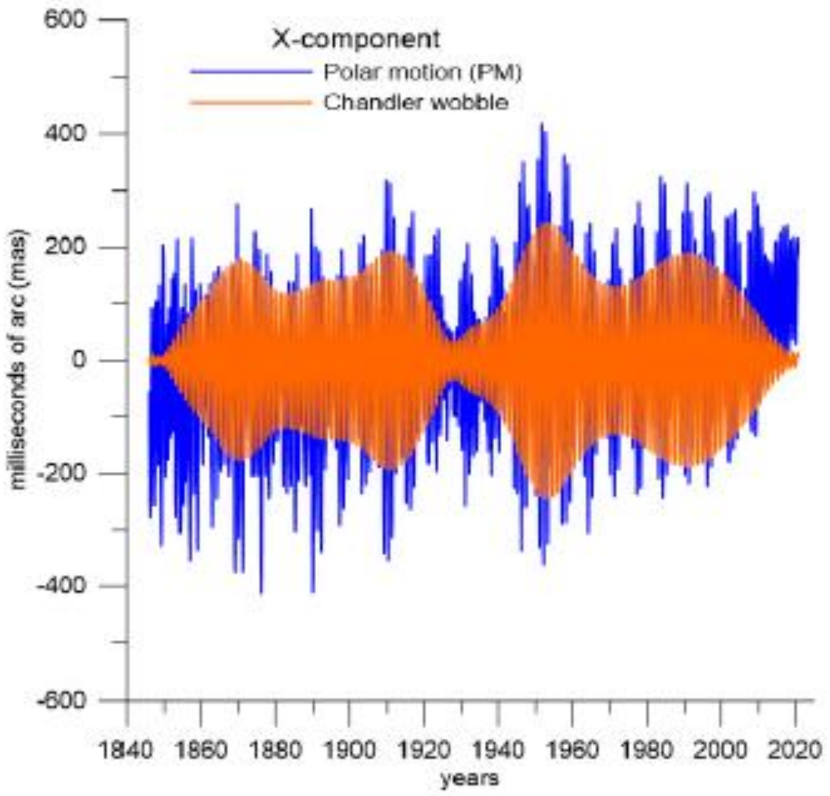

The impulse response of Panteleev's bandpass filter is given by the formula:

$$h(t) = \frac{\omega_0}{2\sqrt{2}} e^{-\left(\frac{\omega_0 |t|}{\sqrt{2}} - i2\pi f_c t\right)} \left(\cos \frac{\omega_0 t}{\sqrt{2}} + \sin \frac{\omega_0 |t|}{\sqrt{2}} \right), \tag{1}$$

with parameters $\omega_0 = 2\pi f_0$, which determine its width and f_c, which determines the center frequency. The filter transfer function is given by:

$$L_h(f) = \frac{f_0^4}{(f - f_c)^4 + f_0^4} \ . \tag{2}$$

We used $f_0 = 0.04$ and $f_c = 0.843$ cycles per year (cpy) [12], selecting the signal around 433-day period. It is important to note, that annual frequency is almost completely damped, but edge-effects of such nattow-band filtering can extent up to 20 years from the initial and final points of time series.

$$\frac{i}{\sigma_c} \frac{dp(t)}{dt} + p(t) = \chi(t),$$

$$p(t) = C(t) \exp\{i\omega_c t\} = A(t) \exp\{i\phi(t)\} \exp\{i\omega_c t\}, \qquad \chi(t) = E(t) \exp\{i\theta(t)\} \exp\{i\omega_c\}.$$

$$E(t)\exp\{i\theta(t)\} = \left[\frac{i}{\sigma_c} \left(\frac{dA(t)}{dt} + i\frac{d\phi(t)}{dt} A(t) \right) + \left(1 - \frac{\omega_c}{\sigma_c} \right) A(t) \right] \exp\{i\phi(t)\},$$

$$E(t) = \frac{i}{\sigma_c} \left[\dot{A}(t) + \left(i\dot{\phi}(t) + \frac{\omega_c}{2Q} \right) A(t) \right].$$

Filtered Chandler wobble and its envelope

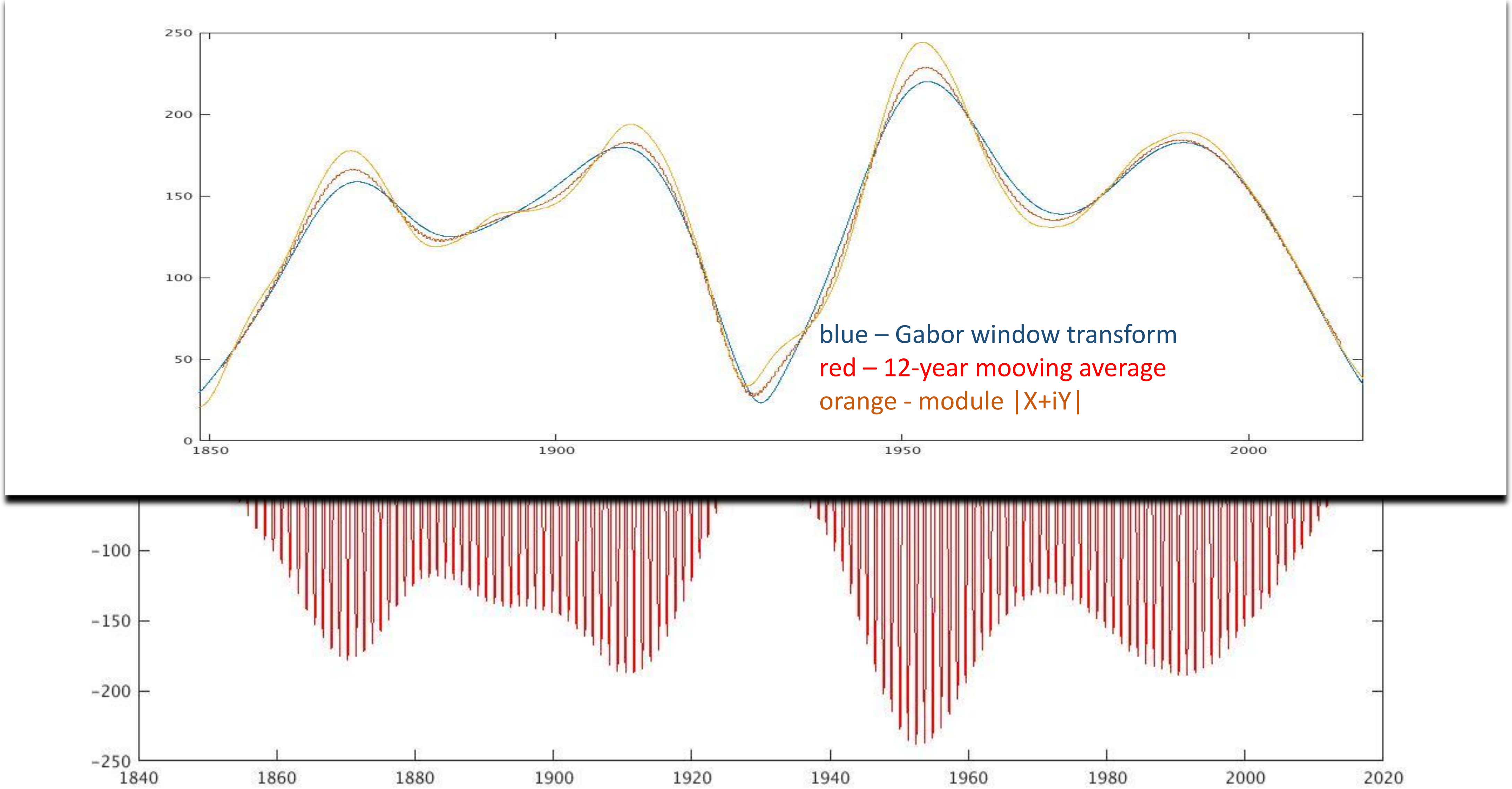

See Doctoral thesis by L. Zotov
http://lnfm1.sai.msu.ru/~tempus/disser/index.htm

Filtered Chandler wobble and its excitation

Chandler excitation envelope

$$E(t) = \frac{i}{\sigma_c}\left[\dot{A}(t) + \left(i\dot{\phi}(t) + \frac{\omega_c}{2Q}\right)A(t)\right].$$

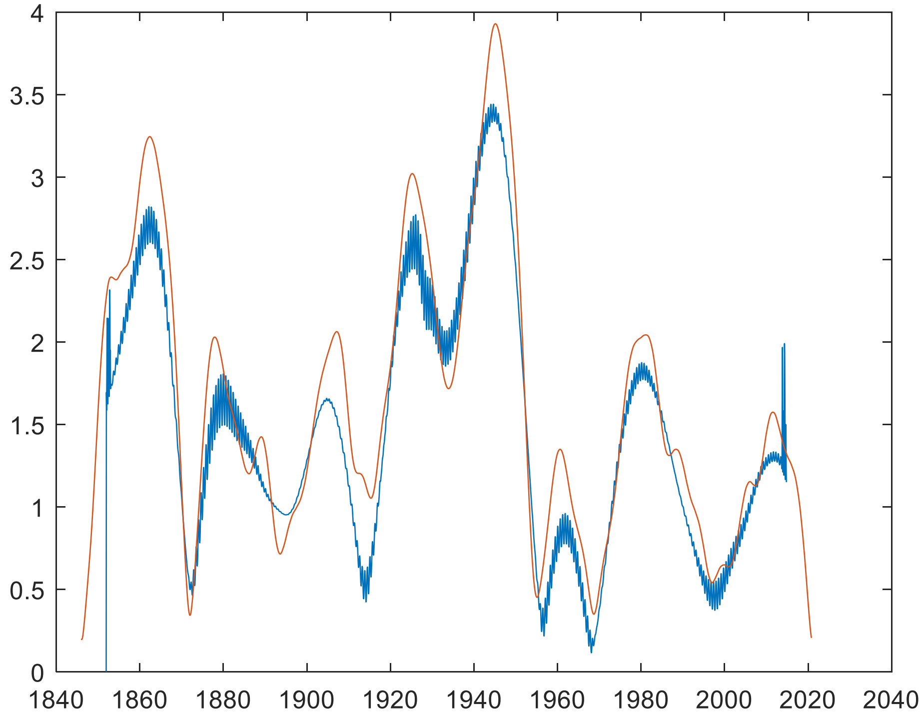

Sum of terms in comparison with reconstructed chandler excitation envelope

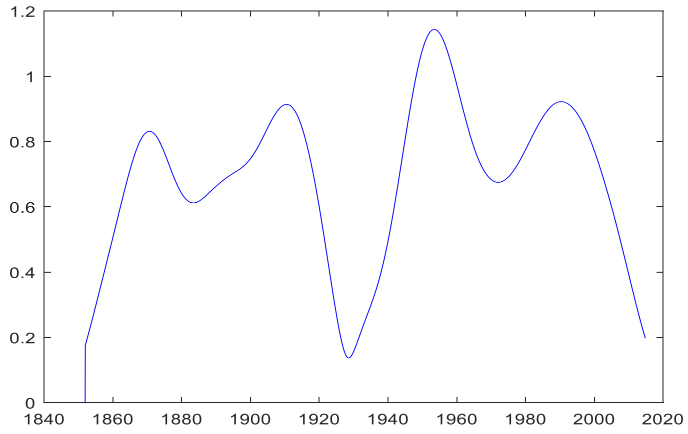

Chandler wobble amplitude A(t) term

Amplitude A(t) derivative

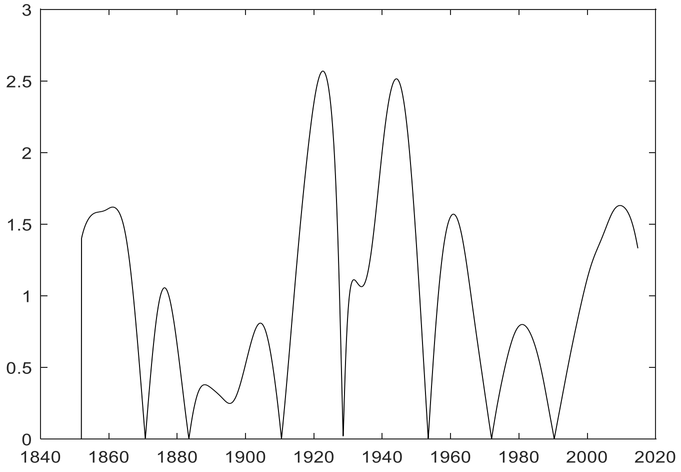

phase ϕ(t) derivative

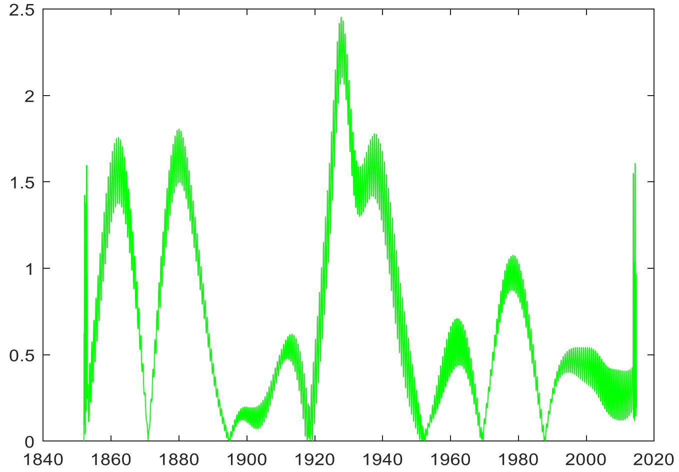

Filtered Chandler wobble and its excitation modeling

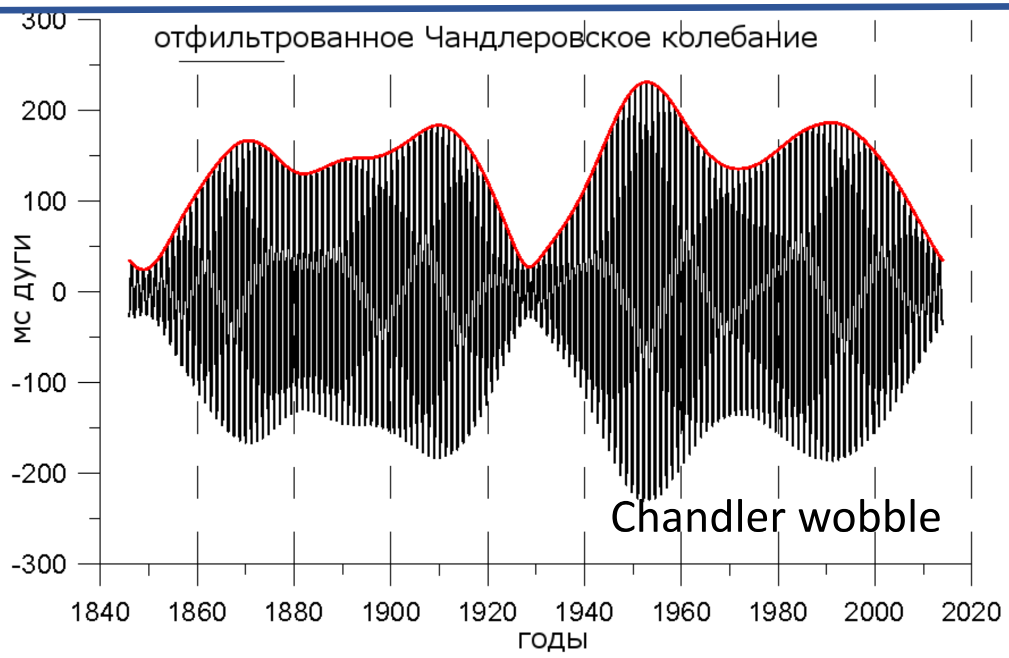

A(t)

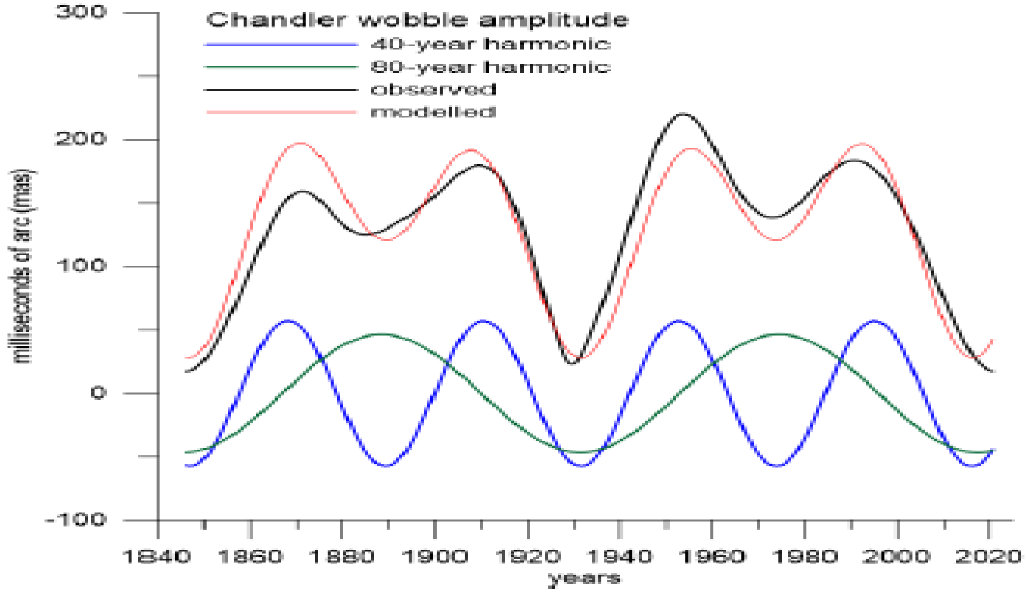

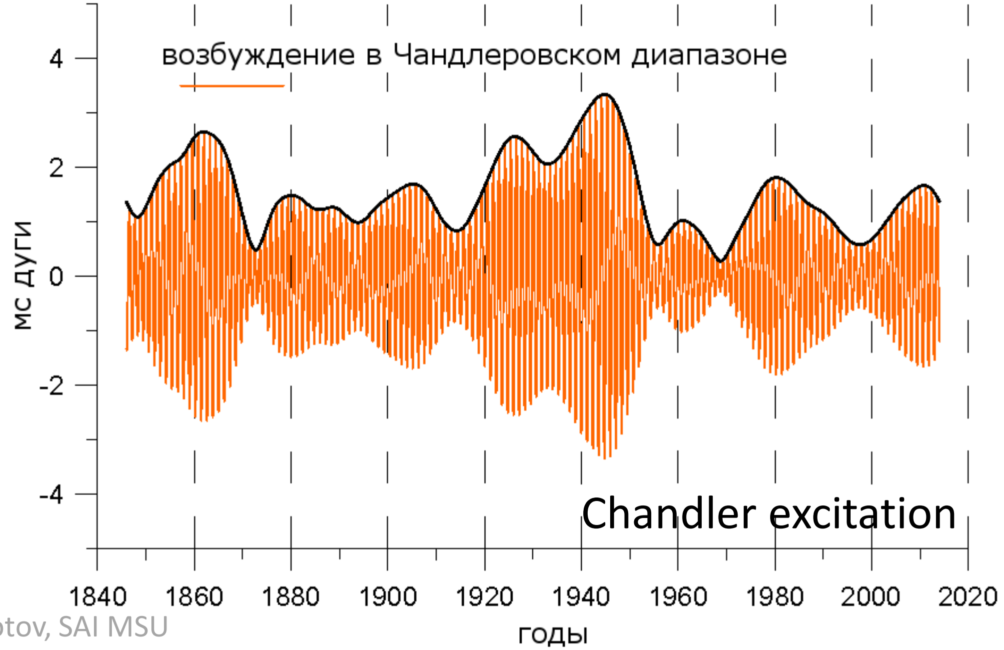

E(t)

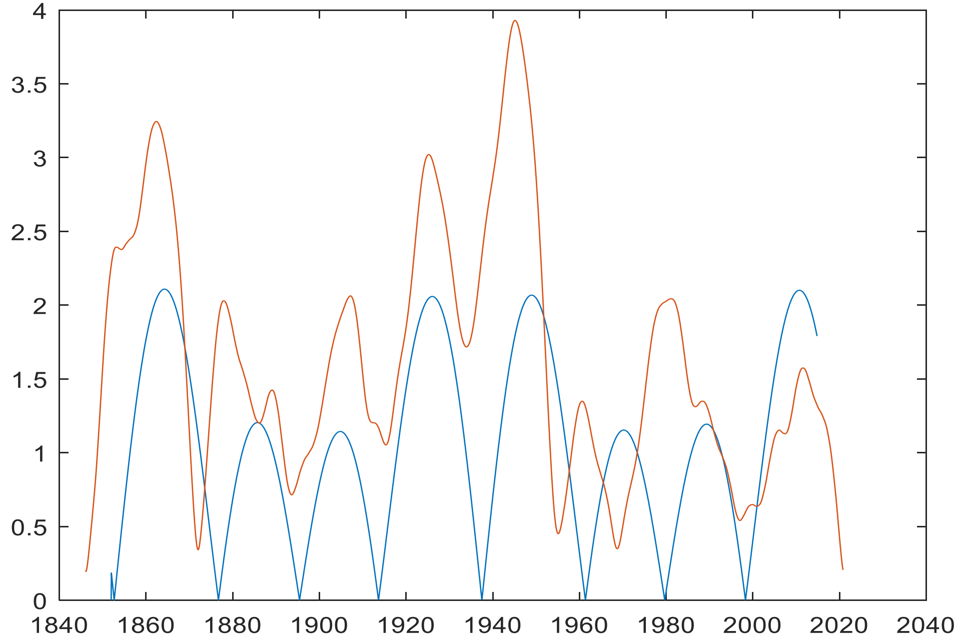

Comparison of excitations for Chandler wobble

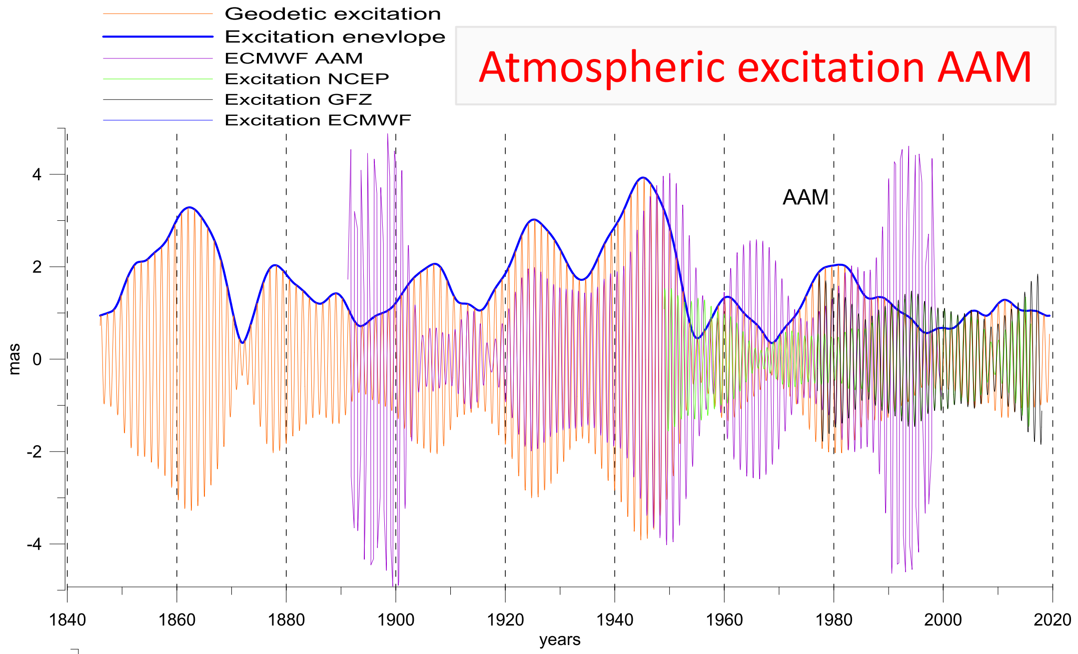

Atmospheric excitation AAM

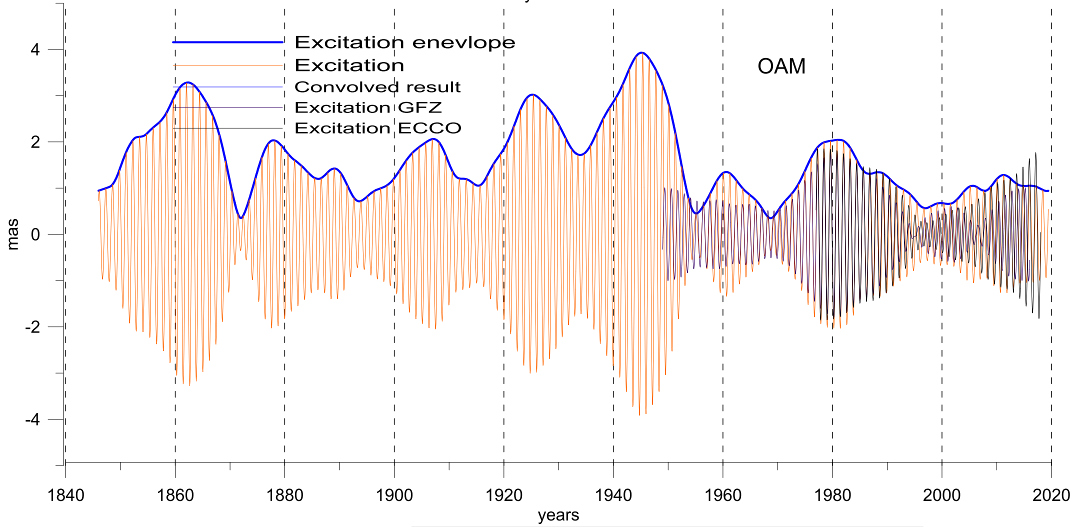

Oceanic excitation OAM

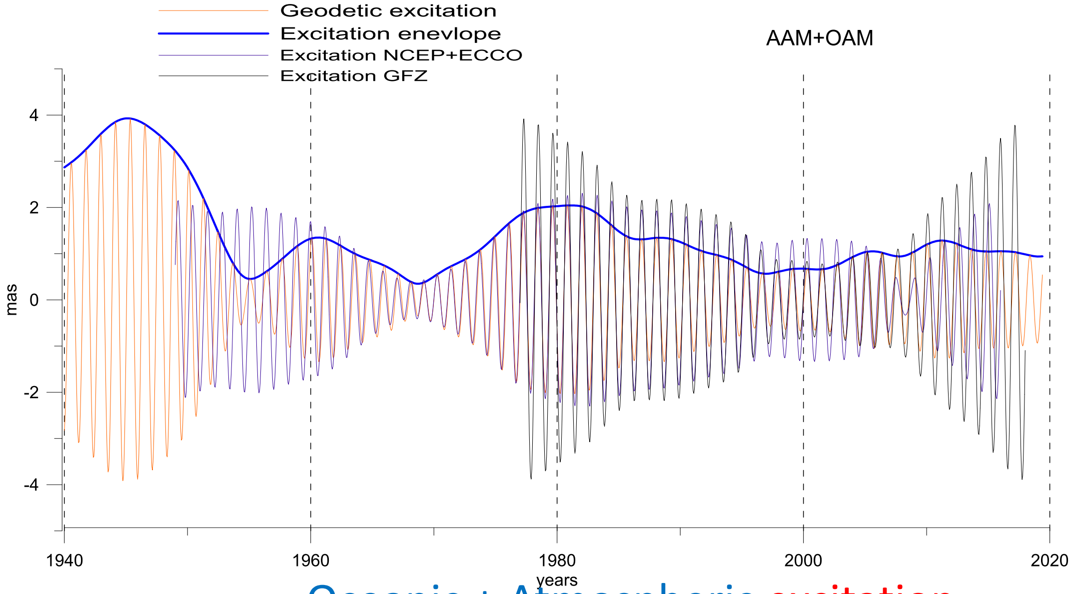

Oceanic + Atmospheric excitation

L.V.Zotov, SAI MSU

Module of the absolute AAM ECMWF wind term in the Chandler frequency band

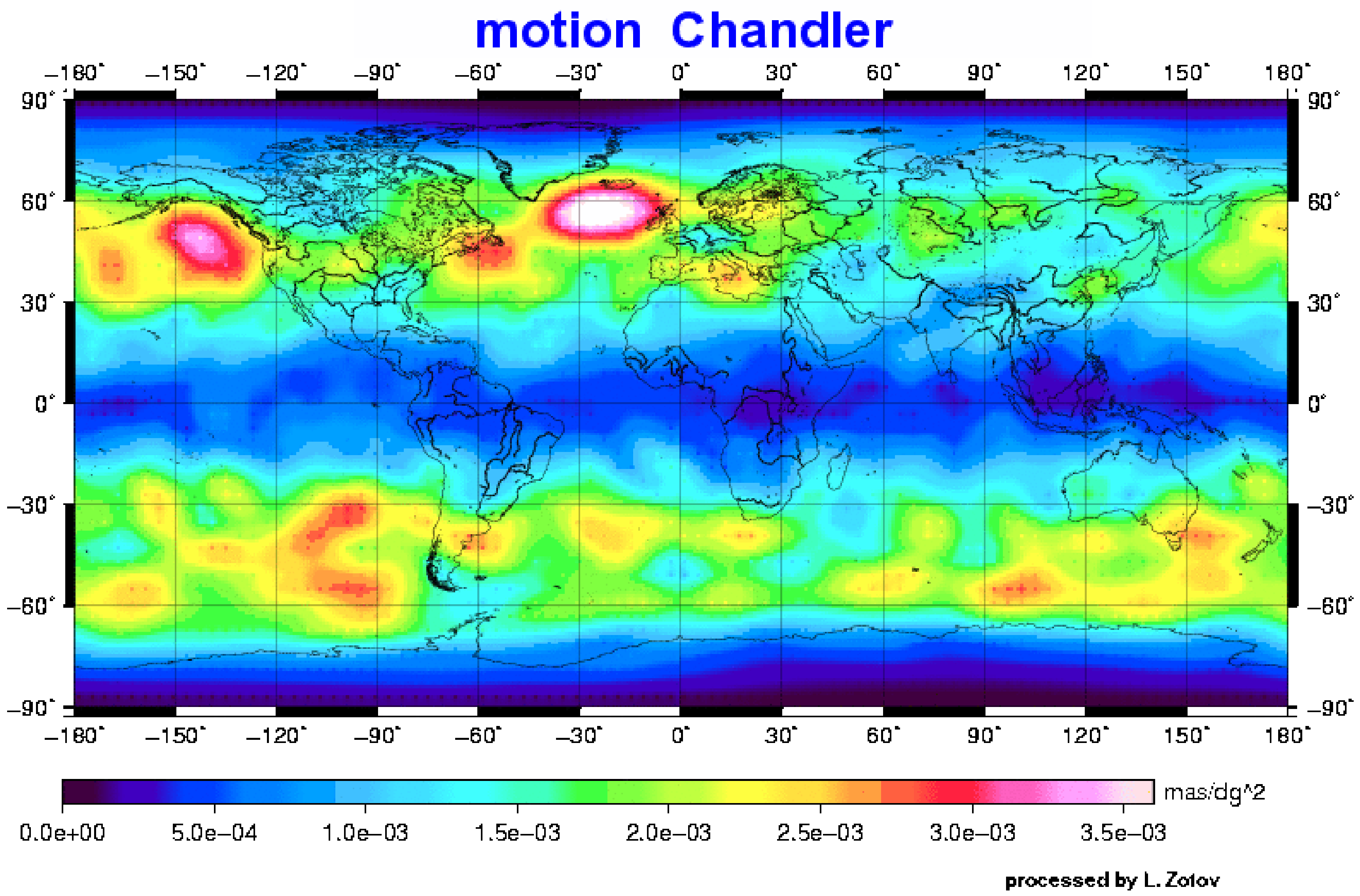

Module of the absolute AAM ECMWF pressure term in the Chandler frequency band

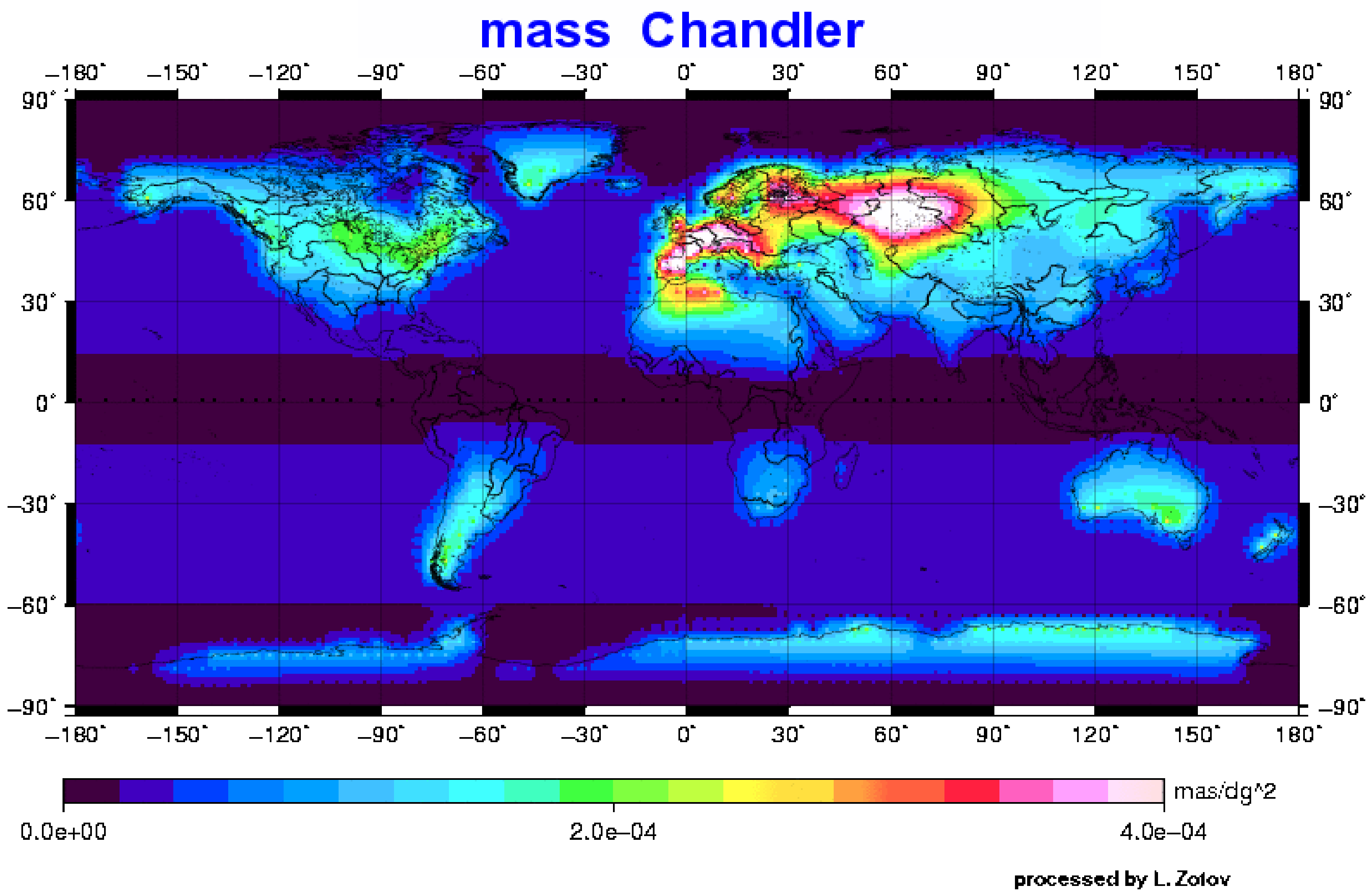

Panteleev's band-pass filters

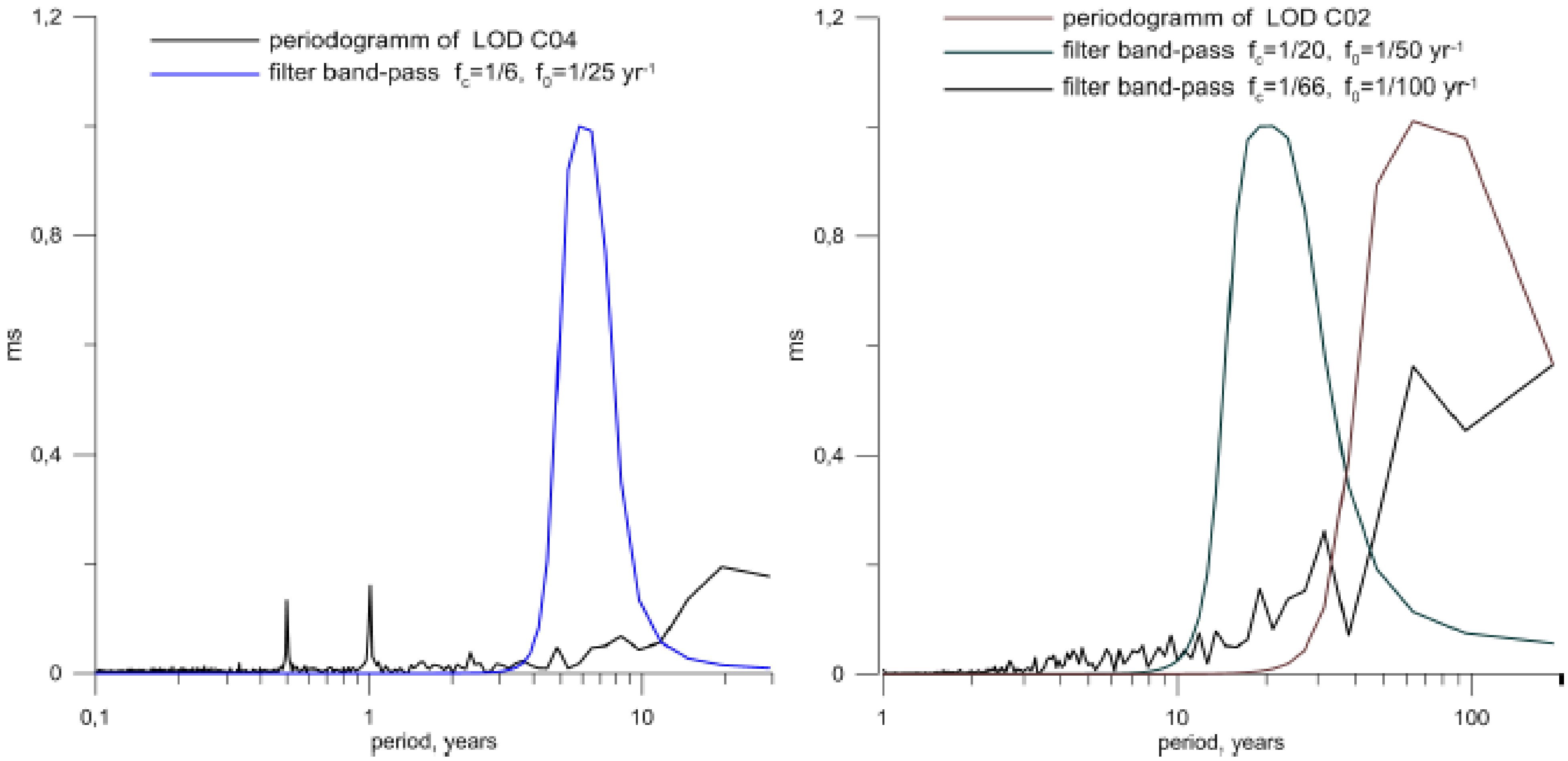

Рис. 5. Periodograms of LOD based of EOP C04 (left) and C02 (right) series and corresponding band-passes of Panteleev's filters.

Comparison of LOD modulations and Chandler wobble amplitude changes

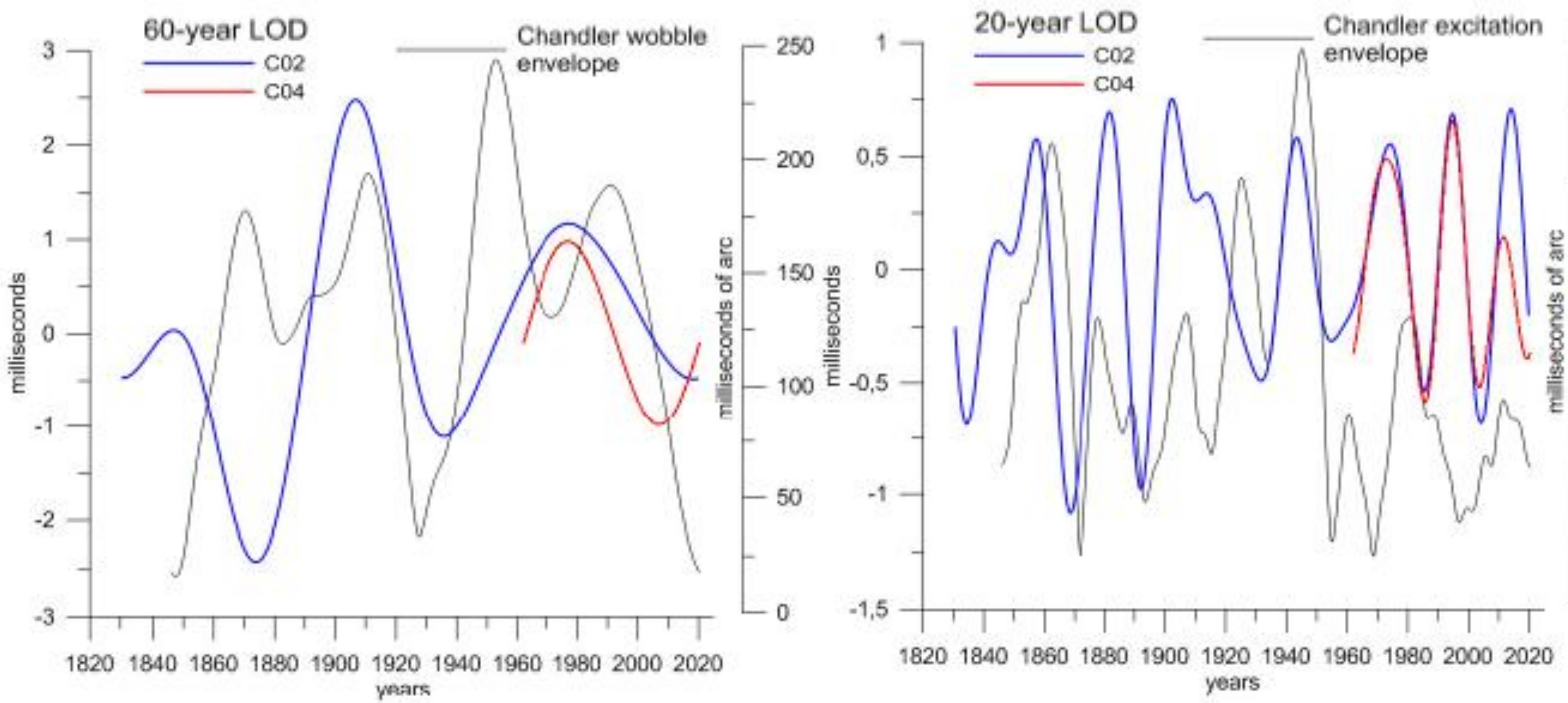

Figure 21. Comparison of the Chandler wobble envelope with 60-year LOD (C02 and C04) variations, left, and of the Chandler excitation envelope with 20-year LOD variations, right.

Low-frequency synchronization in the dynamical system

§2. 同步現象的理論分析

各种不同結构的簡諧振蕩器之方程皆为非綫性方程，它們具有相似的形式与性質，所以在本文中仅对調板振蕩的同步进行理論分析。显然所得結論是适用于任何簡諧振蕩器的。

图 1 所示之調板振蕩器之方程为

$$\frac{d^2V_p}{dt^2} + \frac{1}{RC}\frac{dV_p}{dt} + \omega_0^2 V_p = \frac{-1}{C}\frac{di_p}{dt} \qquad (1)$$

式中 V_p 表板压，i_p 表板流，ω_0 为諧振迴路之固有頻率。即

$$\omega_0 = \frac{1}{\sqrt{LC}}$$

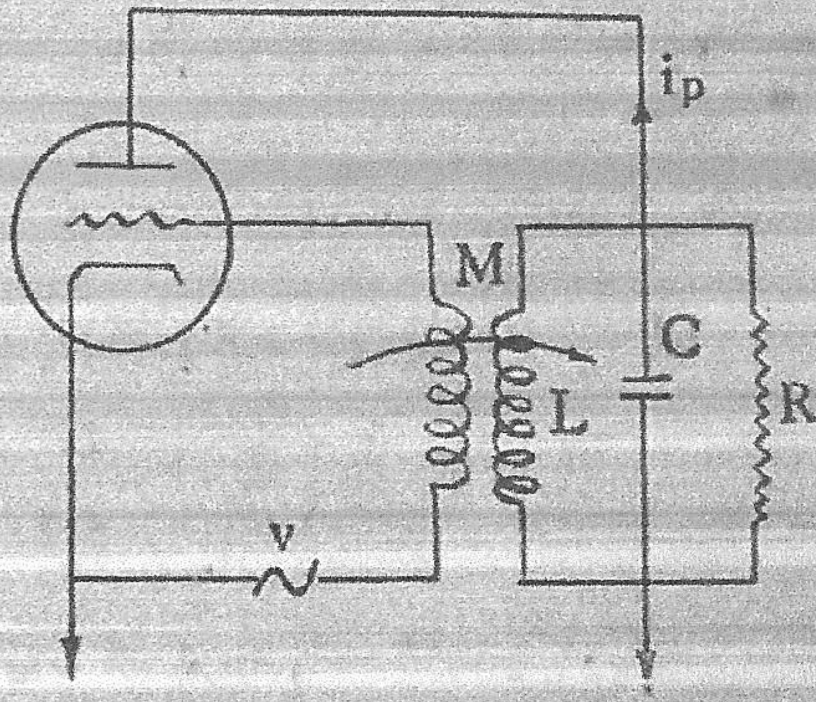

图 1

What if amplitude changes of Chandler Wobble reflects low-frequency synchronization in the dynamical system

ВЗАИМНАЯ СИНХРОНИЗАЦИЯ ДВУХ СВЯЗАННЫХ ГЕНЕРАТОРОВ С ЗАПАЗДЫВАНИЕМ

В. В. Емельянов, Ю. П. Емельянова

$$\dot{A}_1+\frac{i\Delta}{2}A_1+\gamma A_1=\alpha_1 e^{i\theta}\left[(1-k)(1-|A_1(t-1)|^2)A_1(t-1)+k\,(1-|A_2(t-1)|^2)A_2(t-1)\right],$$
$$\dot{A}_2-\frac{i\Delta}{2}A_2+\gamma A_2=\alpha_2 e^{i\theta}\left[(1-k)(1-|A_2(t-1)|^2)A_2(t-1)+k\,(1-|A_1(t-1)|^2)A_1(t-1)\right].$$

参 考 文 献

[1] Хохлов, Р. В., К теорий захвашывания при малой ампридуде внешней силви, Док. А. Н. СССР. 47, 3, 411, 1954.
[2] Райлит, Т. А., Минакова, И. И., Синхронизация лампового генератора синусоидальных кольбаний дродно-кратной гарманической силой Радиотехника, **11**: 7, 50—56, 1956.
[3] К теории нелинейных кольбаний в радиотехнике Р. Ш. Кеваншивили Радиотехника **14**: 9, 17—18, 1959.
[4] Воронин, Э. С., О синхронизации автогенератора модулированной внешней силой радиотехника **14**: 2, 48—56, 1959.

СИНХРОНИЗАЦИЯ ГЕНЕРАТОРА СИНУСОИДАЛЬНЫХ КОЛЬБАНИЙ

Уан Цу

Резюме

Теоретически и экспериментально изучено явлен
под действии низкочастотных сторонних сил. Показан
генератора низкочастотной сторонней силой, и наблю
метров схемы на частотную полосу синхронизации.

$$\frac{d\omega_1}{dt}+\frac{I_3-I_2}{I_1}\omega_2\omega_3=0,$$
$$\frac{d\omega_2}{dt}+\frac{I_1-I_3}{I_2}\omega_3\omega_1=0,$$
$$\frac{d\omega_3}{dt}+\frac{I_2-I_1}{I_3}\omega_1\omega_2=0.$$

???

01

Сложная динамика простой модели распределенной автоколебательной системы с запаздыванием

© Н.М. Рыскин, А.М. Шигаев

$$\dot{A}+\gamma A=\alpha\exp(i\Theta)(1-|A(t-1)|^2)A(t-1).$$

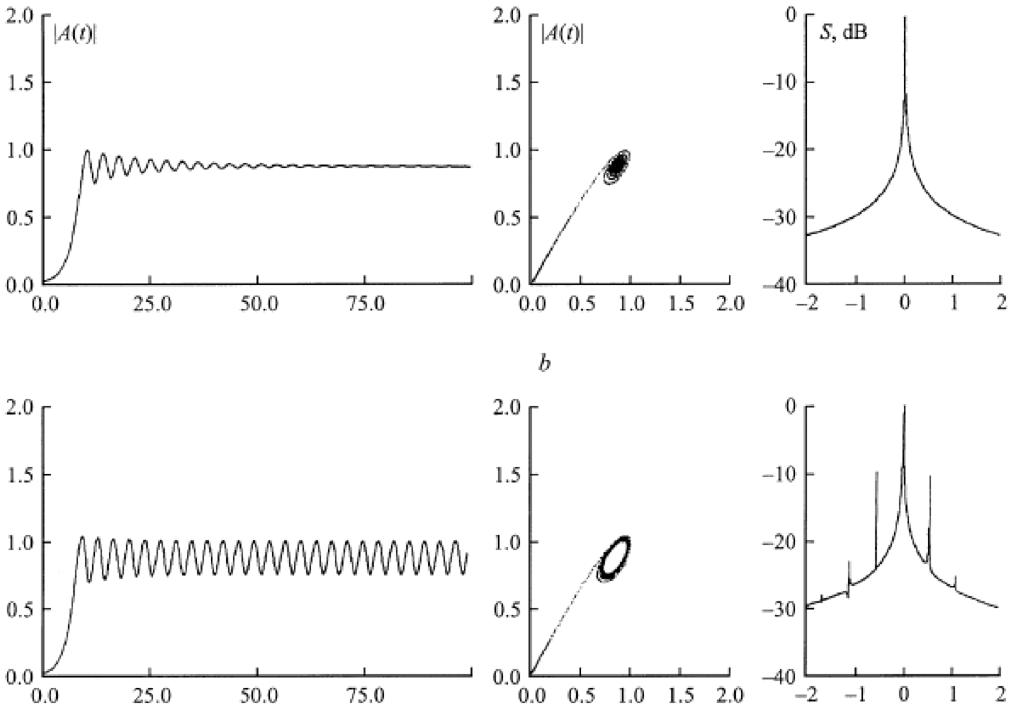

GCOS

GCOS currently specifies 54 ECVs:

ATMOSPHERIC	Surface: air temperature, wind speed and direction, water vapour, pressure, precipitation, surface radiation budget Upper-air: temperature, wind speed and direction, water vapour, cloud properties, Earth radiation budget, lightning Composition: carbon dioxide, methane, other long-lived greenhouse gases, ozone, aerosol, precursors for aerosol and ozone
OCEANIC	Physics: temperature: sea surface and subsurface; salinity: sea surface and subsurface; currents, surface currents, sea level, sea state, sea ice, ocean surface stress, ocean surface heat f ux Biogeochemistry: inorganic carbon, oxygen, nutrients, transient tracers, nitrous oxide , ocean colour Biology/ecosystems: plankton, marine habitat properties
TERRESTRIAL	Hydrology: river discharge, groundwater, lakes, soil moisture, evaporation from land Cryosphere: snow, glaciers, ice sheets and ice shelves, permafrost Biosphere: albedo, land cover, fraction of absorbed photosynthetically active radiation, leaf area index, above-ground biomass, soil carbon, fire, land surface temperature Human use of natual ressources: water use, greenhouse gas fluxes

Essential Climate Variables

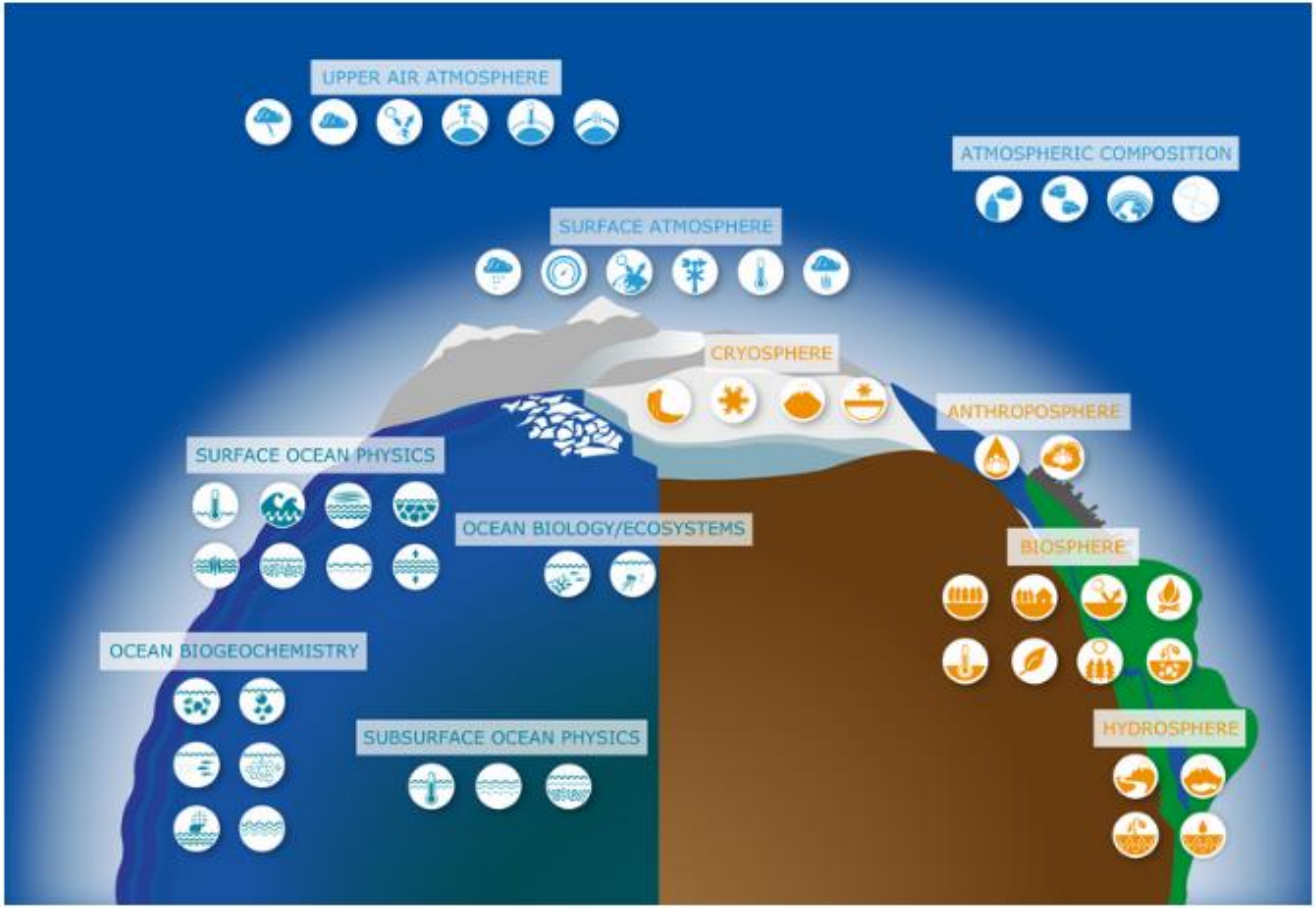

Conclusions

- Climate signals present in excitations of LOD and PM
- Mass term can be accessed through GRACE and GRACE-FO
- Water cycle is very important, hydrological and glaciological changes can shift the axis of the Earth, annual oscillation can also become phase shifted
- Sea level, related to both figure of the Earth and climate can demonstrate forward and backward links to Earth rotation
- Atlantic Ocean gives evident input into Earth temperature variations, which are correlated with Earth rotation velocity on 60 yr scale
- If we can predict climate and ERP together better, then separately, then there is “Granger causality” between them
- We should promote Climate and Earth rotation working group and our ideas. Very few scientists understand the importance of this interdisciplinary scientific field.

Thank you for attention!

The talk is supported by 111 plan (NSFC Grant No. B17033)
of Wuhan University

Earth rotation

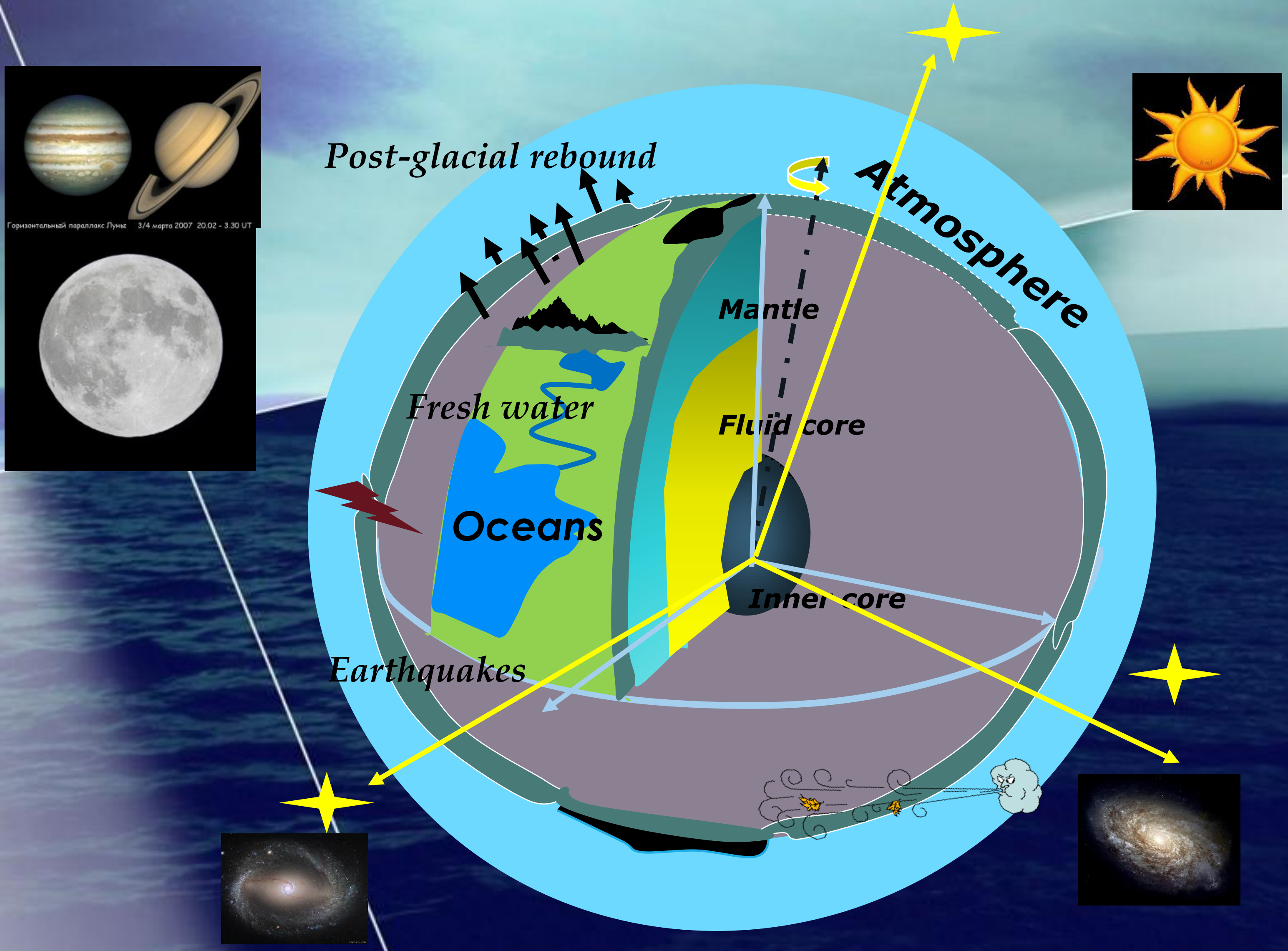

credit: C. Bizouard

О двух гармониках лунного прилива в AAM

Переводим экваториальный AAM из TRF в CRF

$$\chi' = -\chi e^{i\theta(t)}$$

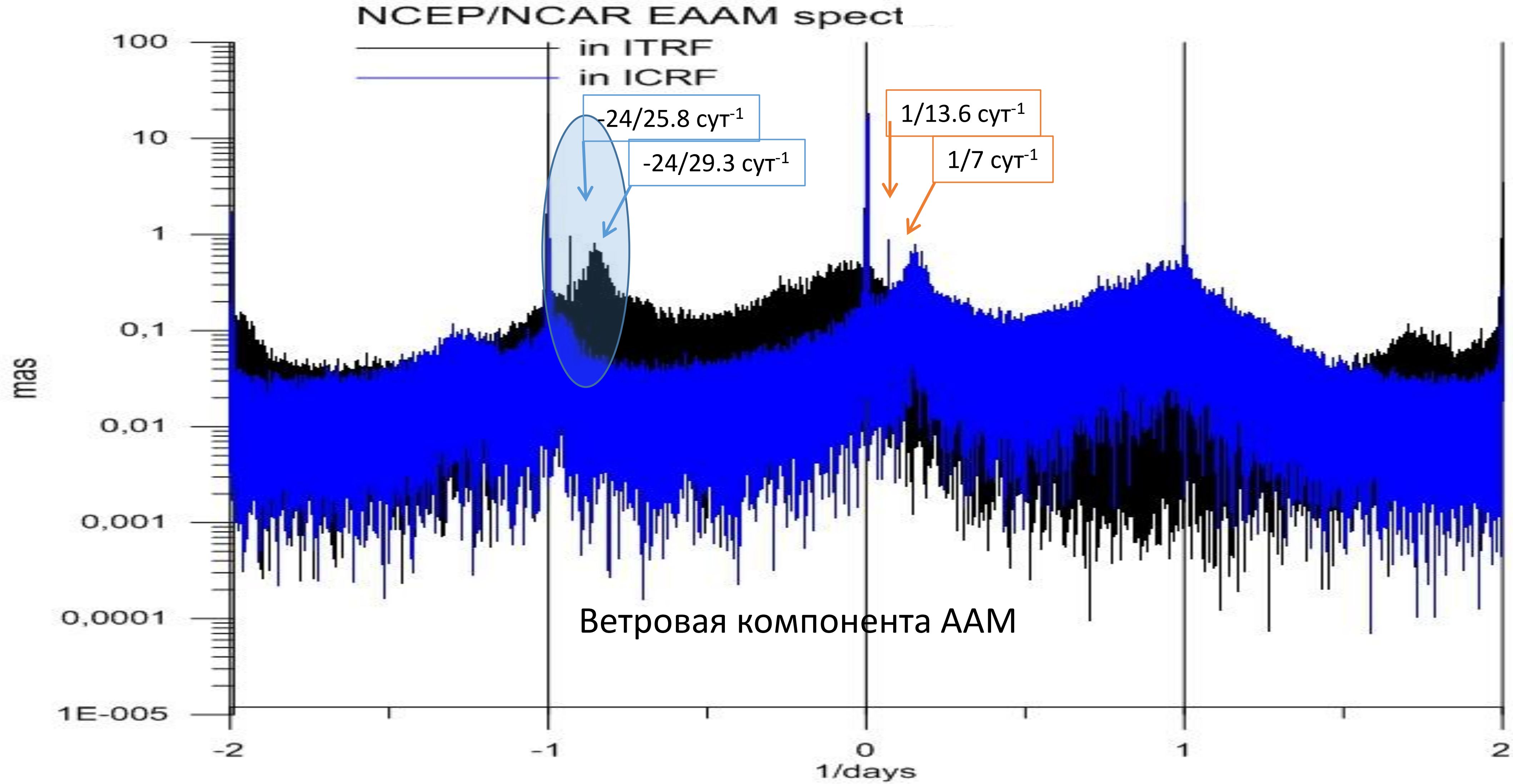

Ветровая компонента AAM

Wavelet-scalogramm of LOD

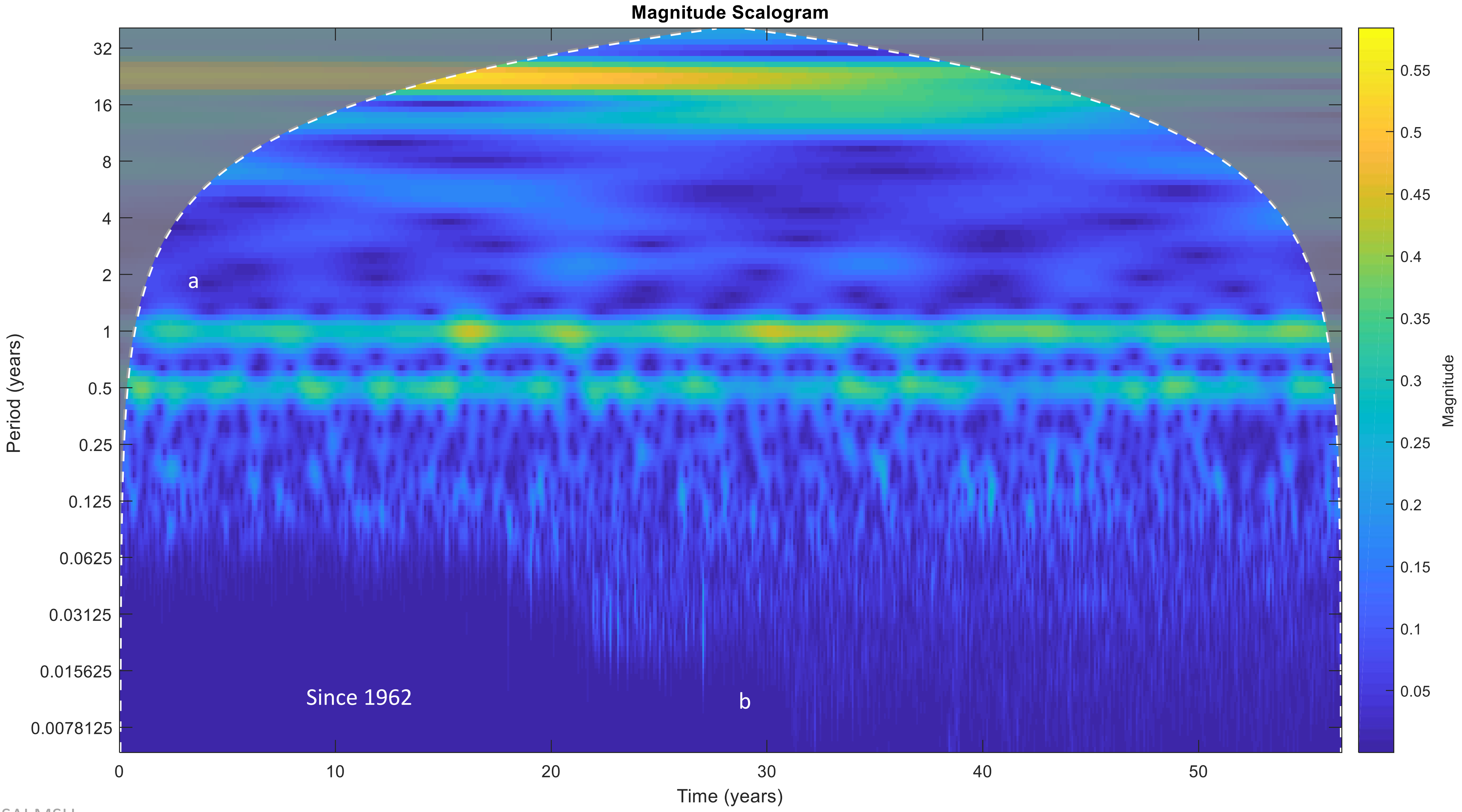

L.V.Zotov, SAI MSU

Earth System Research Laboratory
Physical Sciences Division

PSD STAFF LIST » CECILE PENLAND

Cecile Penland – Scientist

Dynamics and Multiscale Interactions Team

Affiliation: NOAA

Phone: (303) 497-6234

E-mail: cecile.penland@noaa.gov

Curriculum Vitae • Publications

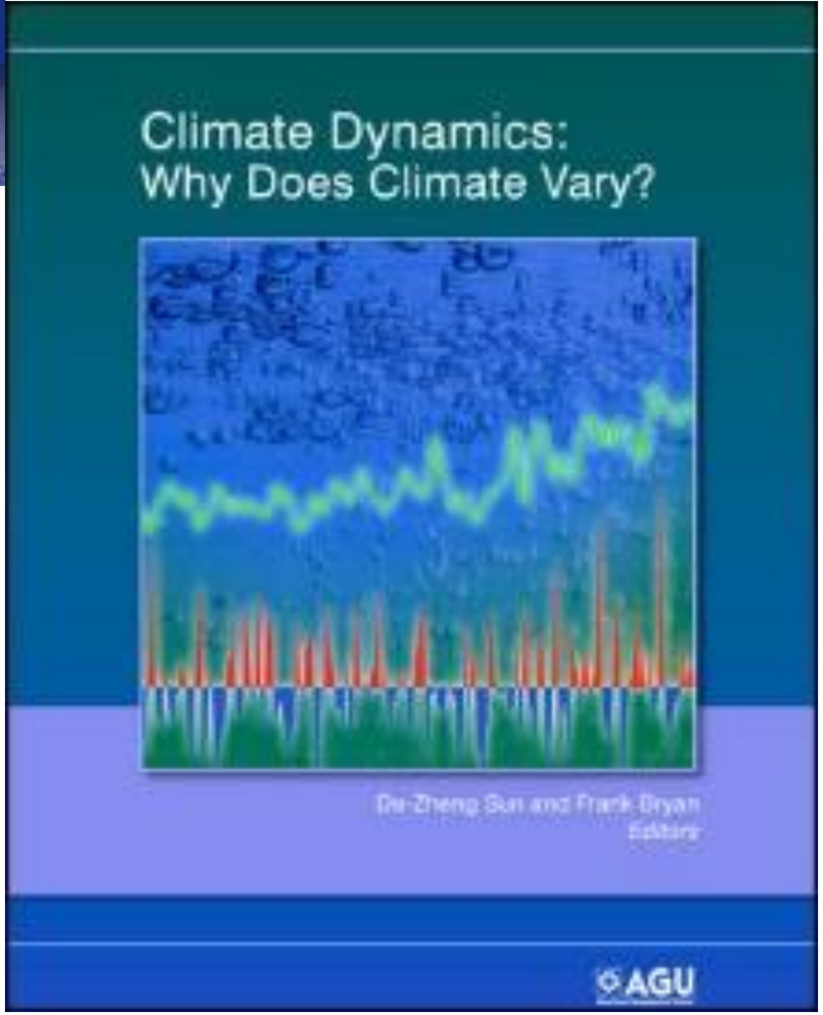

$$\mathbf{x}(t+\tau)=\exp(\mathbf{L}\tau)\mathbf{x}(t)+\int_0^\tau \exp\left(\mathbf{L}[\tau-s]\right)\mathbf{N}(t+s)\,ds\ .$$

Stochastic forcing of north tropical Atlantic sea surface temperatures by the North Atlantic Oscillation

Trends from GRACE in the Ocean Bottom Pressure
Don Chambers data

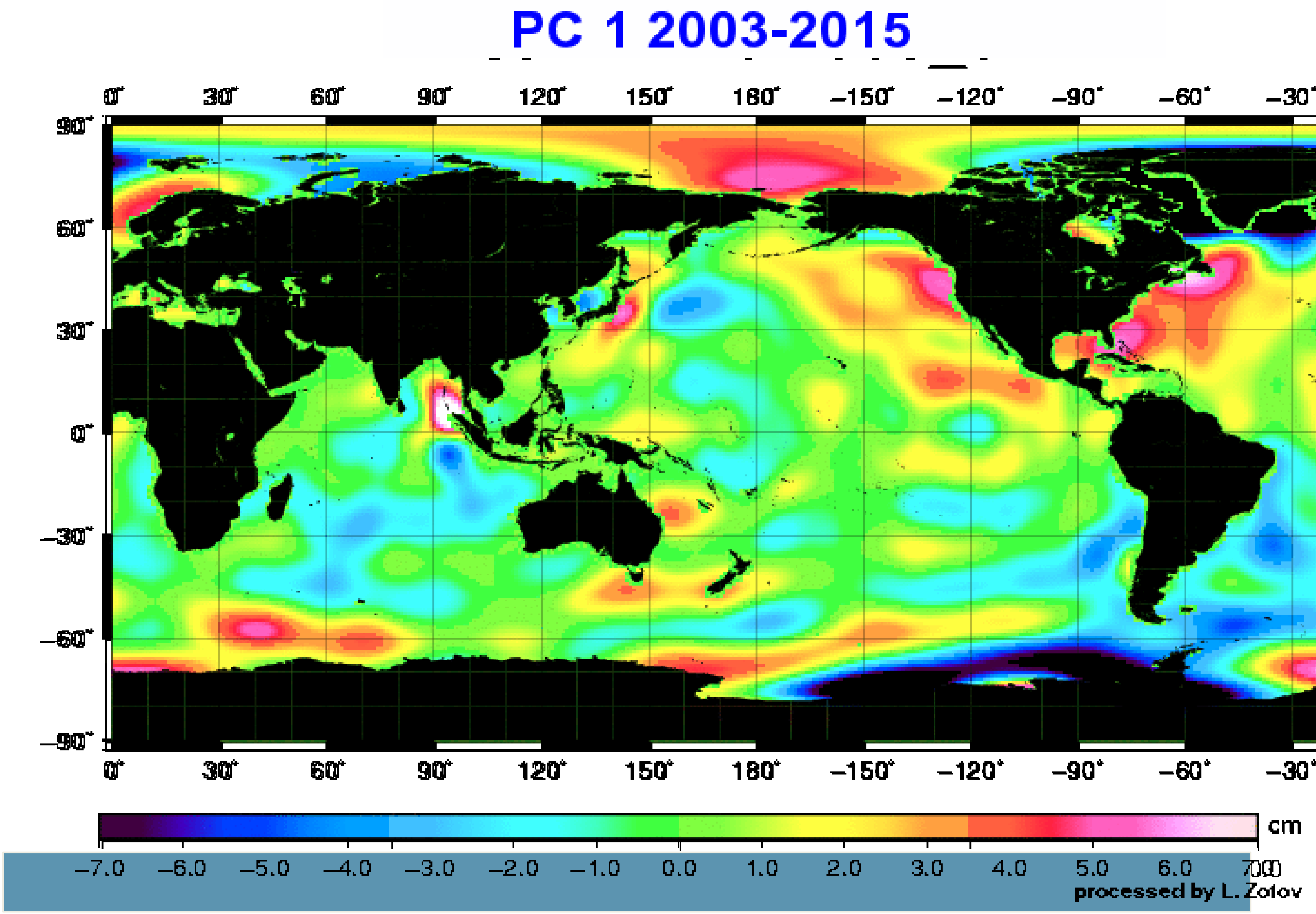

On Estimating the Cross-Correlation and Least-squares Fit of One Dataset to Another with Time Shift

B. F. Chao[1], C. H. Chung[1,2]

A key statistical question to ask is: given the *DOF* of processes *A* and *B*, what is the probability at which the obtained ρ can reject the null hypothesis that *A* and *B* are actually uncorrelated? In the context of statistics, analytical expressions relating the significance of correlation with the *DOF* for random samples can be found in textbooks (e.g., Jenkins & Watts 1968; Bevington & Robinson, 2003). The probability P_c for the correlation value to exceed a certain $|\rho|$ (between 0 and 1) for random samples with $DOF = \nu$ is given by:

$$P_c(\rho;\, \nu) = \frac{1}{\sqrt{\pi}} \frac{\Gamma\,[(\nu+1)/2]}{\Gamma(\nu/2)} \int_{|\rho|}^{1} (1-x^2)^{(\nu-2)/2} dx \qquad (2)$$

where $\Gamma(z) = \int_0^\infty x^{z-1} e^{-x} dx$ (for $Re(z)>0$) is the Gamma function. The significance level is $2P_c$ accounting for both positive and negative ρ values, and the *confidence level* is $1-2P_c$, for given ν.

	P						
ν	**0.20**	**0.15**	**0.10**	**0.05**	**0.01**	**0.005**	**0.001**
60	0.165	0.185	0.211	0.250	0.325	0.352	0.408
70	0.153	0.171	0.195	0.232	0.302	0.327	0.380
80	0.143	0.160	0.183	0.217	0.283	0.307	0.357
90	0.135	0.151	0.173	0.205	0.267	0.290	0.338
100	0.128	0.144	0.164	0.195	0.254	0.276	0.321
900	0.043	0.048	0.055	0.065	0.086	0.093	0.109
950	0.042	0.047	0.053	0.064	0.083	0.091	0.106
1000	0.041	0.046	0.052	0.062	0.081	0.089	0.104
1500	0.033	0.037	0.042	0.051	0.066	0.072	0.085
2000	0.029	0.032	0.037	0.044	0.058	0.063	0.073
3000	0.023	0.026	0.030	0.036	0.047	0.051	0.060
4000	0.020	0.023	0.026	0.031	0.041	0.044	0.052
5000	0.018	0.020	0.023	0.028	0.036	0.040	0.047
10000	0.013	0.014	0.016	0.020	0.026	0.028	0.033

Table S1. Correlation coefficients corresponding to significance levels (of 20% - 0.1%; corresponding to confidence levels of 80% - 99.9%) from Equation (2) in the main text. (ν = degree of freedom, ranging 1-10,000).